Antimicrobial Resistant Plasmid Effects on *Salmonella enterica* serotype Heidelberg

By

Jayelle Renee Friesen-Enns

A Thesis submitted to the Faculty of Graduate Studies of

The University of Manitoba

in partial fulfillment of the requirements of the degree of

MASTER OF SCIENCE

Department of Medical Microbiology and Infectious Diseases and the Max Rady College of Medicine

University of Manitoba
Winnipeg

Copyright © 2023 by Jayelle Renee Friesen-Enns

Abstract

Salmonella enterica serotype Heidelberg is the third most frequently isolated serotype in Canada and is of particular interest due to its resistance to cephalosporin-class antimicrobials. Through national surveillance of Canadian *S.* Heidelberg strains isolated from poultry sources and human infections, we previously demonstrated that human and animal-derived isolates were genetically similar (ST15) and that structurally similar IncI1 plasmids harbouring the $bla_{\text{CMY-2}}$ gene were predominantly responsible for cephalosporin-resistance. Here, we focus on the impact of two variants (pCMYN13-02944A and pCMY12-2460C) of a well-characterized and widely disseminated IncI1plasmid on the core physiology of an *S.* Heidelberg strain isolated from Canadian national surveillance. The plasmids were transferred via conjugation to a susceptible and previously whole-genome sequenced (WGS) *S.* Heidelberg isolate (N13-01291) to form isogenic strain pairs. Illumina WGS was performed on the parent and transconjugants to monitor genetic alteration introduced during conjugation. Plasmid maintenance and viability were assessed using the PMAxx™ (Biotum, Inc., Hayward, CA, USA) photoreactive viability dye followed by quantitative polymerase chain reaction (PCR). Growth curves and Biolog Omnilog® (Biolog, Hayward, CA, USA) phenotypic microarrays were performed to analyze the effects of the plasmids of interest on fitness and growth kinetics. The presence of either plasmid resulted in observable changes in growth kinetics compared to N13-01291. Biofilm assays were performed using 0.1% (w/v) crystal violet staining which determined that N13-01291, N13-01291/pCMYN13-02944A, and N13-01291/pCMY12-2460C are poor biofilm producers. Phylogenomic analysis of the isogenic strain pairs indicated the presence of a shared single nucleotide variant (SNV) and a unique SNV in the presence of either plasmid which affected various changes in growth kinetics. Proteomics were analysed using tandem mass tags and LC-

MS/MS analysis. In the presence of one plasmid (pCMYN13-02944A), there were 341 significantly detected proteins that had a $\log_2$-fold change ≥ 1 and 72 that had a $\log_2$-fold change ≥ 2. In the presence of plasmid (pCMY12-2460C), there were 415 significantly detected proteins that had a $\log_2$-fold change ≥ 1 and 96 proteins that had a $\log_2$-fold change ≥ 2. In conclusion, the presence of either IncI1 plasmid influenced changes in growth and proteomic expression when present in the host isolate N13-01291.

Acknowledgements

I would like to thank my supervisor, Dr. Michael Mulvey for giving me the opportunity to complete my Master of Science degree on antimicrobial resistance in *Salmonella* and for the amazing experiences that came along with the project. I would also like to say a special thank you to Dr. Chand Mangat for providing frequent and much-needed guidance in the lab. I would also like to thank my committee members, Dr. Denice Bay, and Dr. Ann Karen Brassinga for their suggestions and support during this project.

Thank you to all the Antimicrobial Resistance and Nosocomial Infections lab members for their friendship, support, and laughs over the years. Specifically, I would like to thank Sean for always helping me when I needed it, Chand for his expertise, Dave and Jen for always brightening my days, Amrita for supplying endless bioinformatics knowledge, and Shelley for all the technical support. I would also like to say thank you to the Mass Spectrometry and Proteomics Core Facility, specifically Dr. Patrick Chong, for their assistance and guidance. I am also thankful for the funding sources of this project including the Canadian Institute of Health Research and the Joint Programming Initiative on Antimicrobial Resistance, with whom this project was possible.

Finally, I would like to say a huge thank you to my friends and family for their love and support throughout the years and during this degree. Most of all, I would like to thank my husband Nikolas for his endless encouragement and support during these past years.

Table of Contents

Abstract 2

Acknowledgements 4

List of Tables 9

List of Figures 10

List of Abbreviations 12

1. Introduction 14

1.1 Antimicrobial Use and Resistance 14

1.1.1 Use and Overuse of Antimicrobials 14

1.1.2 AMR in Enterobacterales 16

1.1.3 Mechanisms of AMR 19

1.1.3.1 Efflux 19

1.1.3.2 Porins 20

1.1.3.3 Inactivating Enzymes 21

1.1.3.4 Antimicrobial Target Modification 22

1.2 Plasmids 25

1.2.1 Plasmid Classifications 26

1.2.2 Plasmid Maintenance 28

1.2.3 Plasmids in *Enterobacterales* 31

1.2.4 Effects of Plasmids in Gram-negative Bacteria 32

1.2.4.1 Fitness and Growth 33

1.2.4.2 Virulence 34

1.2.4.3 Chromosomal Gene Expression 36

1.3 *Salmonella enterica* 36

1.3.1 Pathogenesis and Virulence of *S. enterica* 37

1.3.2 Sequence Variability in *S. enterica* 40

1.3.3 Treatment of *S. enterica* 41

1.3.4 *Salmonella enterica* serotype Heidelberg 41

1.3.4.1 AMR in S. Heidelberg 42

1.3.4.2 CMY-2-Containing S. Heidelberg Outside of North America 43

1.3.4.3 Epidemiology of S. Heidelberg 44

1.3.4.4 Relevance of S. Heidelberg 45

1.3.4.5 Plasmids in S. Heidelberg 46

1.4 Rationale and Hypothesis 46

2. Materials and Methods 49

2.1 Bacterial Strains and Growth Conditions 49

2.2 Nucleic Acid Manipulation 49

2.2.1 Plasmid Isolation 49
2.2.2 Crude DNA Extraction 50
2.2.3 Nucleic Acid Quantification 50
2.3 Isogenic Strain Pair Formation **51**
2.3.1 Formation of Electrocompetent Isolates 51
2.3.2 Plasmid Transformation 51
2.3.3 Transformation Efficiency Assay 52
2.3.4 Plasmid Conjugation 52
2.3.5 Conjugation Frequency Assay 53
2.4 Determination of Antimicrobial Susceptibility **54**
2.4.1 Detection of *bla*$_{\text{CMY-2}}$ 54
2.4.2 Gel Electrophoresis 54
2.4.3 Antimicrobial Susceptibility Testing 56
2.5 Whole-Genome Sequencing **57**
2.5.1 DNA Extraction 57
2.5.2 Whole-Genome Sequencing 57
2.5.3 WGS Analysis 59
2.5.4 Assembly of Genomes and Plasmids 59
2.5.4.1 Phylogenetic Analysis 59
2.5.4.2 Antimicrobial Gene Detection 60
2.5.4.3 Plasmid Characterization 60
2.6 Plasmid Maintenance and Viability Assays **61**
2.6.1 Protocol and Optimization 62
2.6.2 Targets and Efficiencies 62
2.6.3 Isolates and Controls 63
2.6.4 Determination of Plasmid Retention 63
2.6.5 Statistical Analysis 65
2.7 Growth Assays **65**
2.7.1 Temperature and Media Conditions 65
2.7.2 Statistical Analysis 66
2.8 Phenotypic Microarrays using Biolog Omnilog® **67**
2.8.1 Procedure 67
2.8.2 Analysis of Phenotypic Microarrays 67
2.9 Biofilm Formation Assays **69**
2.9.1 Procedure 69
2.9.2 Statistical Analysis 69
2.10 LC/MS/MS Proteomics **70**
2.10.1 Cell Preparation 70
2.10.2 Cell Lysis 70
2.10.3 Protein Quantification 73
2.10.4 SDS and DTT Treatment of Protein 73
2.10.5 Peptide Digestion 73

2.10.6 Peptide Recovery and Desalting ... 74
2.10.7 Tandem Mass Tag (TMT)-Labelling ... 75
2.10.8 Pre-Scan ... 75
2.10.9 Peptide Fractionation ... 76
2.10.10 Nano-LC-MS/MS Analysis ... 76
2.10.11 Data Processing and Statistical Analysis ... 77
2.10.12 Protein Modelling ... 78

3. Results ... 78

3.1 Isogenic Strain Pair Formation ... **78**
3.1.1 Plasmid pCas Transformation and Efficiency ... 78
3.1.2 Conjugation of pCMY/pCas Plasmids ... 79
3.1.3 Detection of Extended-spectrum β-lactamase Genes ... 80

3.2 Determination of Antimicrobial Susceptibility ... **82**

3.3 Whole Genome Sequencing of Isogenic Strain Pairs ... **84**
3.3.1 Phylogenomic Analysis ... 84
3.3.2 Antimicrobial Gene Detection ... 88
3.3.3 Plasmid Identification and Characterization ... 90
3.3.4 IncI1 Plasmid Comparisons ... 96

3.4 Plasmid Maintenance Assays ... **98**
3.4.1 Determination of Plasmid Retention ... 98

3.5 Growth Assays ... **101**

3.6 Phenotypic Microarrays ... **108**
3.6.1 Metabolic Assays ... 108
3.6.1.1 N13-01291 vs N13-01291/pCMYN13-02944A ... 108
3.6.1.2 N13-01291 vs N13-01291/pCMY12-2460C ... 111
3.6.1.3 N13-01291/pCMYN13-02944A vs N13-01291/pCMY12-2460C ... 116
3.6.2 Chemical Sensitivity Assays and Comparisons to Sensititre® ... 120

3.7 Biofilm Assays ... **126**

3.8 Proteomics ... **131**
3.8.1 General ... 131
3.8.2 Functional Annotation ... 132
3.8.3 Protein Structures ... 136

4. Discussion ... 140

4.1 Comparison of pCMYN13-02944A and pCMY12-2460C ... **140**

4.2 Phylogenomics ... **141**
4.2.1 Shared SNV in the Presence of Either pCMYN13-02944A or pCMY12-2460C ... 141
4.2.2 Unique SNV in the Presence of Plasmid pCMY-N13-02944A ... 142
4.2.3 Unique SNV in the presence of plasmid pCMY-12-2460C ... 143

4.3 Plasmid Effects on Fitness and Pathogenicity 144
4.3.1 Plasmid Viability and Maintenance 144
4.3.2 Growth Curves 145
4.3.2.1 Comparison of Growth Kinetics in the Presence of pCMYN13-012944A vs pCMY12-2460C 145
4.3.2.2 Notable Changes in Growth Kinetics in the Presence of pCMYN13-02944A 147
4.3.2.3 Notable Changes in Growth Kinetics in the Presence of pCMY12-2460C 148
4.4 Proteomic Changes in the Presence of CMY-2 Plasmids 149
4.4.1 Changes in Protein Expression Found in the Presence of Either Plasmid 149
4.4.1.1 Proteins Regulated in the Same Direction 149
4.4.1.2 Proteins Regulated in Opposite Directions 150
4.4.2 Changes in Protein Expression Found in the Presence of pCMYN13-02944A 152
4.4.3 Changes in Proteomic Expression Found in the Presence of pCMY12-2460C 158
4.5 Potential Plasmid Gene Targets Influencing Expression of Chromosomal Genes 162
4.5.1 ProQ/FinO Domain-Containing Protein YafB 162
5. Conclusions 167
5.1 Future Directions 168
References 171
Appendix 185

List of Tables

Table 2.1. Primers used for PCR amplification of *bla*$_{CMY-2}$ gene 56
Table 2.2. Antimicrobial susceptibility breakpoints for *Salmonella*. 59
Table 2.3. Primers used for viability and maintenance assays. 65
Table 3.1. Antimicrobial susceptibility testing results using Sensititre® interpreted using CLSI or NARMS standards 84
Table 3.2. A summary of the identified SNV alterations detected in the core-genomes of N13-01291/pCMYN13-02944A and N13-01291/pCMY12-2460C as compared to the plasmid-free isolate genome 87
Table 3.3. Predicted AMR genotypes and phenotypes of the three isolates using staramr. 90
Table 3.4. Replicon typing and characterization of plasmids identified using MOB-recon 92
Table 3.5. TRAMS results for isolate N13-01291/pCMYN13-02944A using pCVM_29188_101 as a reference 95
Table 3.6. TRAMS results for isolate N13-01291/pCMY12-2460C using pCVM_29188_101 as a reference 96
Table 3.7. Antimicrobial susceptibility testing results from the Sensititre® analyses as compared to the results from the Biolog Omnilog® phenotypic microarray plates 125
Table 3.8. *S.* Heidelberg isolates tested for biofilm formation; these isolates were previously described by Edirmanasinghe et al., 2017 128
Table 5.1. Targets and primer sequences chosen for future RT-qPCR experiments. 170

List of Figures

Figure 1.1 Timelines of the discovery of antibiotics and the discovery of antibiotic resistance .. 19
Figure 1.2. Types of enzymes involved in antimicrobial resistance. 23
Figure 1.3. Hydrolysis of the amide bond in the β-lactam Ring by β-lactamases 24
Figure 1.4. Depiction of plasmid addiction systems adapted from Tsang J. 31
Figure 1.5. Common features of virulence plasmids adapted from Pilla et al 36
Figure 2.1. Phenotypic microarray panel contents for plates 1-20 sourced from Biolog 69
Figure 2.2. Workflow used for the proteomic analysis of *S.* Heidelberg samples 73
Figure 3.1. Extended-spectrum β-lactamase PCR for the identification of *bla*$_{CMY-2}$ 82
Figure 3.2. Minimum spanning phylogenetic tree of core genome SNVs between *S.* Heidelberg isolates N13-01291/pCMYN13-02944A and N13-01291/pCMY12-2460C 88
Figure 3.3. Visualization of Group A IncI1 plasmid "pCMYN13-02944A" isolated from sample N13-02944 93
Figure 3.4. Visualization of Group C IncI1 plasmid "pCMY12-2460C" isolated from sample 12-2460 94
Figure 3.5. Plasmid alignment generated using EasyFig v2.2.2 98
Figure 3.6. Plasmid maintenance assay results for pCMYN13-02944A performed in biological triplicate and technical duplicate using PMAxx™ to isolate DNA from viable cells through qPCR 100
Figure 3.7. Plasmid maintenance assay for pCMY12-2460C performed in biological triplicate and technical duplicate using PMAxx™ to isolate DNA from viable cells through qPCR. 101
Figure 3.8. Growth curves of *S.* Heidelberg isogenic strain pairs for 24 hours at various temperatures in 20 mL LB broth or M9 minimal salts media with 250 rpm shaking 104
Figure 3.9. Growth curves of *S.* Heidelberg isogenic strain pairs for 24 hours at various temperatures in 100 µL LB broth or M9 minimal salts media with 280 cpm shaking 105
Figure 3.10. Growth curves of *S.* Heidelberg isogenic strain pairs for 24 hours 100 µL LB broth with 280 cpm shaking in Epoch™ 2 Microplate Spectrophotometer 106
Figure 3.11. Metabolic assays (PM 1-10) comparing the growth kinetics of isolates N13-01291 indicated in red and N13-01291/pCMYN13-02944A indicated in green 111
Figure 3.12. Metabolic assays (PM 1-10) comparing the growth kinetics of isolates N13-01291 indicated in red and N13-01291/pCMY12-2460C indicated in green 115
Figure 3.13. Metabolic assays (PM 1-10) comparing the growth kinetics of isolates N13-01291/pCMYN13-02944A indicated in green and N13-01291/pCMY12-2460C indicated in red. 120
Figure 3.14. Chemical sensitivity assays (PM 11-20) comparing the growth kinetics of isolates N13-01291 indicated in red and N13-01291/pCMYN13-02944A indicated in green 122
Figure 3.15. Chemical sensitivity assays (PM 11-20) comparing the growth kinetics of isolates N13-01291 and N13-01291/pCMY12-2460C 123

Figure 3.16. Chemical sensitivity assays (PM 11-20) comparing the growth kinetics of isolates N13-01291/pCMYN13-02944A indicated in green and N13-01291/pCMY12-2460C indicated in red 124
Figure 3.17. Biofilm content determination was based on absorbance readings at 600nm after staining with crystal violet 131
Figure 3.18. Functional annotation of 341 significantly ($p<0.05$) detected proteins with a 2-fold or greater change in regulation in the presence of pCMYN13-02944A. 134
Figure 3.19. Functional annotation of 415 significantly ($p<0.05$) detected proteins with a 2-fold or greater change in regulation in the presence of pCMY12-2460C. 136
Figure 3.20. 3D model of UbiB designed using the Phyre2 server 138
Figure 3.21. 3D model of CpxA designed using the Phyre2 server. 139
Figure 3.22. 3D model of MshA_1 designed using the Phyre2 server 140
Figure 4.1. Flagellar assembly proteins that had changes in regulation in the presence of pCMYN13-02944A (green) and pCMY12-2460C (blue) as indicated by imputting GhostKOALA v2.0 annotation data intothe KEGG PATHWAY database via KEGG Mapper 155
Figure 4.2. Quorum sensing proteins that had changes in regulation in the presence of pCMYN13-02944A (green) and pCMY12-2460C (blue) as indicated by imputting GhostKOALA v2.0 annotation data intothe KEGG PATHWAY database via KEGG Mapper 156
Figure 4.3. ABC transporter proteins that had changes in regulation in the presence of pCMYN13-02944A (green) as indicated by imputting GhostKOALA v2.0 annotation data intothe KEGG PATHWAY database via KEGG Mapper 157
Figure 4.4. Bacterial invasion proteins that had changes in regulation in the presence of pCMY12-2460C (green) as indicated by imputting GhostKOALA v2.0 annotation data intothe KEGG PATHWAY database via KEGG Mapper 161
Figure 4.5. Bacterial chemotaxis proteins that had changes in regulation in the presence of pCMY12-2460C (green) as indicated by imputting GhostKOALA v2.0 annotation data intothe KEGG PATHWAY database via KEGG Mapper 162
Figure 4.6. Effects of ProQ/FinO family proteins adapted from Liao and Smirnov 166

List of Abbreviations

ABC ATP-binding cassette

AMC Amoxicillin/clavulanic acid

AMP Ampicillin

AmpC Ampicillin hydrolyzing

AMR Antimicrobial resistance

AZM Azithromycin

BLAST Basic Local Alignment Search Tool

bp Base pair

BSA Bovine serum albumin

CAM Chloramphenicol

CDS Coding sequence

cfu Colony forming unit

CIP Ciprofloxacin

CIPARS Canadian Integrated Program for Antimicrobial Resistance Surveillance

CLSI Clinical and Laboratory Standards Institute

CMY Cephamycinase

Col Colicinogenic

cpm Circulations per minute

CRO Ceftriaxone

CTX-M Cefotaximase

CV Crystal Violet

ddH_2O Double distilled H_2O

DNA Deoxyribonucleic acid

DTT Dithiothreitol

EDTA Ethylenediaminetetraacetic acid

ESBL Extended-spectrum β-lactamase

FOX Cefoxitin

Gen Gentamicin

HCD High energy collisional dissociation

HPLC High-performance liquid chromatography

hqSNV High-quality single nucleotide variants

IAA Iodoacetic acid

IMP Imipenemase

iNTS Invasive non-typhoidal *Salmonella*

IRIDA Integrated Rapid Infectious Disease Analysis

Kb Kilobase

KPC *Klebsiella pneumoniae* carbapenemase

LB Luria-Bertani

LC Liquid chromatography

LC/MS/MS Liquid chromatography with tandem mass spectrometry

MATE Multidrug and toxic compound extrusion family

MCP Methyl-accepting chemotaxis protein

Mem Meropenem

MFS Major facilitator superfamily

MIC Minimal inhibitory concentration

MRSA Methicillin-resistant *Staphylococcus aureus*

NAL Nalidixic acid

NARMS National Antimicrobial Resistance Monitoring System

NCBI National Center for Biotechnology Information

NDM New Delhi metallo β-lactamase

NGS Next-generation sequencing

NML National Microbiology Laboratory

NTS Non-typhoidal *Salmonella*

PRSA Penicillin resistant *S. aureus*

RND Resistance-nodulation-cell-division

rpm Rotations per minute

PBP Penicillin-binding protein

PBRT PCR-based replicon typing

PCR Polymerase chain reaction

pMLST Plasmid MultiLocus Sequence Typing

PMAxx™ Propidium monoazide-xx

PM Phenotypic microarray

RNA Ribonucleic acid

RTF Replication and transfer region

SDS Sodium dodecyl sulfate

SIX Sulfisoxazole

SMR Small multidrug resistance

SNV Single nucleotide variant

SPI *Salmonella* pathogenicity island

ST Sequence types

STR Streptomycin

SXT Trimethoprim/sulfamethoxazole

T3SS Type III secretion system

TBE Tris-borate-EDTA

TET Tetracycline

TIO Ceftiofur

Tm Melting temperature

TMAO Trimethylamine N-oxide

TMT Tandem mass tag

TRAMS Tool for rapid annotation of microbial SNPs

TSA Tryptic soy agar

UEB Urea exchange buffer

UV Ultraviolet

V/cm Volts/cm

VIM Verona integron encoded metallo β-lactamase

VRE Vancomycin-resistant *Enterococci*

VRSA Vancomycin-resistant *S. aureus*

WGS Whole genome sequencing

1. Introduction

This section describes the discovery and use of antimicrobials throughout history, as well as the concurrent existence of bacterial resistance to antimicrobials. It then focuses on antimicrobial resistance (AMR) in *Enterobacterales* and the mechanisms of resistance including plasmid transfer that are found in this family of Gram-negative bacteria. Finally, this section will describe *Salmonella enterica* and the importance of studying AMR in *S. enterica* serotype Heidelberg in Canada. Together, this information justifies the need for a greater understanding of the AMR mechanisms conferred via plasmids in *S. enterica* serotype Heidelberg.

1.1 Antimicrobial Use and Resistance

AMR existed in the natural environment before the implementation of antimicrobials as a therapeutic and is now a rapidly increasing problem in present global healthcare[1]. In the early 20th century, infectious diseases were the causes of approximately 800 deaths per 100,000 people every year[2]. After the discovery and use of antimicrobials in the late 1930s, the number of deaths from infectious diseases decreased by 8.2% per year over the next 14 years[2]. The development of AMR in bacteria is generally driven by selective pressure in the host due to antimicrobial use. Overuse of antimicrobials in animals and humans has led to increased selective pressure for antimicrobial-resistant bacteria, which can result in difficult-to-treat infections in humans and animals.

1.1.1 Use and Overuse of Antimicrobials

The emergence of AMR began before therapeutic use by humans, in fact, as early as 1924 researchers had already identified syphilis that was resistant to Salvarsan[3]. The official discovery of antimicrobials in the 1930s was followed by the "Golden Age" of antimicrobial discovery[4]. The use of sulphonamides and penicillin kick-started the regular usage of

antimicrobials and the search for new antimicrobial agents; however, widespread resistance among *Staphylococcus aureus* was apparent within the first decade of the first clinical trials of penicillin[4,5]. The combination of natural selection leading to AMR and the use of antimicrobials driving this development forward led to increasing resistance in bacteria; by the mid-1950s, 90% of tested strains of *S. aureus* were resistant to penicillin[3].

AMR makes treating infections difficult, lengthens hospital stays, and increases healthcare costs[3]. The use and overuse of antimicrobials increases the development of drug-resistant bacteria and the spread of these resistance genes among related bacteria. Unnecessary use of antimicrobials in human medicine includes: i) taking/prescribing antimicrobials for viral infections, ii) taking/prescribing the wrong type, dose, or duration of antimicrobials, iii) taking antimicrobials in ways other than how they were prescribed, and iv) taking leftover antimicrobials without a prescription or using someone else's antimicrobials[3]. Proper prescribing practices and consideration of antimicrobial stewardship, as well as patient education are key to ensuring that antimicrobial use is beneficial and can help to reduce the rates of AMR.

The use of antimicrobials is not isolated to human medicine, it is also very prevalent in agriculture. In livestock farming, antimicrobials are used for disease treatment, and sub-therapeutically for animal growth promotion, improved feed conversion efficiency (ex. the ability to turn the energy from feed into increased body mass or milk output), and antimicrobial prophylaxis[6]. Globally the regulation of antimicrobial use is quite varied, both in clinical and veterinary use of these drugs. In the Chief Public Health Officer of Canada's 2019 Spotlight report titled "Handle with Care: Preserving Antibiotics Now and Into the Future", it stated that an estimated 1 in 16 Canadians admitted to hospital will develop an infection from a resistance superbug and that a survey performed in 2016 indicated that 7 in 10 Canadians worry about the

risk of nosocomial infections[3]. The current situation of AMR in Canadian communities described by the Chief Public Health Officer of Canada's 2019 Spotlight Report indicated that methicillin-resistant *S. aureus* infections have increased by 60% since 2012[3]. In this report, it is stated that more than 50% of all gonorrhea infections are resistant to at least one antibiotic and that there has been a 5x increase in people carrying the bacteria resistant to carbapenems[3]. Researchers are finding it increasingly difficult to find novel antimicrobials at the rate that AMR is developing in bacteria and the need for antimicrobial stewardship has become critical. The recognition of the problem of AMR has led to antimicrobial stewardship initiatives across the globe including surveillance and education.

1.1.2 AMR in Enterobacterales

AMR is a serious global threat that affects human, animal, and environmental health[7]. While it is difficult to estimate the precise burden of AMR infections it is known that hundreds of thousands of lives are currently lost to AMR infections[8]. In 2014, the UK Prime Minister announced a Review on AMR, and the results of that review estimated that by the year 2050, 10 million people will die each year due to AMR infections[8]. As of February 2022, the Public Health Agency of Canada website (https://www.canada.ca/en/public-health/services/antibiotic-antimicrobial-resistance/antibiotic-resistant-illnesses-bacteria.html) currently has a list of six "Important antibiotic-resistant bacteria" that includes carbapenem-resistant *Enterobacterales*, *Escherichia coli*, and *Salmonella*[9]. Types of resistance genes that are commonly found among the *Enterobacterales* include those against penicillins, cephalosporins, fluoroquinolones, aminoglycosides, and more recently even some last-line antimicrobials including the carbapenems[10]. The incidence of resistance genes in *Enterobacterales* has been rising in past years as well as the co-occurrence of resistance genes leading to multidrug-resistant isolates or

"superbugs"[10]. Figure 1.1 shows a timeline of the discovery of antimicrobials by humans and the discovery/recognition of AMR in bacteria[10].

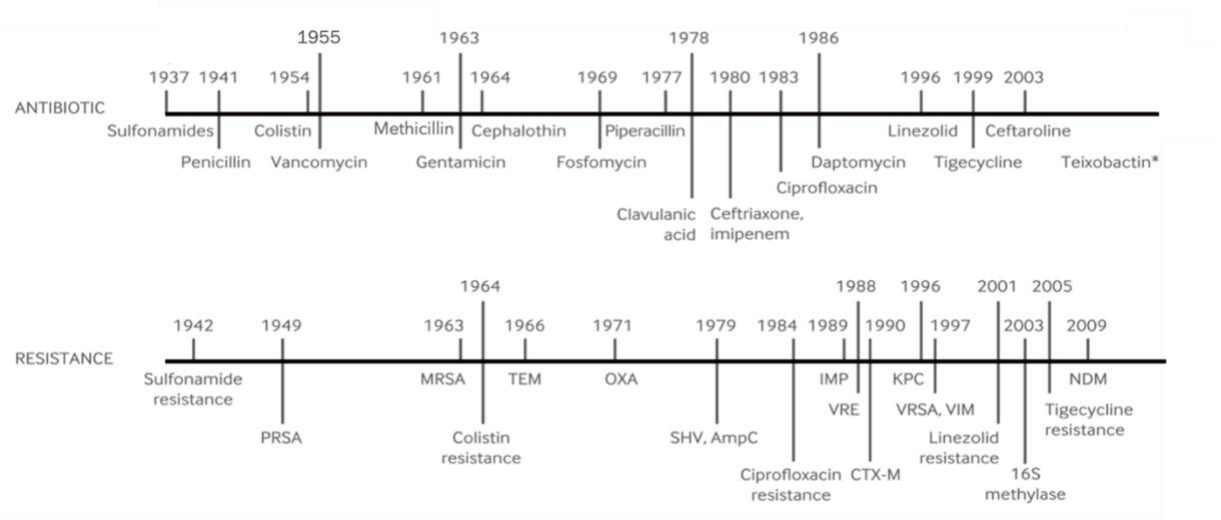


Figure 1.1. Timelines of the discovery of antibiotics and the discovery of antibiotic resistance[10]. Adapted with permission from Iredell et al., 2016[10]. AmpC; ampicillin hydrolyzing; CTX-M; cefotaximase; IMP; imipenemase; KPC; Klebsiella pneumoniae carbapenemase; MRSA; methicillin-resistant Staphylococcus aureus; NDM; New Delhi metallo β-lactamase; PRSA; penicillin-resistant S. aureus; TEM, SHV, and OXA; common and diverse groups of β-lactam hydrolyzing enzymes; VRE; vancomycin-resistant Enterococci; VRSA; vancomycin-resistant S. aureus, VIM; Verona integron encoded metallo β-lactamase.

*Not in clinical use

1.1.3 Mechanisms of AMR

There are many mechanisms that bacteria use to develop AMR, including the alteration and/or acquisition of genes that are specific to drug resistance and the utilization of structural components already present in bacteria. Some bacterial species employ multiple methods to achieve AMR; for example, fluoroquinolone resistance can occur due to three different biochemical routes[11]. These routes include mutations in genes encoding the target site of fluoroquinolones, over-expression of efflux pumps that extrude the drug from the cell, and protection of the fluoroquinolone target site by a protein designated Qnr[11]. Certain mechanisms of AMAR are more commonly found in particular species of bacteria, but many employ similar mechanisms such as efflux pumps, porins, and inactivating enzymes.

1.1.3.1 Efflux

Drug efflux is an important mechanism of drug resistance in Gram-negative bacteria such as *Enterobacterales*[12]. Efflux pumps allow microorganisms to regulate their internal environment by pumping solutes out of the cell, including toxic substances such as antimicrobial agents[12]. One of the first efflux systems described was discovered in the 1980s; it was the TetA efflux system used to pump tetracycline out of the cytoplasm in *E. coli*[11]. Since then, there have been 5 major families of antimicrobial-selective efflux pumps that have been characterized, including the i) major facilitator superfamily (MFS), ii) the small multidrug resistance family (SMR), iii) the resistance-nodulation-cell-division family (RND), iv) the ATP-binding cassette family (ABC), and v) the multidrug and toxic compound extrusion family (MATE)[11]. One of the most well-studied efflux pump systems is the AcrAB-TolC in *Enterobacterales* which belongs to the RND family[11]. The AcrAB-TolC system is composed of three proteins: the AcrB transporter protein, the AcrA linker protein, and the TolC protein channel located in the outer membrane[13]. Efflux systems are believed to play a large role in AMR, and there has also been evidence that

they play a role in quorum sensing or cell-to-cell signalling[12]. Quorum sensing has been shown to play a role in biofilm formation and the expression of virulence factors[12]. Efflux pumps play a role in transporting signal molecules across the cell membrane which can promote the activity of quorum sensing which in turn can exert an effect on biofilm formation and other virulence factors which contribute to AMR[12].

1.1.3.2 Porins

A defining feature of Gram-negative bacteria such as *S. enterica* is the presence of an outer membrane which contains proteins called porins[14]. Porins are outer membrane proteins that act as entry channels and play a role in permeability of the bacterial cell membrane through changes in the number of porins and capacity for movement through these channels[15]. They play a role in AMR by modulating the compounds that can pass through the outer membrane[14]. The change in the structure, number, and type of porins that are present in the outer membrane in response to various conditions such as oxidative stress or anaerobiosis can change the permeability of an antimicrobial[16]. These alterations can change the permeability of antimicrobials and therefore increase the levels of AMR above baseline in the bacterium[17]. Common porins that are found in *S. enterica* include OmpC which regulates cephalosporin resistance and OmpF, which regulates resistance to chloramphenicol and imipenem[15].

The outer membrane of Gram-negative bacteria is composed of a highly hydrophobic lipid bilayer that is filled with a mosaic of proteins[18]. Small hydrophilic drugs such as β-lactams can use porins as a gate to the interior of the cell while other drugs can diffuse freely across the lipid membrane[18]. Another porin protein that has been discovered in *Enterobacterales* species is OmpX. This porin has been shown to play a role in virulence pathways such as biofilm formation, responding to environmental stress, and downregulating other porin proteins[19]. The

diverse roles of porin proteins demonstrate their important role in the development and spread of AMR in *Enterobacterales*.

1.1.3.3 Inactivating Enzymes

One method of AMR is the reduction in the effectiveness of a drug through the action of an enzyme. Enzymes involved in mechanisms of AMR can be subdivided into four categories as outlined in Figure 1.2; i) enzymes that are the targets of antimicrobial drugs, ii) enzymes that modify the cellular targets of antimicrobial drugs, iii) enzymes that metabolize antimicrobial drugs and iv) enzymes that modify antimicrobial drugs[20]. Concerning the latter, β-lactamases in the *Enterobacterales* are important contributors to AMR. Either chromosomally- and/or plasmid-encoded β-lactamases function by hydrolyzing the amide bond of the four-membered β-lactam ring found in drugs such as penicillin and cephalosporins as shown in Figure 1.3[20]. These AMR enzymes mainly emerge by two mechanisms; i) the occurrence of novel mutations in the genes of pre-existing enzymes and ii) the emergence of enzymes with a new structure[20].

β-lactamases are often localized on mobile genetic elements and thus are a large contributor to the rapid spread of resistant bacteria, in fact, bacteria carrying up to eight β-lactamase genes at once have been detected[20]. The most common class of β-lactamases are those belonging to class A including CTX-M, TEM, and SHV lactamases[17,20,21]. When certain mutations occur, they can form extended-spectrum β-lactamases, which have broader drug recognition ranges they are active against[20]. The emergence of bacteria that are resistant to all β-lactam antimicrobials is of great global concern as infections caused by these bacteria are particularly difficult to treat and thus capable of causing significant illness.

1.1.3.4 Antimicrobial Target Modification

Alteration of the target sites in bacteria for antimicrobials is a commonly observed method of resistance[22]. Target sites for antimicrobials often have a role in microbial growth and survival.

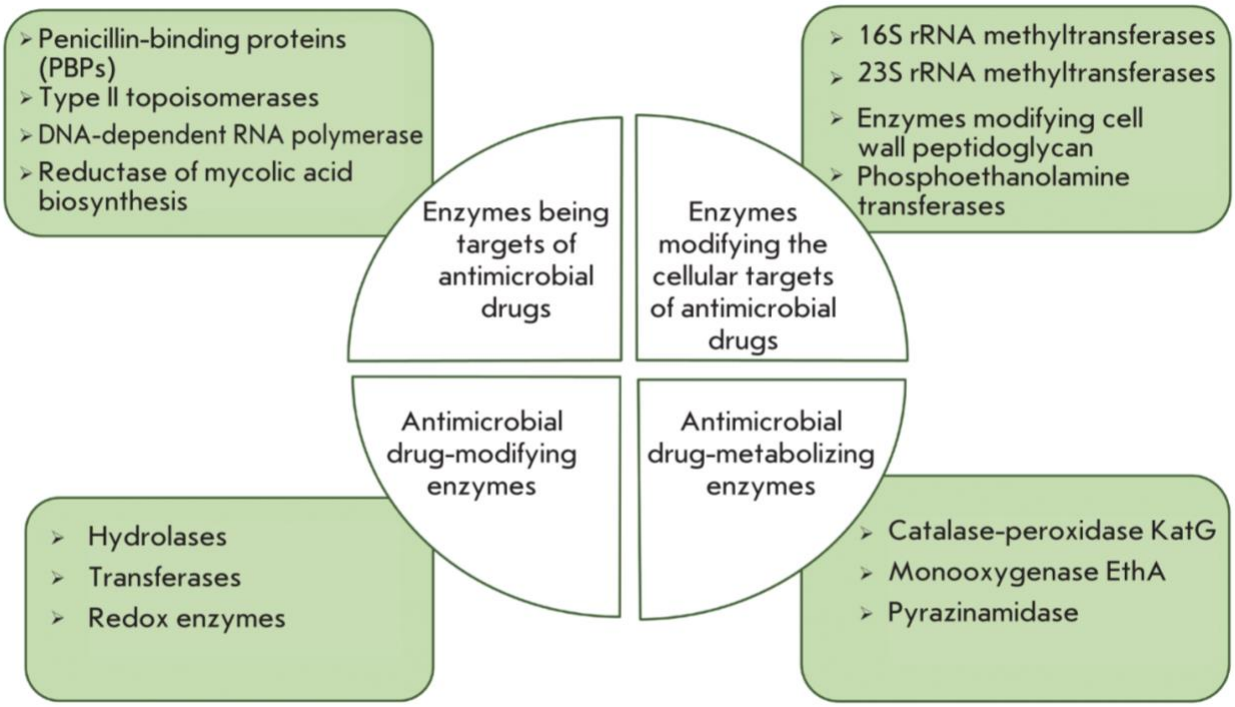


Figure 1.2. Types of enzymes involved in antimicrobial resistance[20].

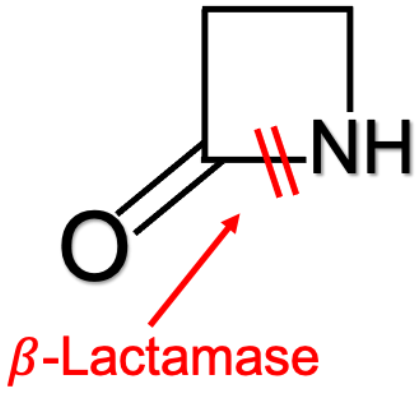


Figure 1.3. Hydrolysis of the amide bond in the β-lactam ring by β-lactamases.

Binding to these sites interferes with these functions which can lead to lethality or difficulties with growth[22]. To avoid this interference, bacteria have evolved various methods to prevent the binding of antimicrobials to their desired target within the host; these methods include protection of the target and modifications of the target site to prevent binding affinity[11].

Target protection is employed by some bacteria and examples of drugs affected by this mechanism include tetracycline, fluoroquinolones, and fusidic acid[11]. One target protection mechanism described in Gram-negative bacteria is the removal of tetracycline by its binding to sites of TetO and TetM; both proteins protect the bacterium from the effects of the drug[11]. A second protective function of the resistance conferred by the protein TetO is to compete for the binding site of tetracycline, thus preventing the binding of the drug[11]. Another target protection mechanism example found in some Gram-negative bacteria is the quinolone resistance protein Qnr, which is plasmid-mediated[11]. The Qnr protein acts as a DNA gyrase mimic/homologue that competes for the DNA binding site of the DNA gyrase and topoisomerase IV[11]. This interaction protects the legitimate DNA gyrase drug target by reducing the opportunities for the quinolone molecule to form a gyrase-cleaved DNA-quinolone complex that is lethal for the bacterium[11]. Target protection mechanisms often only confer low levels of resistance, but in combination with other resistance mechanisms present in the same bacterium they can promote the emergence of highly resistance isolates[11].

Antimicrobial target modification is a more common mechanism of AMR and has been found to affect almost all families of antimicrobial compounds[11,22]. Target changes affecting antimicrobials include point mutations in the genes encoding the target site, enzymatic alterations of the binding site, and replacement or bypass of the original target[11]. In Gram-negative species, one of the most common forms of resistance is β-lactamase-mediated

resistance; however, increasing forms of non-β-lactamase-based resistance to β-lactam drugs is seen[17]. The main target site for β-lactamases are the penicillin-binding proteins (PBPs); alterations in PBP target sites can alter the effectiveness of these drugs[17,23,24]. PBPs are responsible for peptidoglycan synthesis which is important for the structure of the cell wall[24]. The reduced affinity via modification of PBPs can prevent or reduce the binding of β-lactam drugs; thereby, reducing the effectiveness of these drugs. Antimicrobial target modification genes can be encoded on horizontal gene transfer-mediated elements (plasmids, integrons, phage, and transposons), making them very important in AMR[23].

1.2 Plasmids

In general, plasmids are double-stranded, circular DNA molecules capable of autonomous replication[25]. Plasmids are found in bacteria as an extrachromosomal element (although they are capable of chromosomal integration) and generally do not carry genes essential for growth[25]. The length of a plasmid can vary from a few to several hundred kilobase pairs; for example, the size of the largest known plasmid pSCL4 has a length of 1.8 Mbps[26]. Plasmids contain many genes including those for their transfer, stable inheritance, virulence factors, toxin production, and AMR[27]. Due to the vast diversity of plasmids, many types and families of plasmids have been identified, as well as many uses of plasmids for scientific endeavours.

Plasmids initially became a topic of interest when it was discovered that *Bacillus anthracis*, the causative agent of anthrax, harboured two plasmids that conferred virulence properties to this bacterium[28]. The first well-studied plasmid types were AMR (R) plasmids in Japan, colicinogenic "Col" plasmids in Belgium, and fertility "F" plasmids in Paris[28]. The foundations of understanding plasmid biology were laid by these studies on each of these types

of plasmids in *E. coli* and other related *Enterobacterales*. It was soon after the rigorous studies of plasmids began that it was discovered that some plasmids, such as F-type plasmids, were able to assume both autonomous and integrated states, an important feature in the designation of plasmid types. Studies of this kind determined that R plasmids tend to remain extrachromosomal in nature, and indicated that R plasmids harboured conjugative properties localized to a region coined as the "RTF" or replication and transfer region[28]. This discovery showed that the resistance regions of R plasmids were genetically distinct from the transfer region[28].

While many advances in the studies of plasmids were made when plasmids were first discovered and identified, further investigation using more recent sophisticated methods such as WGS has allowed for even greater elucidation in the study of plasmids. An increasing number of plasmids have been identified and characterized over time in Gram-negative and Gram-positive bacteria, and the diversity seen amongst these plasmids is vast. As plasmids were further studied, the use of plasmids as a scientific tool also came into practice, and some plasmids have been modified to be used as important molecular biology cloning vectors. Plasmids have many useful features, and the next sections will investigate a few of them to exemplify the importance of studying plasmids.

1.2.1 Plasmid Classifications

Finding a classification scheme is important for the study of any organism as it aids in the understanding of its distribution and relationship to other organisms. The classification and understanding of plasmids is important for many fields of study, particularly health-related research to examine and relate their clinically relevant traits to drug resistance and virulence factors[27]. The concept of classifying plasmids based on replication control was finally chosen and is known as incompatibility groups. This was based on the fact that plasmids with the same

replication control are not able to coexist in a bacterial cell, while plasmids with different replication controls are usually compatible[27]. Plasmid partitioning mechanisms are also a factor in the Inc group classification; but in general, plasmids featuring the same partitioning mechanism will also share the same replication control mechanism.

Plasmid incompatibility was first described in an F plasmid in the early 1960s, as it was observed that cells carrying integrated and autonomous F plasmids were unable to replicate other autonomous F plasmids[27]. In 1971, Hedges and Datta proposed the classification scheme that is used presently, incompatibility "Inc" groups[25]. The first Inc groups described were: IncI, characterized by the ability to produce type I pili susceptible to phage Ifl; IncN, plasmids related to plasmid N3 which are susceptible to phage Ike; IncF, plasmids producing type F pili susceptible to phage Ff; and IncP, RP4-related plasmids susceptible to the PRR1 phage[25]. To date, there are 27 Inc groups recognized in *Enterobacterales* by the Plasmid Section of the National Collection of Type Cultures in London, United Kingdom.

Testing for incompatibility involves the introduction of a plasmid into a strain with a plasmid, to monitor its genetic markers, and examine the progeny to determine which plasmids are present. Complications in this type of classification do exist and arise when a plasmid does not have a suitable selection marker or does not contain a suitable means of transfer[27]. These complications, as well as the lack of specificity of this method, have led to the formation of other forms of classification, including replicon typing based on the annotation of replication control genes within sequenced plasmids[25]. Autonomous replication control is an important feature of plasmids that takes place under adequate growth conditions in a host cell. The genes required for autonomous replication include *cop* and *inc* which control replication initiation, and *rep* genes required for replication and copy control (i.e., the maximum number of plasmid copies within the

host cell). Basic replicons including these genes can be ligated *in vitro* to a selective marker to form mini-plasmids that will replicate autonomously with characteristics of the parental plasmid[27]. This method was successful in providing classification for both conjugative and non-conjugative plasmids; however, its lack of specificity, particularly in plasmids with multiple replicons, led to the development of the current method of plasmid typing.

Polymerase chain reaction (PCR)-based replicon typing (PBRT) is a method that has been the standard since 2005 for plasmid typing. This method is particularly useful for targeting the major plasmid families that are found in *Enterobacterales*, although it does also have limitations due to its reliance on incompatibility groups which can fail to identify novel plasmid replicons[25]. While these few methods can selectively identify plasmid families, the best way to ensure proper typing is through analysis of the full plasmidic DNA sequence; WGS combined with tools such as PlasmidFinder and in silico plasmid MultiLocus Sequence Typing (pMLST) are useful for plasmid identification. Classification, while complicated, is still very important to understanding plasmids, and further precision methods of identification and classification will need to be determined.

1.2.2 Plasmid Maintenance

To ensure the maintenance of a plasmid in a host, plasmids have developed systems to ensure that their host cannot survive without them. Addiction systems are encoded by plasmids to produce a toxin/antitoxin that will kill cells that have lost their plasmids as shown in Figure 1.4[29]. While addiction systems are diverse, utilizing three general mechanisms to produce interactive toxin-antitoxin pairs: protein-regulated systems, antisense RNA-regulated systems, and restriction/modification systems[29]. The nature of these systems all possess similar properties including toxins and antitoxins encoded by the same operon with the antitoxin encoded

upstream. The product of the toxin is long-lived while the antitoxin is short-lived, and when the toxin and the antitoxin interact the antitoxin is degraded by bacterial proteases[29]. These traits work together to ensure that the toxin is produced and combatted while the plasmid is present, but with the loss of the plasmid, the antitoxin will not remain in the cell while the toxin will, ultimately leading to the death of the cell. This manipulation results in the reliance of the bacterial cell to maintain the plasmid so that the cell can continue to survive.

Another method of plasmid maintenance found in bacterial cells is the conferring of AMR genes. Many plasmids carry AMR genes which the bacteria can pass among bacterial species and disseminate across the globe via horizontal genetic transfer mechanisms. AMR genes can coexist on plasmids with addiction systems, as well as coexist with multiple types of AMR genes. One example of resistance genes that are conferred and spread amongst bacteria are the extended-spectrum β-lactamases (ESBLs) which were first reported in 1985[29]. ESBLs can hydrolyze the amide bond found in the β-lactam ring of many β-lactam-based antimicrobials. ESBLs can be found on large plasmids which also carry genes for resistance to other antimicrobials such as aminoglycosides, trimethoprim, sulphonamides, tetracyclines, and more recently, fluroquinolones[30]. These resistance genes are able to perpetuate the maintenance of the plasmid by conferring resistance and permitting survival in the presence of antimicrobial conditions, however, to pass these plasmids among bacteria, horizontal genetic transfer systems are needed which will be discussed below.

Plasmid transfer can be achieved through a process known as bacterial conjugation which involves the transfer of DNA between bacteria through structures known as sex pili[31]. Conjugation is an extremely important process in *Enterobacterales* as it allows adaptation to various environmental niches through the transfer of genes such as those for AMR hydrocarbon

degradation, pathogenesis, and virulence[31]. There are three main components of the conjugative transfer system which are encoded within the *tra* operon of plasmids; the transferosome, the relaxosome, and the coupling protein, which connects the other two. The transferosome is a transmembrane pore through which DNA is transferred during conjugation, and the relaxosome is a complex of DNA-binding proteins that unwind DNA into a single strand for transfer, as well as signal the initiation of transfer to the transferosome[32].

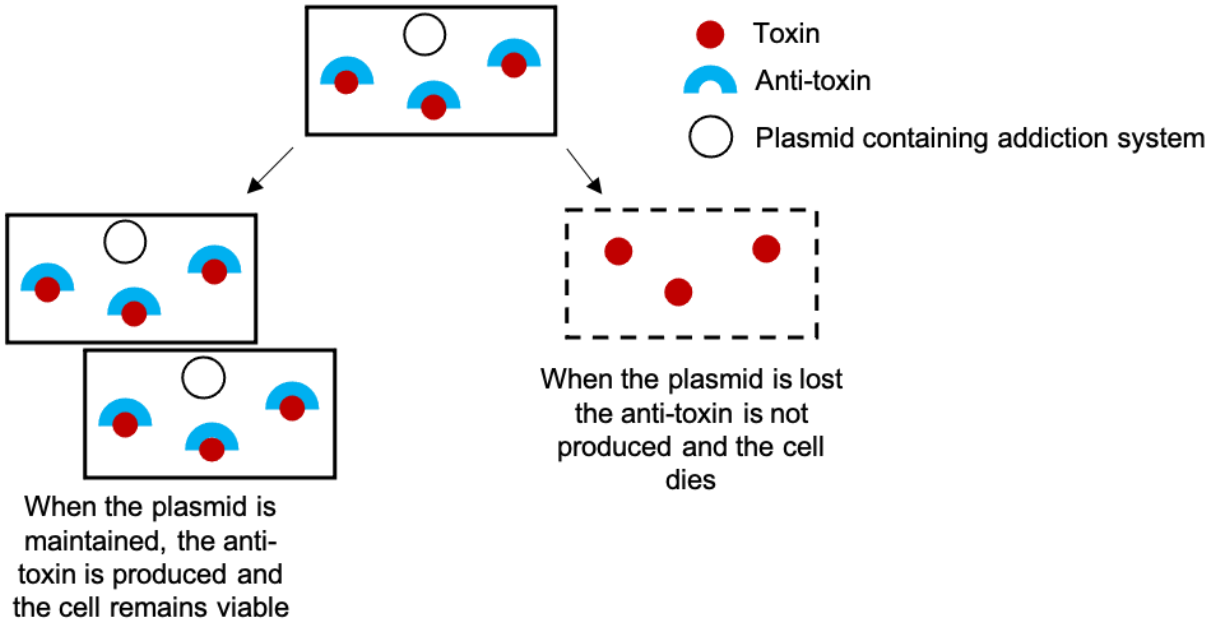


Figure 1.4. Depiction of plasmid addiction systems adapted from Tsang J[29].

Conjugative plasmids found in Gram-negative bacteria generally belong to the IncI, IncP, or IncF families, and conjugation itself is mediated by either collision or the sex pilus[31]. As well, all conjugative systems currently known in Gram-negative bacteria possess an elaborate pilus and two signature nucleoside triphosphate-utilizing proteins. The transferosome found in the conjugative transfer system is a type IV secretion system that uses a type IV pilus to facilitate mating-pair stabilization between bacterial cells, creating a bridge across which the plasmid is transferred. The transfer of plasmids containing useful or unknown genes selects for the survival of the plasmid and often the survival of the host to ensure maintenance.

Finally, a feature of plasmids that not only contributes to maintenance but also confers a selective advantage to its host is the possession of virulence genes. The first virulence genes transferred by plasmids were noted in *B. anthracis* and are the factors behind the high level of pathogenicity possessed by this bacterium. This example that was first seen in *B. anthracis* turned out to be true for many bacteria, particularly *Enterobacterales.* Virulence plasmids are a common finding among the *Enterobacterales* and usually range from 60-200 kb in size with low copy numbers[33]. These plasmids are often essential for the pathogenicity of the organism and members of the same strain without the plasmid are merely commensal organisms. Virulence factors that can be conferred include adhesion genes, secretion systems, toxin production, and regulatory genes. The acquisition of these plasmids can greatly enhance the ability of its host to infect and outcompete other organisms and contributes to the retention of the plasmid.

1.2.3 Plasmids in *Enterobacterales*

Some plasmids are able to replicate only in closely related hosts, while others have acquired a broader host range. In the *Enterobacterales* family, plasmids carrying ESBLs are of increasing relevance as the efficacy of antimicrobials decreases. Studies have shown that the

highly virulent *E. coli* ST131 clone is highly associated with the spread of the *bla*$_{\text{CTX-M-15}}$ ESBL gene through the horizontal transfer of an IncF plasmid[25]. These IncF plasmids are unique in the sense that while belonging to the same family, they are quite varied in size (50-200 kb), as well as containing different numbers and combinations of replicons[25]. While these plasmids are commonly found in ST131, they are not exclusive to it as other members of *E. coli* and other *Enterobacterales* such as *Salmonella enterica* have been isolated with this plasmid. Another commonly found plasmid within *Enterobacterales* is the IncI1 plasmid found in *S.* Heidelberg containing a *bla*$_{\text{CMY-2}}$ ESBL. In a study of *S.* Heidelberg isolates from Quebec in 2012, it was found that all isolates that carried AMR to cefoxitin possessed the same IncI1 plasmid. These examples both indicate the importance of the horizontal transfer of genes via plasmids in the dissemination of AMR among *Enterobacterales.* The plasmid families and genes that are passed among the *Enterobacterales* are incredibly varied and as demonstrated here, have a high relevance to healthcare and the spread of clinically relevant genes.

1.2.4 Effects of Plasmids in Gram-negative Bacteria

Plasmids contain genes for self-survival, maintenance, replication, drug resistance, toxin production, altering chromosomal gene expression, and many genes with unknown functions. Plasmids are generally non-essential to their hosts, but they can provide a significant advantage or burden to their host bacterium[34]. Due to the large variety of functions that plasmids are capable of, their maintenance is highly regulated and the energy burden can be quite large[34]. Aside from resistance genes, plasmids can influence the fitness of their host through the expression of various genes and host factors that will have effects on fitness and growth, virulence, and chromosomal gene expression.

1.2.4.1 Fitness and Growth

Plasmids can exert their effect on host fitness and growth through gene expression or through the energy burden of hosting a plasmid. Alongside the effects that a plasmid may exert on its host, the composition of the growth medium, phase in the growth cycle, temperature, and other external effects can also play a role in bacterial fitness and growth[35]. A study by Cheah et al. in 1987 examined the effects of recombinant plasmid size on cellular processes and growth in *E. coli*[35]. The study hypothesized that an increasing amount of genetic material would decrease the growth rate of host cells and lower the plasmid copy number[35]. This study showed that with increasing plasmid size there was a decrease in maximum cell density in most strains, a decrease in plasmid copy number, and a decrease in growth rate[35]. The mechanism of this burden is likely due to the use of machinery for the replication of plasmid genetic material, and the interactions between the genes of the plasmid that have deleterious interaction with bacterial genes[36].

Another example of the effect plasmid genes can have on fitness and growth are the addiction systems that were mentioned previously. Addiction systems are composed of toxin and antitoxin proteins that are capable of killing the host cell if their plasmid is no longer maintained[29]. These addiction systems exert their toll on the growth of bacteria in two ways: i) through the use of host machinery, and ii) through the post-segregational killing of cells via toxin interaction[29]. Toxins from plasmid addiction systems or those otherwise carried on plasmids are thus able to decrease bacterial growth or to even kill their host bacterium[29]. A final important note to make is that systems that may negatively affect the fitness of bacteria are often found together with genes that may increase the fitness of bacteria such as AMR genes.

1.2.4.2 Virulence

The expression of virulence genes on plasmids can be very important for the fitness and survival of their host in varied environments. Virulence plasmids are often low copy number and can be transferred via conjugation between bacteria[37]. Virulence plasmids are commonly found in the *Enterobacterales* family and can confer a broad range of characteristics to their host[37]. Plasmid-encoded virulence genes can play a critical role in pathogenesis through complex cellular processes such as adhesion, invasion, colonization, and modulation of host immune response as shown in Figure 1.5[37]. In *S. enterica*, virulence plasmids are quite varied, but many of their virulence plasmids contain the virulence locus *spvRABCD*[37]. This particular locus enhances bacterial replication within host cells, particularly in macrophages, and contributes to systemic infection[37]. Although this plasmid virulence locus has a variable sequence between serotypes of *Salmonella*, its constant presence in various serotypes suggests its importance to the species[37]. Other examples of virulence genes that are found on plasmids in *S. enterica* include *pef* which encodes fimbrial structures that mediate adhesion, *rck* which confers resistance to complement killing, and *rsk* which mediates resistance to serum killing by the host[37]. The contribution of plasmid virulence factors that can increase the pathogenesis and survivability of their host help to increase the fitness of the host and allow the host to be benefited by maintaining the plasmid[37].

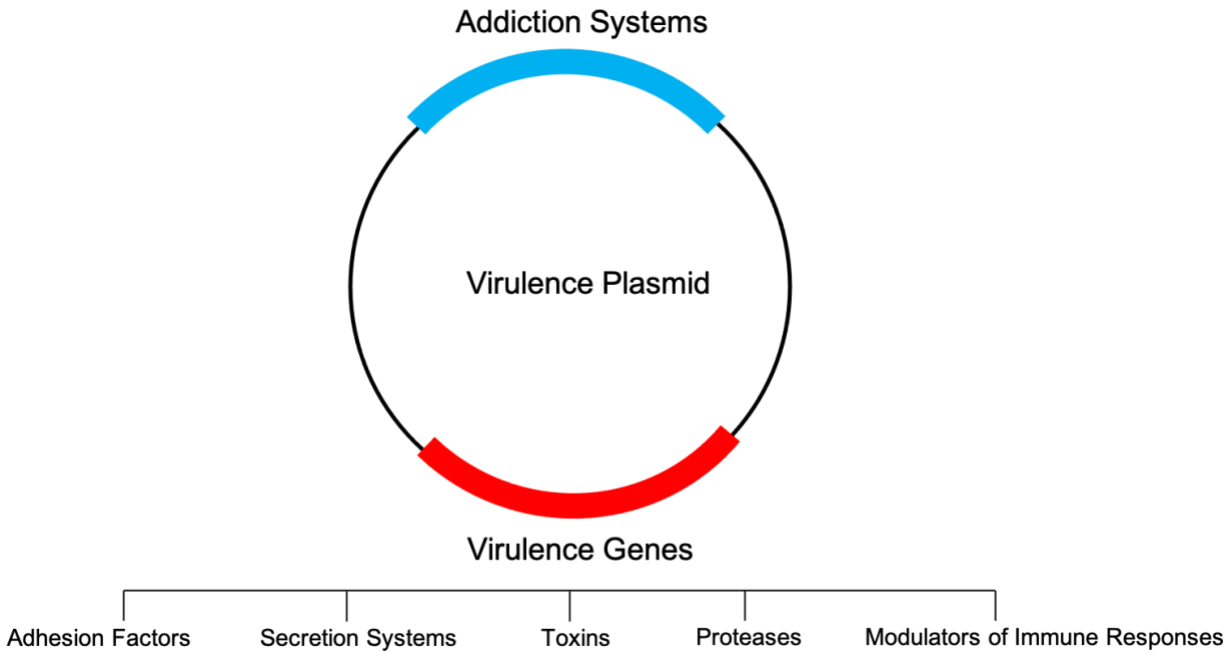


Figure 1.5. Common features of virulence plasmids adapted from Pilla et al[37].

1.2.4.3 Chromosomal Gene Expression

Since plasmids were discovered, it was clear that chromosome regulation of plasmids occurs, but the regulation of the chromosomal genes by plasmids has been explored to a much lesser extent[38]. Recent studies using next-generation sequencing (NGS) have been used to analyze plasmidic and chromosomal adaptive mutations.

In a study by Harrison *et al* in 2015, it was shown that plasmids were able to cause compensatory evolution in their host bacterium, *Pseudomonas fluorescens*[39]. Harrison et al found that the mega-plasmid pQBR103 was able to target the *gacA/gacS* genes and downregulate their expression to compensate for the fitness burden of the plasmid[39]. While phenomena such as this are still underexplored, compensatory evolution could help to explain the widespread occurrence of plasmids despite their great fitness burden[39,40]. This particular study has led to further exploration of the concept of compensatory evolution and mathematical models have been developed to examine this possibility[41,42]. It is very likely that there are further effects that plasmid-encoded genes have effects on host chromosomal gene regulation and that further research in this area will bring greater understanding to this influence.

1.3 *Salmonella enterica*

Salmonella enterica is a diverse species of rod-shaped Gram-negative facultative anaerobes that are capable of causing disease[43]. This species consists of more than 2600 serotypes which can be divided into typhoidal and non-typhoidal *Salmonella* serotypes (NTS) based on surface antigens[44]. All serotypes of *Salmonella* are capable of causing disease in humans even though a few serotypes are host specific; for example, *Salmonella enterica* serotype Dublin is highly host-adapted to cattle[45]. When host-specific serotypes cause disease in humans, it is often invasive and can lead to severe symptoms and even death[45].

S. enterica serotype Heidelberg is an invasive non-typhoidal *Salmonella* (iNTS) that is the third most frequently isolated serotype in humans in Canada[46]. In a 2008 study conducted on the prevalence of *S.* Heidelberg, it was found that this serotype is common in retail poultry and meats and this serotype includes clones of multi-drug resistant strains[47]. *S.* Heidelberg is capable of causing salmonellosis, which is a type of foodborne poisoning caused by ingestion or contact with food or drink that has been contaminated with *S. enterica*[47]. Salmonellosis is capable of causing extraintestinal infections and severe septicemia which leads to an estimated 1,000,000 illnesses and 380 deaths per annum in the United States[48,49]. Treatment for *Salmonella* infection can include electrolyte replacement in severe cases due to loss of nutrients and hydration from diarrhea. Routine antimicrobial treatment is not recommended for mild cases due to the selective pressure for AMR it causes. However, in young children, the elderly and immunocompromised patients, antimicrobial therapy is used. The first line of antimicrobial treatment for adults includes fluoroquinolones such as ciprofloxacin or levofloxacin, followed by trimethoprim-sulfamethoxazole, cefixime, and azithromycin[50].

S. Heidelberg continues to be a burden to health and well-being in Canada and the United States. Increasing levels of AMR in *S.* Heidelberg are particularly troubling with resistance to first and second-line treatment drugs. These next sections will examine the pathogenesis, resistance, and relevance of *S.* Heidelberg and highlight the importance of further studies of this serotype.

1.3.1 Pathogenesis and Virulence of *S. enterica*

Many serotypes of *Salmonella* are host-specific and the course of infection depends on factors such as the inoculation dose and the immune status of the host[43]. *Salmonella* commonly colonizes poultry, including chickens. Birds harbouring many *Salmonella* serotypes are

asymptomatic but can convey infection to humans. Salmonellosis is spread via the fecal-oral route and can cause foodborne outbreaks. After ingestion of contaminated food or water, *Salmonella* passes through the stomach and has to counterbalance intestinal peristalsis to adhere to the gut of the host[51]. Common symptoms of salmonellosis include nausea, vomiting, fever, chills, and abdominal pain. Some factors that aid in infection are the varied virulence factors that are found among serotypes; these will be described below.

Salmonella species possess many virulence factors including adherence factors, toxins, and flagella. Adherence factors are cell-surface components of bacteria that can facilitate bacterial adhesion to a host. Bacterial adhesins help to gain access to an intracellular niche within the host and can increase survival by residing within macrophages or by evading antimicrobials[52]. Host adhesion is essential during pathogenesis to trigger biofilm formation or protein translocation which can lead to host cell invasion and systemic dissemination of the bacteria[51]. *S.* Heidelberg carries 99 gene clusters that are associated with adhesion including the fimbrial operons *fimAICDHF* (type 1 fimbriae), *lpfABCDE* (long polar fimbriae), and *agflcsgABCEFG* (thin aggregative fimbriae). Fimbriae are appendages that are found on many Gram-negative bacteria that mediate infection of host cells[51]. *Fim* fimbriae are characterized by mannose-sensitive hemagglutination and binding to host cells[51]. The functions of the various subunits of the type 1 fimbria work together to bind the host cell to facilitate invasion. Long polar fimbriae genes result in the formation of structures similar to type IV fimbriae and play a role in the adhesion of *S.* Heidelberg to Peyer's patches[51]. Peyer's patches are small areas of lymphatic tissue found in the small intestine that are considered possible sites of entry for *Salmonella* to cause infections, and therefore the *lpf* gene cluster can be very important in determining the virulence of *Salmonella*. Finally, thin aggregative fimbriae are structures that are

morphologically distinct from type 1 and long polar fimbriae and are assembled via the nucleation-precipitation pathway. These fimbriae lead to auto-aggregation as well as biofilm formation and adhesion to various surfaces[51].

Non-fimbrial adhesion factors are also encoded within the *S.* Heidelberg genome, and these are generally related to biofilm formation and adhesion to abiotic surfaces. Non-fimbrial adhesion factors in *S.* Heidelberg include the proteins MisL, RatB, ShdA, and SinH[52]. MisL and ShdA are monomeric auto-transported adhesins with poorly researched functions. ShdA has been shown to bind to fibronectin and has indicated importance in intestinal adhesion[51]. MisL is encoded by a gene within *Salmonella* pathogenicity island 3 (SPI-3). Like ShdA, this poorly described protein has been shown to contribute to bacterial shedding and intestinal colonisation[51].

Toxins are proteins that are produced by bacteria that interfere with host functioning in some detrimental way. Isolates of *S.* Heidelberg have been found to carry putative hemolysin, hemolysin-coagulated, and hemolysin expression regulator proteins[52]. The mechanism of action of hemolysin itself is unknown; however, it has been shown to contribute to virulence. Another toxin that has been found in *S.* Heidelberg is colicin; a protein expressed by some gram-negative bacteria that functions to inhibit the growth of one or more bacterial species by promoting the formation of bacterial cell lesions whilst protecting these lesions for itself[53]. Gene clusters encoding the colicin-binding catecholate siderophore receptor, its uptake protein, colicin Ia, the corresponding immunity protein, and the colicin V production protein were all found in a 2015 study examining non-typhoidal serotypes of *Salmonella*[52].

S. enterica is a motile species of bacteria via the flagella they possess. At least 40 flagella-associated proteins can be found in all isolates of *S.* Heidelberg, including an N-terminally truncated version of FlgE, a flagellar hook protein, which is unique to this serotype. The flagellum is a complex apparatus found in many bacteria[52]. The principal subunit of the flagella is encoded by the structural flagellin gene *fliC* in *S.* Heidelberg which plays a role in innate immunity as an antigen of the adaptive immune response[54]. As well, flagella can function as adhesins and aid in host invasion. The many virulence factors including the few that are named here all play important roles in the virulence and pathogenesis of *S.* Heidelberg infection in humans. These factors combined with their defence against modern medicine are the reason this serotype poses such a severe threat to human health.

1.3.2 Sequence Variability in *S. enterica*

S. enterica genome size and genomic features vary greatly among serotypes. The Heidelberg genome size varies around an average of 4.75Mbp and carries an average G+C content of 52.91%. There is an average of about 4596 coding DNA sequences per *S.* Heidelberg genome[55]. A 2017 study analyzing whole genome sequences of 113 cefoxitin-resistant and susceptible isolates of *S.* Heidelberg from Quebec in 2012 found that many Heidelberg isolates carried large plasmids that confer AMR. All plasmids that were found in this study were determined to belong to plasmid incompatibility group IncI1 and carried 95-99% identity to a previously isolated plasmid found in *S.* Kentucky (pCVM29188_101)[46]. Transmission of mobile genetic elements such as insertion sequences and plasmids are common among *S.* Heidelberg isolates and leads to the genetic variability of this serotype.

1.3.3 Treatment of *S. enterica*

Non-typhoidal *Salmonella* can cause gastroenteritis with symptoms of diarrhea, abdominal cramping, and fever[50]. The first step in the treatment of *S. enterica* involves the diagnosis, which is done through the isolation of the pathogen in stool cultures or in the case of bacteremia or severe illness, through blood cultures[50]. Laboratory isolation can involve overnight enrichment broth incubation, Gram-staining, and/or nucleic acid amplification tests[50]. Once *S. enterica* has been identified as the cause of illness and susceptibility results have been determined, treatment can ensue. Treatment of *Salmonella* gastroenteritis generally involves supportive management with fluids to avoid dehydration, and antimicrobial therapy if needed[50]. Antimicrobial therapy is indicated in neonates, the elderly, the immunocompromised, and when the illness is severe[50]. The most commonly used agents to treat *S. enterica* are fluoroquinolones (e.g. 500mg ciprofloxacin orally twice daily), but other appropriate antimicrobial choices include trimethoprim-sulfamethoxazole, cefixime, or azithromycin[50]. The incidence of antimicrobial-resistant isolates of *Salmonella* has been increasing in past years which has led to increasing difficulty with treatment[56]. If a *Salmonella* infection has been found to be resistant to first-line antimicrobials, such as ciprofloxacin, then antimicrobial susceptibility testing can be done and 3rd generation cephalosporins such as cefotaxime are often used. *Salmonella* infections are often self-limiting and resolve on their own and if needed, antimicrobial treatment is generally effective in resolving the illness.

1.3.4 *Salmonella enterica* serotype Heidelberg

In Canada, *Salmonella enterica* serotype Heidelberg is the third most frequently isolated serotype in humans and is often more invasive than other non-typhoidal serotypes[46]. In a 2008 study conducted on the prevalence of *S. enterica* serotype Heidelberg, it was found that this

serotype was common in retail poultry and meats and this serotype includes clones of multi-drug resistant strains[47]. In this study, we hope to further understand how IncI1 plasmids that contain the *bla*$_{\text{CMY-2}}$ gene influence the fitness of an *S.* Heidelberg.

1.3.4.1 AMR in *S.* Heidelberg

S. Heidelberg contains clones of multi-drug resistant strains including resistance to third-generation cephalosporins[46]. A study observing *S.* Heidelberg AMR from 2002-2006 showed that 67% of Heidelberg isolates from humans and poultry were resistant to at least one microbial agent and 16.4% of the isolates showed resistance to at least 5 antimicrobials through antimicrobial susceptibility testing[47]. At the time of this study, all isolates were shown to be susceptible to ceftriaxone; however, in a study of *S.* Heidelberg isolates from 2012 in Quebec, 57.5% of isolates examined were shown to be resistant to ceftriaxone[46,47].

Four major mechanisms confer AMR to bacteria; efflux, porin alterations, alteration of antimicrobial target sites, and finally, the production of enzymes that degrade antimicrobials[57]. The production of enzymes known as β-lactamases and extended-spectrum β-lactamases are likely the most important mechanism of resistance in *S.* Heidelberg as these confer resistance to the most commonly prescribed treatments for ciprofloxacin-resistant *Salmonella* infection[57]. β-lactamases confer resistance by hydrolyzing the amide bond in the four-membered β-lactam ring of antimicrobials such as penicillin and ampicillin and thus render it inactive[20]. While extended-spectrum β-lactamases (ESBLs) function in the same way, they are also able to hydrolyze broad-spectrum cephalosporins such as ceftriaxone[1].

As described previously, AMR is often conveyed via genes carried on plasmids. The plasmidic cephamycinase CMY-2 has been isolated from a large number of *S.* Heidelberg

isolates[58]. The 3.2kb *bla*$_{CMY-2}$ gene that when translated contains a serine active site at position 64 in the polypeptide chain and is therefore characterized as a class C β-lactamase[58]. As previously mentioned, plasmids belonging to IncI1 are commonly found in *S.* Heidelberg and can integrate into the chromosome[46]. These plasmids carry transfer genes and can diffuse across bacterial populations through horizontal gene transfer mechanisms from a wide spectrum of ecological and epidemiological compartments and thus increase the concern for the spread of resistance in *S.* Heidelberg[59].

1.3.4.2 CMY-2-Containing S. Heidelberg Outside of North America

S. Heidelberg is one of the most prevalent causes of salmonellosis in the United States and Canada however, in recent years, it has been detected outside of North America[60]. In 2013, Cejas *et al*. released a paper indicating the first detection of a CMY-2 plasmid-containing *S.* Heidelberg outside of North America in Buenos Aires, Argentina[60].

In Argentina, *Salmonella* samples are collected from human, animal, food, feed, and environment origins and submitted to the Centro Nacional de Referencia for characterization[60]. *S.* Heidelberg is not commonly found among these isolates, and before 2012, a CMY-2-containing isolate had never been identified. Detection of the first CMY-2-containing *S.* Heidelberg isolate was obtained from the diarrheal stool sample of an HIV adult inpatient and underwent antimicrobial susceptibility testing using minimal inhibitory concentrations (MICs) based on the Clinical and Laboratory Standards Institute (CLSI) guidelines[60]. This particular isolate was found to be resistant to ampicillin, cephalothin, cefoxitin, ceftriaxone, and ceftazidime[60].

In recent years, *S.* Heidelberg has become increasingly common in South America[61,62]. A study published in 2020 by Souza *et al*. performed β-lactam susceptibility testing on isolates of *S.* Heidelberg found in a Brazilian poultry production chain[61]. Of 62 isolates tested, 37 *S.* Heidelberg isolates were found to contain the *bla*$_{\text{CMY-2}}$ gene, indicating that the prevalence of CMY-2-containing Heidelberg isolates in South America has considerably increased since their first detection in 2012[61]. CMY-2-containing isolates of *S.* Heidelberg continue to be found in South America and are now commonly isolated from poultry origin[62]. Current studies have indicated that *S.* Heidelberg containing the *bla*$_{\text{CMY-2}}$ gene outside of North America is becoming increasingly common and it is likely that CMY-2-containing Heidelberg will continue to disseminate globally.

1.3.4.3 Epidemiology of *S.* Heidelberg

Salmonella infection affects approximately 550 million people each year. People of all ages can be infected; however, the incidence is highest in children under the age of 5[45]. Epidemic outbreaks of *S.* Heidelberg present a significant public health and economic burden in Canada and the United States[47]. While *S.* Heidelberg is the third most common serotype in Canada and the fifth most common serotype in the United States, it is not one of the top serotypes across the other continents[63].

In 2004, an outbreak of *S.* Heidelberg infection was reported in Edmonton, Alberta. A total of 32 outbreak bases were reported with the likely cause determined as fecal-oral transmission from improper food handling. Stool samples were taken from 5 employees at the restaurant where the outbreak occurred and one employee was determined to be *S.* Heidelberg positive[63].

Multiple multi-state outbreaks of *S.* Heidelberg have been recorded in the United States including two in 2011 followed by an outbreak in 2013 and 2016[64]. These outbreaks were all determined to be caused by contact with animals or uncooked poultry. The largest number of cases from these outbreaks was 278 in 2013. The longest and most recent recorded outbreak of *S.* Heidelberg was from January 2015 to August 2017. This outbreak was linked to contact with dairy calves and consisted of a total of 54 people infected from 15 different states, with 33% of the infected individuals under the age of 5[65].

AMR testing from outbreaks indicates an increase in AMR over the years. Antimicrobial susceptibility testing on the isolates from the 2015-2017 outbreak indicated that all isolates were resistant to amoxicillin-clavulanic acid, ampicillin, cefoxitin, ceftriaxone, streptomycin, sulfisoxazole, and tetracycline as well as reduced susceptibility to ciprofloxacin[65]. Comparisons of isolates from the early 2000s to now indicate an increase in resistance to ciprofloxacin and ceftriaxone, which is a third-generation cephalosporin. Third generation cephalosporins are one of the last antimicrobial options that we currently have to treat multi-drug resistant *Salmonella* infection and if drug resistance continues to rise, *Salmonella* infection may become untreatable.

1.3.4.4 Relevance of *S.* Heidelberg

S. Heidelberg presents a large economic and healthcare burden in North America as a consistent member of the top ten causes of foodborne disease. Outbreaks of foodborne illness from *S.* Heidelberg have been occurring regularly in North America for at least two decades with the most recent outbreak ending in August 2017. The multitude of virulence factors that can be found in Heidelberg isolates are indicative of the level of infection they can cause in humans. Further studies are required to understand this serotype to develop more treatment and

prevention strategies to hopefully allow the battle against *S.* Heidelberg to be more positive in the future.

1.3.4.5 Plasmids in *S.* Heidelberg

Many plasmid types have been found in *S. enterica* serotype Heidelberg isolates. In recent years, *S.* Heidelberg has been found to cause more invasive infections and has been found to carry multidrug resistance. An analysis of multidrug-resistant isolates of *S.* Heidelberg by Han *et al.* found that these bacteria contained plasmids from the IncI1, IncHI2, IncA/C, and IncFIB families, as well as a plasmid that was unclassified to an Inc group[66]. These plasmids were found to carry multiple resistance genes and virulence genes, which contribute to the increasing pathogenesis and drug resistance found among *S.* Heidelberg isolates[66]. Other studies have found that ColE1 plasmids are important for the fitness of *S.* Heidelberg in poultry environments, where the isolates are commonly found[67,68]. Often, similar plasmids belonging to the same Inc group are found among resistant Heidelberg isolates such as the Group A, B, and C IncI1 plasmids found among cefoxitin-resistant Heidelbergs[46]. The diversity of plasmids found in *S.* Heidelberg exceeds that which has been discussed here; it is suffice to state that the plasmids found in these isolates play a large and complex role in the fitness and dissemination of resistance genes among Heidelberg isolates.

1.4 Rationale and Hypothesis

The use of antimicrobials in medicine and agriculture has resulted in considerable advancements for the health of humans and animals; however, it has also led to the widespread dissemination of AMR among bacteria. The use and overuse of antimicrobials has led to increasing selective pressure among bacteria to develop and acquire AMR genes. The increasing number of illnesses and deaths due to these AMR bacteria has led to the need for a greater

understanding of how certain bacteria become resistant to antimicrobials and if there are plasmidic factors aside from known AMR genes that contribute to high levels of AMR in certain bacteria such as plasmid-influenced changes in fitness, genomic expression, or proteomic expression. Plasmids are important vectors for the conferral and transfer of AMR genes, and studies analyzing these possible physiological effects are often not performed in their natural bacterial hosts.

As previously stated, *S.* Heidelberg is frequently isolated from humans and poultry in Canada and they frequently contain group A and C IncI1 CMY-2 plasmids that confer resistance to amoxicillin-clavulanic acid, ampicillin, cefoxitin, ceftiofur, and ceftriaxone[46]. A comparison of studies examining *S.* Heidelberg AMR in Canada from 2002-2006 and 2012 shows that resistance to ceftriaxone had increased by up to 57.5% in merely 6 years and that this resistance was largely due to group A and C IncI1 plasmids[46,47]. These studies indicate that there is an existing knowledge base regarding the role of IncI1 CMY-2 plasmids in conferring AMR, however, there is a further need for studies analyzing the role of these plasmids on factors such as fitness, genomic expression, and proteomic expression in their natural host, *S.* Heidelberg.

We hypothesize that IncI1 plasmids containing the CMY-2 antimicrobial resistance gene play a role in *Salmonella enterica* serotype Heidelberg fitness through alterations in growth, gene expression, and proteomic expression.

Based on this hypothesis, we expect that the IncI1 CMY-2 plasmid-free isolate N13-0291 will display observable changes in fitness when it contains an IncI1 CMY-2 plasmid. This will be studied through the formation of two isogenic strain pairs of *S.* Heidelberg isolate N13-01291; i) N13-01291/pCMYN13-20944A: *S.* Heidelberg isolate N13-01291 containing the group A

IncI1 plasmid sourced from *S.* Heidelberg isolate N13-02944A, and ii) N13-01291/pCMY12-2460C: *S.* Heidelberg isolate N13-01291 containing the group C IncI1 plasmid sourced from *S.* Heidelberg isolate 12-2460C. These isolates will be analyzed for the presence of antimicrobial resistance through β-lactamase PCR and antimicrobial susceptibility testing (AST). WGS will be used to examine isogenicity of the strain pairs through phylogenomic analysis, for confirmation of plasmid presence, prediction and detection of antimicrobial resistance, and changes in genomic expression due to the presence of a plasmid. Plasmid maintenance and viability will be confirmed using the photosensitive viability dye PMAxx™. This is done to confirm that plasmids will be maintained in growth assays performed without the presence of a CMY-2 plasmid-selective antimicrobial, as this will remove antimicrobial presence as a confounding factor for any observed changes in growth.

Subsequently, fitness will be analyzed and compared for differences between isolates due to the presence of a plasmid through the performance of growth assays, phenotypic microarrays, and assays for biofilm formation. Finally, alterations in proteomics will be analyzed through the comparison of changes in protein expression in the presence of a plasmid as compared to the plasmid-free isogenic isolate. Together, these results will indicate whether pCMYN13-02944A and pCMY12-2460C play a role in altering the fitness, gene expression, and proteomic expression of *S.* Heidelberg N13-01291.

2. Materials and Methods

2.1 Bacterial Strains and Growth Conditions

The enteric strain used in this study was *Salmonella enterica* serotype Heidelberg which was collected and typed as a part of the Canadian Integrated Program for Antimicrobial Resistance Surveillance (CIPARS)[69,70]. *S. enterica* isolates N13-02944 from a chicken stool sample which harbored a group A CMY-2 plasmid and 12-2460 from human stool which harbored a group C CMY-2 plasmid were used as donors for the plasmid-free recipient *S. enterica* sample N13-01291 from chicken cecal sample. Plasmids A and C from the donor samples carry resistance to amoxicillin-clavulanic acid, ampicillin, cefoxitin, ceftiofur, and ceftriaxone encoded on $bla_{\text{CMY-2}}$. These isolates were obtained from Dr. M. Mulvey, Public Health Agency of Canada, Winnipeg, MB. All bacterial strains were stored at -80°C using Microbank™ 2 mL cryovials (Pro-Lab Diagnostics, Richmond Hill, ON, Canada).

2.2 Nucleic Acid Manipulation

2.2.1 Plasmid Isolation

Plasmid isolation from *S. enterica* serotype Heidelberg strains was performed using a QIAGEN® Plasmid Midi Kit (Qiagen, Hilden, Germany). Strains were subbed twice onto LB plates with growth overnight at 37°C. A single colony was then inoculated into 125 mL of Luria-Bertani (LB) broth and grown overnight. A 100 mL volume of overnight culture was harvested by centrifugation at 6000 x g for 15 minutes at 4°C. The supernatant was removed, and the bacterial pellet was resuspended in 4 mL Buffer P1. A total of 4 mL of Buffer P2 were added to this solution and mixed by inverting, followed by incubation at room temperature for 5 minutes. To this solution, 4 mL of Buffer P3 was added and mixed by inversion, followed by incubation on ice for 15 minutes. This sample was then centrifuged at 20,000 x g for 30 minutes at 4°C.

During this time, a QIAGEN®-tip 100 (Qiagen, Hilden, Germany) was equilibrated by the addition of 4 mL Buffer QBT. After incubation, the supernatant was added to the QIAGEN®-tip 100 (Qiagen, Hilden, Germany) and washed twice with 10 mL of Buffer QC. DNA was eluted using 5 mL of 65°C Buffer QF into a clean 15 mL tube. Plasmid DNA was then precipitated by adding 3.5 mL of isopropanol to the eluted DNA. This solution was then mixed and centrifuged at 15,000 x g for 30 minutes at 4°C. The supernatant was decanted. The DNA pellet was washed with 2 mL of 70% ethanol and centrifuged at 15,000 x g for 10 minutes. The supernatant was decanted, and the pellet was air-dried for 10 minutes before re-dissolving DNA in water for storage at -20°C.

2.2.2 Crude DNA Extraction

One loop of culture was inoculated into a microcentrifuge tube containing 0.1mm glass disruptor beads (Chemglass Life Sciences, Vineland, NJ, USA) and 600 µL neutralization buffer. Tubes were then heated at 95°C for 2-5 minutes followed by vortexing on a Vortex Genie for 2 minutes. Samples were then centrifuged at 6,000 x g for 2 minutes.

2.2.3 Nucleic Acid Quantification

DNA and RNA quantification were performed using a Qubit™ dsDNA High Sensitivity Assay Kit (Invitrogen, Carlsbad, CA, USA), Qubit™ RNA High Sensitivity Assay Kit (Invitrogen, Carlsbad, CA, USA), and a Qubit™ 4 Fluorometer (Invitrogen, Carlsbad, CA, USA). Qubit™ working solution was prepared by diluting the Qubit™ reagent 1:200 in Qubit™ buffer (Invitrogen, Carlsbad, CA, USA). Standards were prepared by combining 10 µL of positive and negative controls provided in the kit with 190 µL of the Qubit™ working solution (Invitrogen, Carlsbad, CA, USA) in Qubit™ assay tubes. Sample tubes were prepared by combining 1-20 µL of the sample with 180-199 µL of Qubit™ working solution (Invitrogen, Carlsbad, CA, USA) for

a final volume of 200 µL in Qubit™ assay tubes. All assay tubes were then vortexed for 2-3 seconds and then incubated for 2 minutes at room temperature. The standards were then inserted into the Qubit™ 4 Fluorometer to calibrate the machine, following which the sample assay tubes were inserted and read.

2.3 Isogenic Strain Pair Formation

Isogenic strain pairs were formed through a multistep workflow with the goal of obtaining two isolates that would be identical aside from the presence of a plasmid of interest.

2.3.1 Formation of Electrocompetent Isolates

The following procedure was adapted from Binotto *et al.*, 1991[71]. Strains were removed from an 80°C freezer storage and subbed twice on LB plates with overnight growth. A single colony was then incubated overnight at 37°C and then 20 µL of overnight culture was then inoculated into 20 mL of LB broth in a 125 mL flask. This culture was then grown to an optical density of approximately 0.6 at 600 nm and 10 mL of this sample was then placed on ice for 15 minutes to arrest bacterial growth. These cells were then pelleted by centrifugation at 3000 rpm at 4°C for 10 minutes. The supernatant was removed, and the cells were washed with 5 mL of cold dH_2O. Centrifugation and washing were repeated twice under the same conditions. The final pellet was resuspended in 1 mL of dH_2O and pelleted by centrifugation at 21,000 x g at 4°C. The supernatant was removed, and the pellet was stored at -80°C or transformed immediately.

2.3.2 Plasmid Transformation

Electrocompetent cells and isolated pCas kanamycin-resistant plasmids were removed from the 20°C freezer and allowed to thaw. Once thawed, 30 µL electrocompetent cells were added to cold 1 mm electroporation cuvettes along with 2 µL of 10 ng isolated plasmid. A

BioRad MicroPulser™ (Bio-Rad, Hercules, CA, USA) was manually set to 1.25 kV and electroporation was performed. Cuvette was removed from the MicroPulser™ (Bio-Rad, Hercules, CA, USA) and 900 µL of Super Optimal broth with Catabolite Repression (SOC) (0.5% w/v yeast extract, 2% w/v tryptone, 10 mM NaCl, 2.5 mM KCl, 10 mM $MgCl_2$, 10 mM $MgSO_4$, 20 mM glucose) (Invitrogen, Carlsbad, CA, USA) was immediately added. This solution was then placed in a 1.5 mL Eppendorf tube and incubated at 30°C for 1 hour. After incubation, cells went through a serial dilution and 100 µL was plated separately on LB and LB + 25 µg/mL kanamycin plates for transformation efficiency tests and grown overnight at 30°C.

2.3.3 Transformation Efficiency Assay

Transformation efficiencies were calculated by determining the number of colony-forming units (cfu) that could be produced by transforming 20 ng of the plasmid into 30 µL of electrocompetent cells. Calculations were performed using the following equation[72]:

$$TE = \frac{\frac{colonies}{\mu g}}{dilution}$$

TE = transformation efficiency
Colonies = number of colonies counted on the plate
Ug = the amount of DNA transformed expressed in ug
Dilution = the total dilution of the DNA before plating

Colony counts were performed in a dilution series on selective and non-selective media.

2.3.4 Plasmid Conjugation

Successful transformants of N13-01291 containing the kanamycin-resistant pCas plasmid were suspended in 3 mL of LB broth (Difco, Franklin Lakes, NJ, USA). The isolates containing the conjugation plasmids (N13-02944 and 12-2460) were also suspended in 3 mL of LB broth

(Difco, Franklin Lakes, NJ, USA). Both isolates were allowed to grow at 37°C until they reached an optical density of ~0.6 at 600nm. At this time, 1 mL of the N13-01291/pCas transformant was combined with 1 mL of the isolate containing the CMY-2 donor plasmid. This solution was left at room temperature for 24 hours and then serially diluted on LB plates (Difco, Franklin Lakes, NJ, USA) containing 25 μg/mL kanamycin and 10 μg/mL cefoxitin per plate. These plates were grown at 30°C for 16-18 hours. Successful colonies were then streaked on LB plates (Difco, Franklin Lakes, NJ, USA) containing 10 μg/mL cefoxitin and grown at 37°C for 16-18 hours to remove the temperature-selective plasmid pCas. To confirm the conjugation of the CMY-2 plasmid and the curing of the kanamycin selection plasmid, colonies were streaked separately on 25 μg/mL kanamycin-containing LB plates (Difco, Franklin Lakes, NJ, USA) and 10 μg/mL cefoxitin-containing LB plates (Difco, Franklin Lakes, NJ, USA). The growth of colonies was compared via replica plating and selecting replica colonies that grew on cefoxitin but not kanamycin, as these were considered to contain the CMY-2 plasmid with successful curing of the pCas plasmid. The results of this assay generated the isogenic strain pairs that were used in further experiments. The parent isolate containing the group A plasmid (pCMYN13-02944A) isolated from N13-012944 will be henceforth designated as N13-01291/pCMYN13-02944A and the parent isolate containing the group C plasmid (pCMY12-2460C) isolated from 12-2460 will henceforth be designated as N13-01291/pCMY12-2460C.

2.3.5 Conjugation Frequency Assay

Conjugation frequency of the IncI1 plasmids was calculated by determining the ratio of the number of transconjugants to the number of recipient cells[73]. Colony counts were performed in a dilution series on selective and non-selective media.

2.4 Determination of Antimicrobial Susceptibility

2.4.1 Detection of *bla*$_{CMY-2}$

Detection of an AmpC-type β-lactamase known as *bla*$_{CMY-2}$ was carried out on some isolates and extracted plasmids using PCR[74]. The total reaction volume of 25 µL contained 22 µL of 2X master mix containing primers found in Table 2.1. A total of 0.5 µL AmpliTaq Gold (5 U/µL, Roche) and 2.5 µL DNA template were added. The PCR cycling conditions consisted of an initial denaturation at 95℃ followed by 30 cycles of denaturation at 94℃ for 30 seconds, annealing at 63℃, elongation at 72℃ for 90 seconds, followed by a final extension at 72℃ for 7 minutes.

2.4.2 Gel Electrophoresis

Visualization of PCR products was performed by loading the PCR products onto a 1.5% agarose gel (Fisher-Scientific, Ottawa, ON, Canada) and electrophoresis was performed using 0.5X Tris-borate-EDTA (TBE) buffer (89 mM Tris-borate, 2 mM EDTA, pH 8.3) (Sigma-Aldrich, St. Louis, MO, USA). Approximately 5 µL of the PCR product was mixed with 2.5 µL loading dye (0.25% w/v bromophenol blue, 40% w/v sucrose) and then loaded onto the gel. The gel was then electrophoresed for 60 minutes at 7.5 volts/cm (V/cm).

Once electrophoresis was complete, the gel was stained with an ethidium bromide solution (0.5 µg/mL) for 30 minutes and visualized using ultraviolet light from the AlphaImager® HP System (Alpha Innotech, San Leandro, CA, USA). Determination of the PCR product sizes was done by running 5 µL of a 100 bp ladder (Roche, Mississauga, ON, Canada) alongside the samples.

Table 2.1. Primers used for PCR amplification of *bla*$_{CMY-2}$ gene[74].

Name	Gene	Sequence (5'-3')	Tm (℃)	Product Size
CMY2-A	*bla*$_{CMY-2}$	TGATGCAGGAGCAGGCTATTCC	73.2	323
CMY2-B	*bla*$_{CMY-2}$	CTAACGTCATCGGGGATCTGC	72.8	

2.4.3 Antimicrobial Susceptibility Testing

Antimicrobial susceptibility testing (AST) was performed by broth microdilution method using the Sensititre® Automated Microbiology System (Trek Diagnostic Systems Ltd, Oakwood Village, OH, USA) plate CMV4AGNF in accordance with the Clinical and Laboratory Standards Institute (CLSI) when available[75–77]. AST was completed on the plasmid-free parent isolate N13-01291 and on the isogenic strain pairs formed from this isolate; N13-01291/pCMYN13-02944A and N13-01291/pCMY12-2460C. Antimicrobial susceptibilities were determined for amoxicillin/clavulanic acid (AMC), ampicillin (AMP), azithromycin (AZM), cefoxitin (FOX), ceftriaxone (CRO), chloramphenicol (CAM), ciprofloxacin (CIP), gentamicin (GEN), meropenem (MEM), nalidixic acid (NAL), streptomycin (STR), sulfisoxazole (SIX), tetracycline (TET), trimethoprim/sulfamethoxazole (SXT). Isolates were subbed twice from 80℃ and grown on tryptic soy agar (TSA) (Difco, Detroit, MI) containing 5% sheep's blood agar at 37℃ for 18-24 hours. Colonies were inoculated into tubes containing double distilled H_2O (ddH_2O) and adjusted to the 0.5 McFarland standard (Remel, Lenexa Kansas). Turbidity was automatically read by the nephelometer on the Sensititre®. Next, 10 µL of suspended cells were transferred to Mueller-Hinton broth (MHB) tubes (Difco, Franklin Lakes, NJ, USA) that contained a substrate strip (Trek Diagnostics). Dosing heads (Sensititre®) were put on the MHB tubes (Difco, Franklin Lakes, NJ, USA) and the sample was vortexed for 10 seconds. Automated inoculation of plates coated with a fluorogenic substrate (Sensititre®) was carried out. Samples were immediately covered and placed in the Sensititre® Aris for incubation at 37℃ for 18 hours. At the end of the incubation, antimicrobial susceptibilities were automatically read by fluorescence. Minimum inhibitory concentrations (MICs) for all drugs except azithromycin and streptomycin were determined based on the breakpoints used by the CLSI; azithromycin and streptomycin

interpretations were performed using standards set by the National Antimicrobial Resistance Monitoring System (NARMS) since CLSI interpretive standards were unavailable. These standards can be found in Table 2.2[75–77]. The quality control reference strain used was *Escherichia coli* ATCC 25922*;* reference ranges for these isolates can be found in appendix Table A1.

2.5 Whole-Genome Sequencing

2.5.1 DNA Extraction

DNA extraction and purification for WGS was performed with the Epicentre MasterPure™ Complete DNA and RNA Purification Kit (Illumina Inc. San Diego, CA, USA) as per the manufacturer's protocol. Cultures stored at -80℃ in Microbank™ vials containing beads were used to inoculate 3 mL of LB broth and then incubated for 18-24 hours at 37℃ in a shaking incubator at 300 rpm. A 300 µL aliquot of this culture was centrifuged at 3000 rpm for 3 minutes and the supernatant was discarded. Cell pellets were mixed with 300 µL Tissue and Cell Lysis Solution containing 1 µL Proteinase K (50 µg/µL) (Illumina Inc., San Diego, CA, USA) and incubated at 65℃ for 15 minutes with vortexing every 5 minutes. The samples were then cooled to 37℃, mixed with 1 µL RNase A (5 mg/mL) (Illumina Inc., San Diego, CA, USA) and incubated for 30 minutes to ensure cell lysis.

2.5.2 Whole-Genome Sequencing

Whole-genome sequencing was performed to analyze the plasmid sequence and to determine if the strain pair genomes remained isogenic. Sequencing libraries were prepared by the Genomics Core Facility at the National Microbiology Laboratory with Nextera XT Library Prep Kits and sequenced on the Nextseq 500/550 platform using Nextseq 500/550 150 cycle kits (Illumina Inc., San Diego, CA, USA).

Table 2.2. Antimicrobial susceptibility breakpoints for *Salmonella*[75–77].

Antimicrobial	Testing Range (ug/mL)	Interpretive Categories and MIC Breakpoints[a] (µg/mL)		
		Susceptible	Intermediate[c]	Resistant
Amoxicillin-clavulanic acid	1.0/0.05 – 32/16	≤ 8/4	16/8	≥ 32/16
Ampicillin	1 – 32	≤ 8	16	≥ 32
Azithromycin[b]	0.25 – 32	≤ 16	N/A	≥ 32
Cefoxitin	0.5 – 32	≤ 8	16	≥ 32
Ceftiofur[b]	0.12 – 8	≤ 2	4	≥ 8
Ceftriaxone	0.25 – 64	≤ 1	2	≥ 4
Chloramphenicol	2 – 32	≤ 8	16	≥ 32
Ciprofloxacin	0.015 – 4	≤ 0.06	0.12 – 0.5	≥ 1
Gentamicin	0.25 – 16	≤ 4	8	≥ 16
Nalidixic acid	0.5 – 32	≤ 16	N/A	≥ 32
Streptomycin[b]	32 – 64	≤ 32	N/A	≥ 64
Sulfisoxazole	16 – 512	≤ 256	N/A	≥ 512
Tetracycline	4 – 32	≤ 4	8	≥ 16
Trimethoprim/sulfamethoxazole	0.12/2.38 – 4/76	≤ 2/38	N/A	≥ 4/76

[a]CLSI guideline version M100 – 30th edition was used for all antimicrobials unless otherwise indicated[76]

[b]Breakpoints based on NARMS[77]

[c]N/A = not applicable

2.5.3 WGS Analysis

Bioinformatic analyses were performed using the Integrated Rapid Infectious Disease Analysis (IRIDA) v21.05 platform which is an open-source platform for public health genomics or in the National Microbiology Laboratory (NML) Galaxy platform which is a web-based platform for data-intensive biomedical research[78,79]. Additionally, the tool for rapid annotation of microbial SNPs (TRAMS) was used to annotate any SNPs found in the microbial genomes[80]. Read quality was assessed using the FastQC tool (Galaxy version 0.72)[81].

2.5.4 Assembly of Genomes and Plasmids

Reads were assembled into contigs with the Shovill v1.1.0 tool which uses SPAdes v3.11.1 at its core and annotated with Prokka v1.13[82–84]. Assembly quality was assessed using the QUAST quality assessment tool for evaluating and comparing genome assemblies[85]. The QUAST tool uses the Nucmer aligner from MUMmer v3.23 to align assemblies to a reference genome and then determine quality metrics based on those alignments[85,86].

2.5.4.1 Phylogenetic Analysis

Phylogenetic analysis was performed using the SNVPhyl pipeline v2.0 available through the IRIDA platform[78,87]. The SNVPhyl pipeline is a single nucleotide variant phylogenomics pipeline for microbial genomic epidemiology that is able to identify high-quality single nucleotide variants (hqSNVs) and then construct whole-genome phylogenetic trees from a collection of WGS reads and a reference genome[87]. The SNVPhyl pipeline includes: repeat region identification, reference mapping, variant calling using two methods, variant consolidation, SNV alignment generation, creation of a maximum likelihood phylogeny and outputs a phylogenetic dendrogram and a SNV matrix[87]. Repeat identification identifies internal repeat regions in the reference genome using MUMmer v3.0 tool which are then excluded from

analysis[87]. The mapping/variant calling stage uses the SMALT v0.7.4 tool to align reads against a reference strain in order to generate a read pileup which is evaluated to determine the mapping quality based on a defined coverage threshold[87]. The variant calling stage then uses FreeBayes v1.3.5 and the SAM-tools and BCFtools packages to call SNVs; both methods need to have identified the SNV in order to validate the presence of a SNV in the variant consolidation stage[87]. The SNV alignment generation stage then examines the SNV calls to generate a table that identifies variants; this table can also be used to re-generate the SNV alignment[87]. This can be used to generate the final output phylogeny by running this SNV alignment through PhyML with the GTR+γ model as default and tree support values estimated using PhyML's approximate likelihood ratio test[87–89].

2.5.4.2 Antimicrobial Gene Detection

Identification of resistance genes was performed using the Staramr tool on the Galaxy platform[79,90]. The Staramr tool scans input genome assemblies against the ResFinder, PlasmidFinder, and Pointfinder databases to identify AMR genes, resistance mutations, and plasmids[90–93]. The output from this analysis includes multi-locus sequence typing (MLST), resistance genotypes, predicted resistance phenotypes, and plasmid typing predictions.

2.5.4.3 Plasmid Characterization

Plasmid analysis was performed on the Galaxy platform using MOB-suite tools (Galaxy version 3.0.0), and TRAMS (Galaxy version 1.0.0), while alignments were created with EasyFig[79,80,94,95]. The MOB-recon tool was used to type and extract plasmid contigs from the whole genome sequences and the MOB-typer tool from the MOB-suite was also used to determine plasmid replicon types and mobility in silico[94]. The MOB-suite tools are a set of modular tools that are used to reconstruct and type plasmids in order to characterize them[94]. The

default thresholds in the MOB-suite are optimized for *Enterobacterales* plasmids and broadly group reference plasmids with similar sequence content to determine similarities in sequence clusters[94]. MOB-recon is an ensemble-based approach that uses marker sequence databases of existing replicons and relaxases along with a reference database that is then able to assemble and extract plasmid sequences[94]. The MOB-typer provides replicon typing using relaxase gene typing, oriT predictions, and conjugative transferability predictions together against their reference database[94]. The TRAMS tool was then used to annotate plasmid SNPs using the previously characterized *bla*$_{\text{CMY-2}}$ IncI1 plasmid pCVM_29188_101 from *S.* Kentucky (GenBank accession CP001121.1)[80,96]. Comparison of plasmid pCMYN13-02944A and pCMY12-2460C was performed using Easyfig v2.2.2 to align the plasmid sequences[95]. Easyfig is a Python-based application that can be used to generate figures of multiple genomes in order to compare multiple sequences; it can also be used to generate NCBI BLAST comparisons[95].

2.6 Plasmid Maintenance and Viability Assays

Plasmid maintenance and viability assays were performed using a dye called propidium monoazide-xx (PMAxx™) (Biotum Inc., Fremont, CA, USA). PMAxx™ (Biotum Inc., Fremont, CA, USA) is a cell membrane-impermeable viability PCR dye that acts as a photoreactive DNA-binding dye. This dye binds to DNA with high affinity and upon photolysis with visible light, PMAxx™ (Biotum Inc., Fremont, CA, USA) becomes covalently attached to DNA. PCR cannot amplify this modified DNA. Due to its cell membrane-impermeable characteristics, only dead cells are susceptible to this DNA modification. This allows the differentiation between viable and non-viable cells, which is the foundation of the viability assays performed in this study. This experiment was performed to confirm that the CMY-2 plasmid was maintained in live

Salmonella cells throughout growth assays performed in the absence of a CMY-2-selective antimicrobial.

2.6.1 Protocol and Optimization

Single colonies from LB plates (Difco, Franklin Lakes, NJ, USA) were inoculated into 3 mL LB broth (Difco, Franklin Lakes, NJ, USA) and grown overnight at 37°C with 250 rpm shaking. Overnight cultures were standardized to $OD_{600} \approx 1.0$. A total of 400 µL were aliquoted into ultra-clear microcentrifuge tubes. Negative controls were heat inactivated at 95°C for 5 minutes; killing was confirmed by plating 10 µL of heat-inactivated bacteria on LB (Difco, Franklin Lakes, NJ, USA). A 2.5 µL aliquot of 5 mM PMAxx™ (Biotum Inc., Fremont, CA, USA) and 100 µL aliquot of Gram-negative enhancer were added to each 400 µL aliquot of bacteria. Tubes were then incubated at room temperature for 10 minutes in the dark. Samples were then exposed to directly overhead light for 5 minutes. Light used was an Illume LED Multi-Colour and Pure White A-19 Smart Bulb set to 750 lumens and 6224 K or 465.94 nm white light emission. Samples were then pelleted by centrifuging at 5,000 x g for 10 minutes and DNA was extracted as described previously. This protocol was optimized by comparing different lengths of light exposure from 0-30 minutes of exposure in 5-minute increments and the distance from the light from <5 cm to 30 cm in 5 cm increments. The optimal time of light exposure was determined to be 5 minutes with directly overhead light as this provided the optimal curves after qPCR occurred.

2.6.2 Targets and Efficiencies

Detection of *invA and bla*$_{CMY-2}$ was carried out using the primers in Table 2.3 and the Applied Biosystems ViiA™ 7 Real-Time PCR System (Applied Biosystems, Foster City, CA, USA). The total reaction volume of 20 µL contained 10 µL 2X Forget-Me-Not master mix, 2 µL

10 µM primer mix, 2 µL DNA template, 3 µL 0.1X ROX and 3 µL dH_2O. The qPCR cycling conditions consisted of holding at 95℃ for 5 minutes followed by 40 cycles at 95°C for 5 seconds and 60°C for 30 seconds.

2.6.3 Isolates and Controls

The isolates that were examined for viability and plasmid retention included N13-01291, N13-01291/pCMYN13-02944A, and N13-01291/pCMY12-2460C. Each isolate was grown at 37℃ for 24 hours until the stationary phase was reached. Positive controls were taken from the logarithmic growth phase (OD_{600} ≈0.7) of each plasmid-containing isolate as this is when the cells should have all been viable. Negative controls were created by heat-inactivating bacterial samples of each plasmid-containing isolate at 95℃ for 5 minutes and killing of bacteria was confirmed by plating 10 µL of each negative control on LB plates.

2.6.4 Determination of Plasmid Retention

Plasmid retention was determined by comparing samples at stationary phase with and without PMAxx™ (Biotum Inc., Fremont, CA, USA) alongside control samples. Each isolate was analyzed for the chromosomal *invA* gene and the plasmidic *bla*$_{CMY-2}$ gene. The positive controls were used to determine the ratio of chromosome copies to plasmid copies in a live cell. This data was then compared to the data from isolates that were taken from stationary phase to see if the plasmid was maintained throughout the growth cycle.

Table 2.3. Primers used for viability and maintenance assays.

Name	Gene	Sequence (5'-3')	Tm (℃)	Product Size	Reference
CMY2-A	*bla*$_{CMY-2}$	TGATGCAGGAGCAGGCTATTCC	73.2	323	[74]
CMY2-B	*bla*$_{CMY-2}$	CTAACGTCATCGGGGATCTGC	72.8		
invA-F	*invA*	ATTCTGGTACTAATGGTGATGATC	57.6	288	[97]
invA-R	*invA*	GCCAGGCTATCGCCAATAAC	60.5		

2.6.5 Statistical Analysis

Each isolate examined for viability was grown in biological triplicate and technical duplicates were taken from each biological replicate resulting in six samples testing for each condition. The mean and standard deviation of the C_T for each set of samples was taken and used for calculations. Next, the mean C_T of each target without the dye was subtracted from the mean C_T of each target with the dye to determine the amount of DNA from live cells that was present for each target. The amount of chromosomal DNA (using target *invA*) from live bacterial cells was compared to the amount of plasmidic DNA (using target CMY-2) from live bacterial cells to determine the ratio of plasmids to chromosomal DNA. The following equation was used to determine the number of copies of each template based on its length in base pairs and the amount in nanograms detected via qPCR:

$$number\ of\ copies = \frac{amount\ x\ 6.022x10^{23}}{length\ x\ 6.5x10^{11}}$$

This equation uses the assumption that the average weight of a base pair is 650 Daltons and that one mole of a base pair weighs 6.5 x 10^{11} ng; therefore, the molecular weight of a double stranded DNA template can be estimated by multiplying the length of the template in base pairs by this number. A student's t-test was used to compare the mean ratio of chromosomal to plasmidic DNA and determine if there was a significant difference using $p < 0.05$.

2.7 Growth Assays

2.7.1 Temperature and Media Conditions

S. Heidelberg samples from cryo-bead stocks were streaked for colony isolation on LB plates (Difco, Franklin Lakes, NJ, USA) supplemented with 50 µg/mL ampicillin (Sigma-Aldrich, St. Louis, MO, USA) and 10 µg/mL cefoxitin (Sigma-Aldrich, St. Louis, MO, USA) for

plasmid selection. Two to three colonies from each plate were transferred to a new Luria broth (LB) plate (Difco, Franklin Lakes, NJ, USA) supplemented with antibiotic, streaking for isolation. One colony from each plate was then inoculated into 2 mL of LB broth (Difco, Franklin Lakes, NJ, USA) using a sterile loop and incubated at 37℃ for 16 hours. For manual growth assays, a 100 µL volume of this overnight culture was used to inoculate 10 mL of LB broth (Difco, Franklin Lakes, NJ, USA) for a 1:100 dilution. Absorbance readings were measured at 600 nm using 500 µL of culture in a cuvette every hour for 24-48 hours using an Eppendorf Biophotometer (Eppendorf, Hamburg, Germany). For automatic growth assays, 1 µL of the overnight culture described previously was used to inoculate 100 µL of LB broth (Difco, Franklin Lakes, NJ, USA) for a 1:100 dilution in 96-well Corning® Costar™ plates (Sigma-Aldrich, St. Louis, MO, USA). These plates were read at 600 nm every 5 minutes for 24-48 hours in an Epoch™ 2 Microplate Spectrophotometer (BioTek Instruments, Winooski, VT, USA) was used. To control for plate evaporation during this timeframe, the outer wells of the plate were left empty.

2.7.2 Statistical Analysis

All manual growth curves were performed in biological triplicate and technical duplicate. All growth curves performed by the Epoch™ 2 Microplate Spectrophotometer (BioTek Instruments, Winooski, VT, USA) were performed in biological sextuplicate. Timepoints were determined by taking the average of the biological replicates. The slope of the line between each time point was used to represent the growth rate of each isolate. These slopes were compared using a two-tailed student's t-test assuming unequal variance with an alpha of 0.05.

2.8 Phenotypic Microarrays using Biolog Omnilog®

2.8.1 Procedure

Phenotypic microarrays (PMs) were performed using phenotypic microarray panels 1 to 20 from Biolog (Biolog, Hayward, CA, USA) which contained metabolic and chemical sensitivity tests for bacteria. The array layout for the phenotypic microarrays is shown in Figure 2.1, the contents of each well can be found in the Figures A1-20 of the appendix. PM panels were prepared for incubation according to the manufacturer's protocol. The Biolog Omnilog® PM system (Biolog, Hayward, CA, USA) which works as both an incubator and plate reader was used to analyze the growth kinetics of *S.* Heidelberg over 24 hours at 37℃ in each PM panel.

2.8.2 Analysis of Phenotypic Microarrays

The Biolog Omnilog® PM System Biolog (Biolog, Hayward, CA, USA) comes equipped with a File Management/Kinetic Plot module that lets the user assemble several panels of data into a single data list. Kinetic plots were generated using this software to represent changes in wells over time. The changes seen reflect a combination of growth and respiration of the organism being tested.

The Biolog Omnilog® PM System Biolog (Biolog, Hayward, CA, USA) also comes equipped with the Omnilog® PM PAR Module Software that displays a comparison of the data in two separate data lists via parametric analysis. This software was used to generate comparisons between two separate isogenic strain pairs.

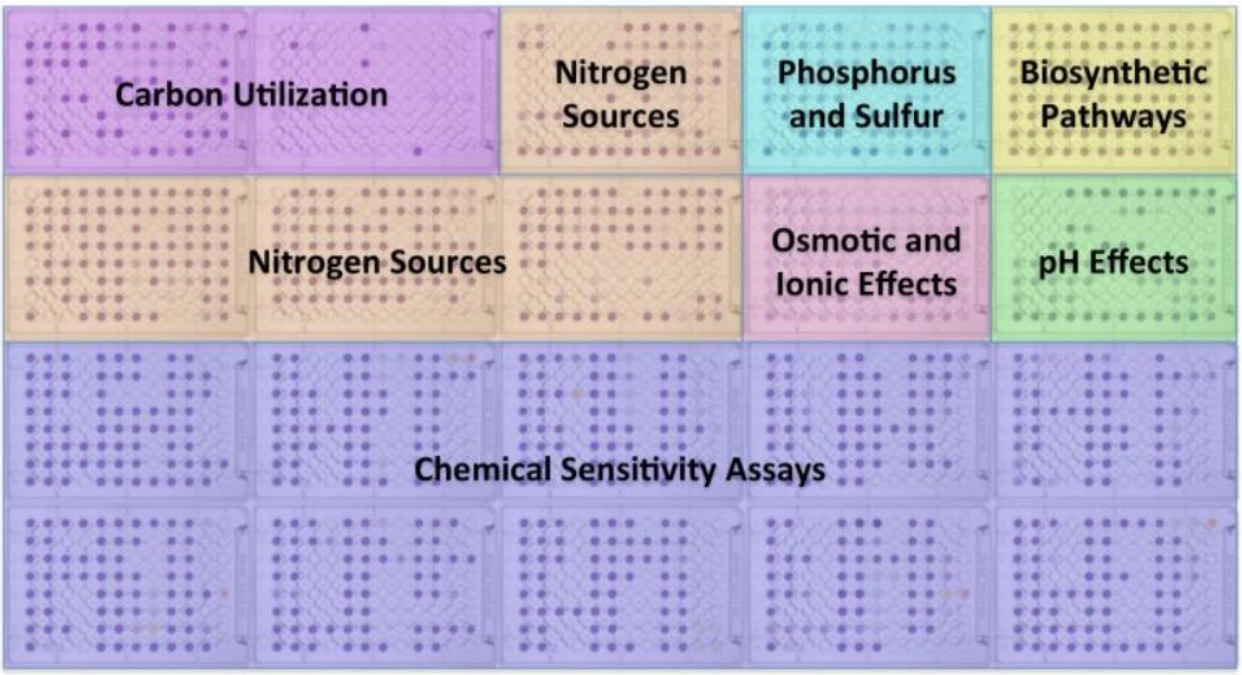


Figure 2.1. Phenotypic microarray panel contents for plates 1-20 sourced from Biolog (Biolog, Hayward, CA, USA).

2.9 Biofilm Formation Assays

2.9.1 Procedure

The following procedure was adapted from Merritt *et al.*, 2005[98]. Cultures were removed from storage at -80°C and subbed twice on LB (Difco, Franklin Lakes, NJ, USA). A single colony was then selected and inoculated in 3 mL of LB (Difco, Franklin Lakes, NJ, USA) overnight at 37℃. Overnight cultures were normalized to an optical density at 600 nm to approximately 1.0. A 96-well Corning™ Costar™ flat bottom cell culture microplate was prepared by pipetting 90 µL of LB broth (Difco, Franklin Lakes, NJ, USA) into each well. Ten µL of each homogenized sample was then pipetted into designated wells, leaving the outer edge wells empty. Plates were incubated for 24 hours at 37°C. After incubation, loose cells and media were discarded and rinsed away. To each well, 125 µL of 0.1% Crystal Violet (CV) (w/v) was added and incubated at room temperature for 30 minutes. The plate was then rinsed with water and dried overnight. The following day, 125 µL of 30% acetic acid in water (v/v) was added to each well to solubilize the CV for 15 minutes. 125 µL of solubilized CV was transferred to a new flat-bottomed optical plate. The absorbance of each well was measured at 600 nm using 30% acetic acid as a blank. The positive control strain used to indicate strong biofilm formation was *E. coli* DSM 1103/ATCC 25922 and the negative control strain was *S. enterica* serotype Typhimurium LT2 which does not form biofilms; a no bacteria control was used as a second negative control.

2.9.2 Statistical Analysis

A two-tailed student's t-test was used to examine for differences between the control and each group.

2.10 LC/MS/MS Proteomics

A visual summary of the proteomic workflow can be found in Figure 2.2. Proteomics methods were adapted from Adkins *et al.* 2006, Leibler *et al.* 2009, and Wisniewski *et al.* 2009 by the staff at the NML in MS Standard Operating Procedure 017[99–101].

2.10.1 Cell Preparation

Samples were prepared by growing bacterial isolates in LB broth at 37℃ until they reach an optical density of approximately 0.6 at 600nm (indicating the logarithmic growth phase). Samples were centrifuged at 5000 x *g* for 10 minutes at 4℃ to pellet the cells and the supernatant was discarded. To this pellet, 5 mL of ddH_2O was added to resuspend the pellet. This suspension was then transferred to a 50 mL falcon tube and centrifuged at 5000 x *g* for 10 minutes at 4℃ to pellet the cells; the supernatant was discarded. These pellets were then resuspended in 1 mL of ddH_2O, centrifuged at 5000 x *g* for 5 minutes at 4℃, the supernatant was discarded, and the pellets were stored at -80℃ until used.

2.10.2 Cell Lysis

Cell pellets were thawed and resuspended in 500 µL sterile, cold Milli-Q H_2O, then combined with 50 µL of 0.1 mm glass beads (Scientific Industries Inc., Bohemia, NY, USA), vortexed briefly to mix, and heated for 5 minutes at 95℃ to denature the samples and inactivate proteases. Samples were then vortexed for 3 minutes to lyse the cells, followed by centrifugation at 3000 rpm for 1 minute to pellet the beads and cell debris. The protein extract in the supernatant was then removed and transferred to a 15 mL conical tube. Following this step, 500 µL of Milli-Q water was added to the sample tube containing the bead mixture, which was then vortexed for 1 minute, and centrifuged at 3000 rpm for 1 minute. The protein extract was

removed and pooled in the same 15 mL. This step was repeated approximately 6 times, or until the supernatant was transparent. The pooled protein extract was stored at -80℃.

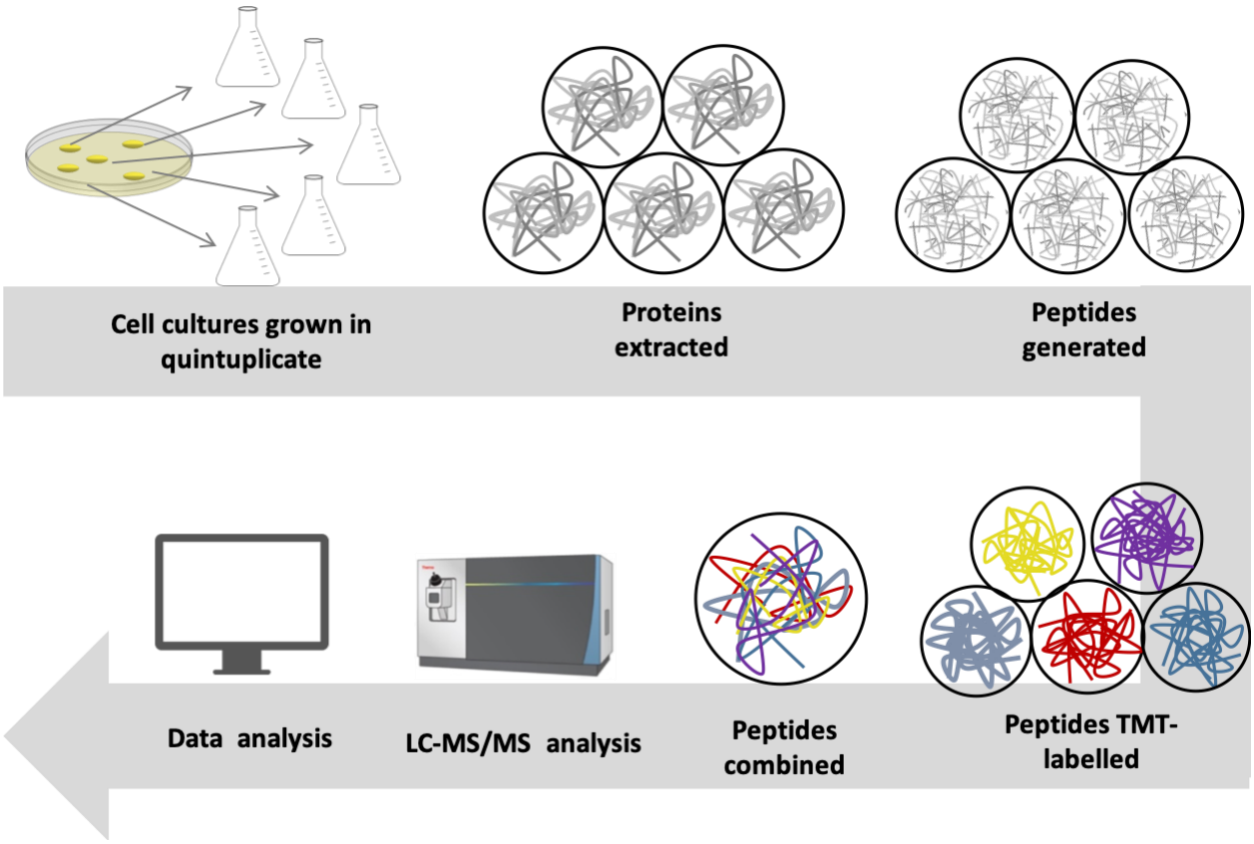


Figure 2.2. Workflow used for the proteomic analysis of *S.* Heidelberg samples. Cell cultures for protein extraction were grown in quintuplicate; replicates are indicated by circles. Proteins and peptides are indicated within the circles with colours representing different TMT labels. These peptides were then analyzed using LC-MS/MS and subsequent data analysis using Scaffold Q+ v4.4.

2.10.3 Protein Quantification

The protein extract was quantified using a Bicinchoninic Acid (BCA) Protein Assay Kit, with bovine serum albumin (BSA) as a standard (Pierce Protein Research Products, Thermo Fisher Scientific). The microplate procedure provided by the manufacturer was used for quantification.

2.10.4 SDS and DTT Treatment of Protein

The protein extract was thawed, and the volume of extract required to yield 100 µg of protein based on the BCA assay was removed. The volume was topped up to 100 µL with sterile Milli-Q water and then concentrated in an Eppendorf Vacufuge Plus speed vac. Once the sample was dried down, 10 µL of 0.5 M HEPES (4-(2-hydroxyethyl)-1-piperazineethanesulfonic acid), pH 8.0 and 30 µL of Milli-Q water was added to the protein pellet. This solution was vortexed on the lowest setting for 10 minutes until the protein was fully suspended. To this suspension, 20 µL of 10% sodium dodecyl sulfate (SDS) was added and gently mixed to yield a final concentration of 2% SDS. This solution was then heated at 95°C for 5 minutes and allowed to cool to room temperature. Finally, 10 µL of 1 M dithiothreitol (DTT) was added to the solution, heated at 95°C for 5 minutes, allowed to cool, and the sample was frozen at -80°C until peptide digestion.

2.10.5 Peptide Digestion

SDS and DTT-treated samples were thawed at room temperature. Up to 200 µg of lysate was mixed with an equal volume of urea exchange buffer (UEB). This mixture was incubated at room temperature for 10 minutes. During this incubation, a Nanosep® 10K membrane cartridge was prepared by running 200 µL of MS-grade water through the cartridge at 10,000 x *g* for 1 minute followed by 200 µL UEB through the cartridge at 10,000 x *g* for 2 minutes. After

incubation, 300 µL of the sample was placed on the cartridge membrane and centrifuged at 10,000 x *g* for 12 minutes in a microcentrifuge. This step was repeated until the entire sample had passed through the cartridge membrane. The cartridge membrane was then washed three times with 250 µL UEB and centrifuged at 10,000 x *g* for 12 minutes.

A total of 100 µL of 50 mM iodoacetic acid (IAA) was added to the cartridge. The cartridge was placed in a thermomixer and shaken at 600 rpm for 1 minute at room temperature. Following mixing, the cartridge was incubated in the dark for 20 minutes at room temperature. The sample was then centrifuged at 10,000 x *g* for at least 10 minutes until all the buffer had passed through the column. 100 µL of UEB was added to the filter and centrifuged for 15 minutes; this was repeated twice more. Following this, 150 µL of 50 mM HEPES was spun through the column twice at 10,000 x *g* for 10 minutes each. The cartridge was then transferred to a fresh collection tube. To each cartridge, 50 µL trypsin (Promega) solution (48.5 µL of 50 mM HEPES and 1.5 µL of 1 µg/µL trypsin (Promega)) was added. Nanosep® cartridge was then placed in a thermomixer and shaken at 600 rpm for 1 minute to mix with the protein at room temperature. Tubes containing the cartridges were then placed in humidity chambers (50 mL Falcon tubes containing 1 mL of water) and incubated overnight at 37°C.

2.10.6 Peptide Recovery and Desalting

Following overnight incubation, the digested protein from the Nanosep® cartridge was moved into an Eppendorf lo-bind microfuge tube. The extruding rim of the Nanosep® cartridge was removed and 50 µL of 50 mM HEPES was added to the cartridge membrane. The solution was then shaken for 2 minutes at 600 rpm at room temperature in a thermomixer. The cartridge was then inverted and spun at 10,000 x *g* for 3 minutes at room temperature. Following this, 50 µL of MS-grade H_2O was added to the cartridge and placed on a thermomixer and shaken at 600

rpm for 3 minutes at room temperature to remove the peptide bound to the membrane. The cartridge was then inverted and spun at 10,000 x *g* for 3 minutes at room temperature. A 50 µL aliquot of 50 mM HEPES was then added to the cartridge and mixed at 600 rpm for 3 minutes at room temperature, followed by inversion and centrifugation at 10,000 x *g* for 3 minutes at room temperature. The flow-through was collected and stored at -80°C until labelling.

2.10.7 Tandem Mass Tag (TMT)-Labelling

Tandem mass tag (TMT) labels from the 10-plex TMT kit (Thermo Fisher Scientific) were brought to room temperature and centrifuged at maximum speed for 2 minutes. 45 µL acetonitrile was added to each label and allowed to dissolve for 5 minutes. Labels were vortexed and spun down. Digested protein extract was resuspended in 59 µL 100 mM HEPES and shaken at 600 rpm for 10 minutes. Resuspended peptide samples were then spun down and added to TMT-labelled tubes. Peptide-label mixtures were then incubated at room temperature overnight. The next day, 8 µL of 5% hydroxylamine quenching reagent was added to each tube and incubated for 30 minutes. Samples were dried down in a vacuum centrifuge (Savant Speed/Vac Concentrator, Thermo Fisher Scientific) and stored at -80°C until pre-scan. All methods following this step were performed by the Proteomics Core at the NML.

2.10.8 Pre-Scan

The trypsin-digested TMT-labelled samples were brought up to a final volume of 35 µL using water. Equal volumes (1 µL) of each labelled sample were mixed with nano-LC buffer A (2% acetonitrile, 0.1% formic acid) to a final volume of 60 µL and analyzed by nano-LC/MS/MS using a 2-hour gradient to ensure one-to-one mixing of all samples. Histograms of count versus ratio for each TMT report ion pair were generated using the peak list from Proteome Discoverer (v2.2, Thermo Fischer Scientific) and an in-house Perl script. The media ratio (histogram

centroid) for each report ion pair was used to make minor corrections to the final 10-plex mixing volumes, with the final mixing volumes calculated to yield unity median TMT ratios, for a total volume of 40 µL of the TMT 10-plex mix.

2.10.9 Peptide Fractionation

The TMT 10-plex mixed samples were spiked with 4 µL of 200 mM ammonium formate (Fisher Scientific, EMD), pH 10, to match LC buffer A (20 mM ammonium formate, pH 10). Sample (40 µL) was loaded onto a Waters XBridge C18 guard column (10 mm long, 2.1 mm inner diameter, 3.5 µm particles) on a micro-flow 1200 Series HPLC pump (Agilent Technologies). Peptides were then separated on a Waters XBridge C_{18} analytical column (10 cm long, 2.1 mm inner diameter, 3.5 µm particles) using an 80-min gradient of 3-75% LC buffer B (20 mM ammonium formate, 90% acetonitrile, pH 10) at a constant flow rate of 150 µL/min. A total of 12 fractions were collected across the peptide elution profile. These fractions were concentrated to near-dryness under vacuum centrifugation and resuspended in 80 µL of nano-LC buffer A (2% acetonitrile, 0.1% formic acid).

2.10.10 Nano-LC-MS/MS Analysis

Each sample was separately analyzed using a nano-flow Easy nLC 1200 connected in-line to an Orbitrap Fusion Lumos mass spectrometer with a nanoelectrospray ion source at 2.1 kV (Thermo Fisher Scientific, San Jose, CA, USA). The peptide samples were loaded (1 µL) and eluted off an Easy Spray column (50 cm long, 75 µm inner diameter, 2 µm particles, Thermo Fisher Scientific, San Jose, CA, USA). with 100% buffer A (2% acetonitrile, 0.1% formic acid) for a total volume of 6 µL, and then separation and elution of peptides was performed using a linear gradient of 2-28% buffer B (80% acetonitrile, 0.1% formic acid) over 100 min, 28%-38% buffer B for 15 minutes, 38%-100% buffer B for 5 minutes and a wash at 100% buffer B for 10

minutes at a constant flow rate of 250 nL/min. The total LC/MS/MS run-time was about 175 minutes, including the loading, linear gradient, column wash, and equilibration.

Data was acquired using these settings: Dynamically choosing the topmost abundant precursor ions from each survey scan that could be fragmented in 2 seconds, each isolated in the quadrupole (0.7 *m/z* isolation width) and fragmentation by HCD (36% normalized collision energy). The survey scans were acquired in the Orbitrap over *m/z* 375-1500 with a target resolution of 120000 at *m/z* 200, and the subsequent fragment ion scans were also acquired in the Orbitrap with a target resolution of 50000 at *m/z* 200. The lower threshold for selecting a precursor ion for fragmentation was 5.0e4. Dynamic exclusion was enabled using a *m/z* tolerance of 10 ppm, a repeat count of 1, and an exclusion duration of 15s.

2.10.11 Data Processing and Statistical Analysis

All spectra were processed using Proteome Discoverer (v2.2, Thermo Fisher Scientific) and database searching was done with Mascot v2.6.2 (Matrix Science)[102,103]. Searches were performed against a subset of the National Center for Biotechnology Information protein (NCBIprot) database created for a Salmonella h-12-4374 species (4713 sequences)[104]. The decoy database option was selected, and the following search parameters were used: Carbamidomethyl (C) was selected as a fixed modification, Oxidation (M) as a variable modification, fragment ion mass tolerance of 0.5 Da, parent ion tolerance of 10 ppm, and trypsin enzyme with up to 1 missed cleavage. TMT 10plex was selected as the Quantitation method. Mascot search results were imported into Scaffold Q+ v4.4 (Proteome Software) and filtered using 0.1% FDR for peptides, 1.0% FDR for proteins, and at least 2 peptides per protein[103]. Resulting Log2 quantitative values were imported into Perseus v1.6.5 (Max Plank Institute); then all the proteins that did not have a least 3 valid log2 LFQ intensities from ID were filtered out[105].

2.10.12 Protein Modelling

Proteins were modelled using Phyre2 (Protein Homology/analogY Recognition Engine V2.0) web portal for protein modelling, prediction, and analysis[106]. Phyre2 was used to analyze the effect of the amino acid variants detected in the presence of the CMY-2 plasmids.

3. Results

3.1 Isogenic Strain Pair Formation

Two similar plasmids were separately inserted into isolates of N13-01291 to form isogenic isolates of *S.* Heidelberg containing each plasmid of interest to examine the effects of the plasmid on the host regarding genomic expression, fitness, and proteomic expression. These two transconjugants were labelled N13-01291/pCMYN13-02944A and N13-01291/pCMY12-2460C. pCMYN13-02944A was extracted from isolate N13-02944 and pCMY12-2460C was extracted from isolate 12-2460. Isolation of the CMY-2 plasmids was confirmed to be successful via PCR amplification of the CMY-2 gene from isolated DNA of each transconjugant. Isogenicity of the strain pairs was examined using PCR with confirmation by WGS which will be discussed in section 3.3.

3.1.1 Plasmid pCas Transformation and Efficiency

Plasmid transformation was performed in order to mark the CMY-2 plasmid-free isolate so it could be differentiated from the CMY-2 donor strain after conjugation was complete. The temperature-sensitive plasmid pCas was transformed into isolate N13-01291 for use as a marker of successful transconjugation of the CMY-2 plasmids[107]. After transformation and plating, successful growth of the cells on plates containing 25 μg/mL kanamycin indicated successful

transformation of the pCas plasmid into isolate N13-01291 forming N13-01291/pCas. A control plate was used to discount spontaneous colony growth and kanamycin-resistant colonies were re-streaked onto kanamycin-containing plates to confirm presence of pCas.

Transformation efficiency is a marker of the amount of plasmid taken up by cells, and is generally used as a measure of success to obtain clones containing the desired plasmid[108,109]. A transformation efficiency between 10^6 and 10^8 is generally considered adequate for most applications however transformation efficiencies of $>1x10^{10}$ cfu/μg is considered acceptable for more difficult or low throughput cloning such as in this experiment[108]. The average transformation efficiency of the pCas plasmid into isolate N13-01291 was calculated to be 7.21 x 10^4 cfu/μg: indicating a successful level of propagation of the pCas plasmid.

3.1.2 Conjugation of pCMY/pCas Plasmids

Due to the large size of the CMY-2 plasmids of interest, conjugation was performed to mediate the individual transfer of each CMY-2 plasmid into the CMY-2 plasmid-free isolate N13-01291. Conjugation frequency was determined to examine the rate of plasmid transfer via conjugation between the isolates and the rate of mating-pair formation[73]. Plasmid transfer via conjugation is an important mechanism for the transmission of AMR, and higher rates of conjugation frequency can result in the successful propagation of a plasmid in a competitive environment where other donor plasmids are present[73].

Two CMY-2 plasmids were conjugated successfully into the parent strain containing the selection plasmid pCas to form N13-01291/pCas/pCMYN13-02944A and N13-01291/pCas/pCMY12-2460C. Successful conjugation was indicated by growth on LB plates containing 25 μg/mL kanamycin and 10 μg/mL cefoxitin as well as PCR detection of the CMY-2

gene. The conjugation frequency of pCMYN13-02944A was determined to be an average of 0.61 units and the conjugation frequency of pCMY12-2460C was determined to be 0.495 units. This result indicates that there are minor differences in conjugation frequency between the two plasmids leading to possible effects on fitness and survivability of the plasmid in conjugative environments.

3.1.3 Detection of Extended-spectrum β-lactamase Genes

After plasmid conjugation and subsequent curing of the pCas plasmid as described in section 2.3.4 and confirmation of the resumption of kanamycin susceptibility in N13-01291/pCMYN13-0244A and N13-01291/pCMY12-2460C, β-lactamase gene PCR amplification was performed to confirm the presence of *bla*$_{\text{CMY-2}}$ as demonstrated in Figure 3.1.

The positive control used for PCR was *Klebsiella pneumoniae* N09-0080 as it contains all six genes used for β-lactamase multiplex PCR: CMY-2 (323 bp), OXA-1 (464 bp), CTX-M (593 bp), TEM (708 bp), and SHV (1016 bp). This control was used to compare the size of the PCR product isolated from the strain of interest to the known size of the *bla*$_{\text{CMY-2}}$ gene product.

A DNA-free sample was used as a negative control to ensure the absence of DNA contamination in the PCR master mix. CMY-2 gene PCR products separated by agarose gel electrophoresis determined that pCMYN13-02944A and pCMY12-2460C were individually transferred successfully into separate replicates of N13-01291.

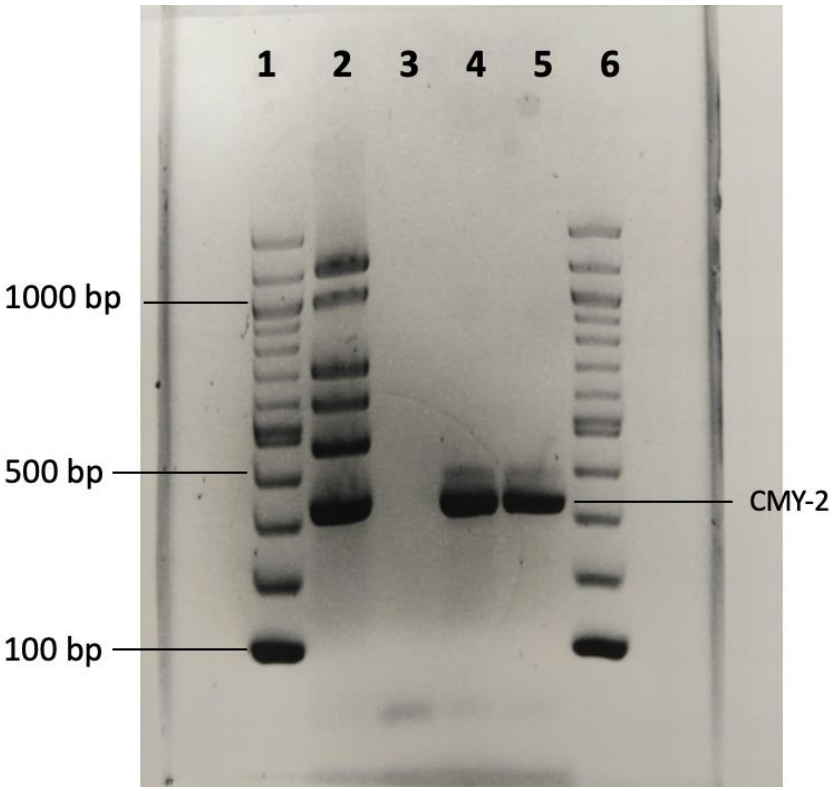


Figure 3.1. Extended-spectrum β-lactamase PCR for the identification of *bla*$_{\text{CMY-2}}$. Visualized using 1.5% agarose gel electrophoresis with one sample per lane. Lanes 1 and 6 contain the DNA molecular weight standard, a 100 bp ladder. Lane 2 contains the positive control, *Klebsiella pneumoniae* N09-0080, consisting of CMY-2 (323 bp), OXA-1 (464 bp), CTX-M (593 bp), TEM (708 bp), and SHV (1016 bp). Lane 3 contains no DNA template as negative control. Lane 4 contains N13-01291/pCMYN13-02944A. Lane 5 contains N13-01291/pCMY12-2460C. Lanes 4 and 5 were found to be CMY-2 positive which confirms the presence of the CMY-2-carrying plasmids.

3.2 Determination of Antimicrobial Susceptibility

Antimicrobial susceptibility testing using the Sensititre® was determined for all three *S. enterica* isolates to determine the baseline susceptibility of the CMY-2 plasmid-free parent and determine plasmid effects on antimicrobial susceptibility. Antimicrobials tested included: Amoxicillin/clavulanic acid, ampicillin, azithromycin, cefoxitin, chloramphenicol, ciprofloxacin, gentamicin, meropenem, nalidixic acid, streptomycin, sulfisoxazole, tetracycline, and trimethoprim/sulfamethoxazole. These results are summarized in Table 3.1 and discussed below.

Isolate N13-01291 (plasmid-free parent) was susceptible to all antimicrobials tested. Isolates containing either plasmid were also susceptible to azithromycin, ciprofloxacin, gentamicin, meropenem, nalidixic acid, sulfisoxazole, tetracycline, and trimethoprim/sulfisoxazole. Isolates containing either pCMYN13-02944A or pCMY12-2460C showed resistance to amoxicillin/clavulanic acid, ampicillin, cefoxitin, ceftriaxone, and streptomycin. The isolate containing pCMY12-2460C showed intermediate resistance to chloramphenicol while the isolate containing pCMYN13-02944A was susceptible to chloramphenicol. Another notable difference was found in the strain susceptibilities to gentamicin where all isolates were susceptible; however, in the presence of either plasmid, the MIC was increased from 0.5 (S) in N13-01291 to 4 (S) in N13-01291/pCMYN13-02944A and 2 (S) in N13-01291/pCMY12-2460C. These findings indicate that the presence of pCMYN13-02944A or pCMY12-2460C results in multidrug resistance.

Table 3.1. Antimicrobial susceptibility testing results using Sensititre® interpreted using CLSI or NARMS standards[75–77].

	MIC Interpretive Standard (µg/mL)[b]		
Antimicrobial	**N13-01291**	**N13-01291/pCMYN13-02944A**	**N13-01291/pCMY12-2460C**
Amoxicillin/Clavulanic Acid	≤ 1 S	> 32 R	> 32 R
Ampicillin	2 S	> 32 R	> 32 R
Azithromycin[a]	4 S	4 S	8 S
Cefoxitin	2 S	> 32 R	> 32 R
Ceftriaxone	≤ 0.25 S	32 R	32 R
Chloramphenicol	8 S	4 S	16 I
Ciprofloxacin	≤ 0.015 S	≤ 0.015 S	0.03 S
Gentamicin	0.5 S	4 S	2 S
Meropenem	≤ 0.06 S	≤ 0.06 S	≤ 0.06 S
Nalidixic Acid	4 S	4 S	4 S
Streptomycin[a]	16 S	64 R	64 R
Sulfisoxazole	≤16 S	≤ 16S	32 S
Tetracycline	≤ 4 S	≤ 4 S	≤ 4 S
Trimethoprim/Sulfamethoxazole	≤ 0.12 S	≤ 0.12 S	≤ 0.12 S

[a]Based on NARMS standards

[b]S = susceptible, I = intermediate, R = resistant

3.3 Whole Genome Sequencing of Isogenic Strain Pairs

WGS analysis of isolates N13-01291, N13-01291/pCMYN13-02944A, and N13-01291/pCMY12-2460C was performed to analyze and compare genomic content with and without the plasmids of interest. The genomes of these isolates were successfully assembled and annotated using Shovill v1.1.0 and Prokka v1.13[82,84]. For isolate N13-01291, the assembled genome had 72 times coverage and was 4748038 bp in length including a 37808 bp IncX1 plasmid and a 2707 bp ColpVC plasmid. The genome of N13-01291/pCMYN13-02944A had 103 times genome coverage and was 4845661 bp in length, of which the IncI1 plasmid pCMYN13-02944A was 95570 bp in length, the IncX1 plasmid was 37808 bp in length, and the ColpVC plasmid was 2707 bp in length. The genome of N13-01291/pCMY12-2460C had 137 times coverage and was 4849011 bp in length, of which the IncI1 plasmid 60C was 99573 bp in length, the IncX1 plasmid was 37808 bp in length, and the ColpVC plasmid was 2707 bp in length. A basic local alignment search tool (BLAST) analysis was performed to analyze sequence similarities between the two genome assemblies which indicated a sequence identity of 99.55%[110].

Differences in genome sizes between N13-01291/pCMYN13-02944A and N13-01291/pCMY12-2460C are likely attributed either sequencing error or to the presence of insertion sequences or phages which are encoded by highly repetitive sequences that are difficult for short-read sequencers to identify accurately.

3.3.1 Phylogenomic Analysis

Single nucleotide variant (SNV) analysis of the core genomes of isolates was performed on the plasmid-containing isolate sequences against the plasmid-free parent N13-01291 as a reference to determine isogenicity and examine the effect of the plasmids on the formation of

SNVs. The core-genome SNVs identified between isolates are outlined in Table 3.2; this analysis was performed in biological triplicate and SNVs were identified in each replicate. In the presence of pCMYN13-02944A there was a unique core-genome SNV identified in N13-01291; a thymine to adenine mutation at position 16541 which resulted in a glutamine to leucine non-conservative missense mutation in UbiB. In the presence of pCMY12-2460C there was a unique core-genome SNV identified in N13-01291; a thymine to guanine mutation at position 64390 which resulted in a leucine to arginine non-conservative missense mutation in CpxA. In the presence of either CMY-2 plasmid, an identical core-genome SNV was identified; a cytosine to adenine mutation at position 311798 which resulted in an aspartate to a tyrosine nonconservative missense mutation in MshA_1. A minimum spanning phylogenetic tree was generated using this SNV data from the SNVPhyl pipeline to examine the relatedness of the isolates using isolate N13-01291 as a reference, this can be found in Figure 3.2[87,111].

Table 3.2. A summary of the identified SNV alterations detected in the core-genomes of N13-01291/pCMYN13-02944A and N13-01291/pCMY12-2460C as compared to the plasmid-free isolate genome.

Gene	Reference Nucleotide[b]	N13-01291/pCMYN13-02944A Nucleotide	N13-01291/pCMY12-2460C Nucleotide	Amino Acid Position	Amino Acid Change
mshA_1	C	A	A	256	D to Y
ubiB	T	A	T	38	Q to L
cpxA	T	T	G	278	L to R

[a]Amino acids are based on single letter naming convention
[b]Reference genome used for all assembly analyses was the N13-01291 core genome

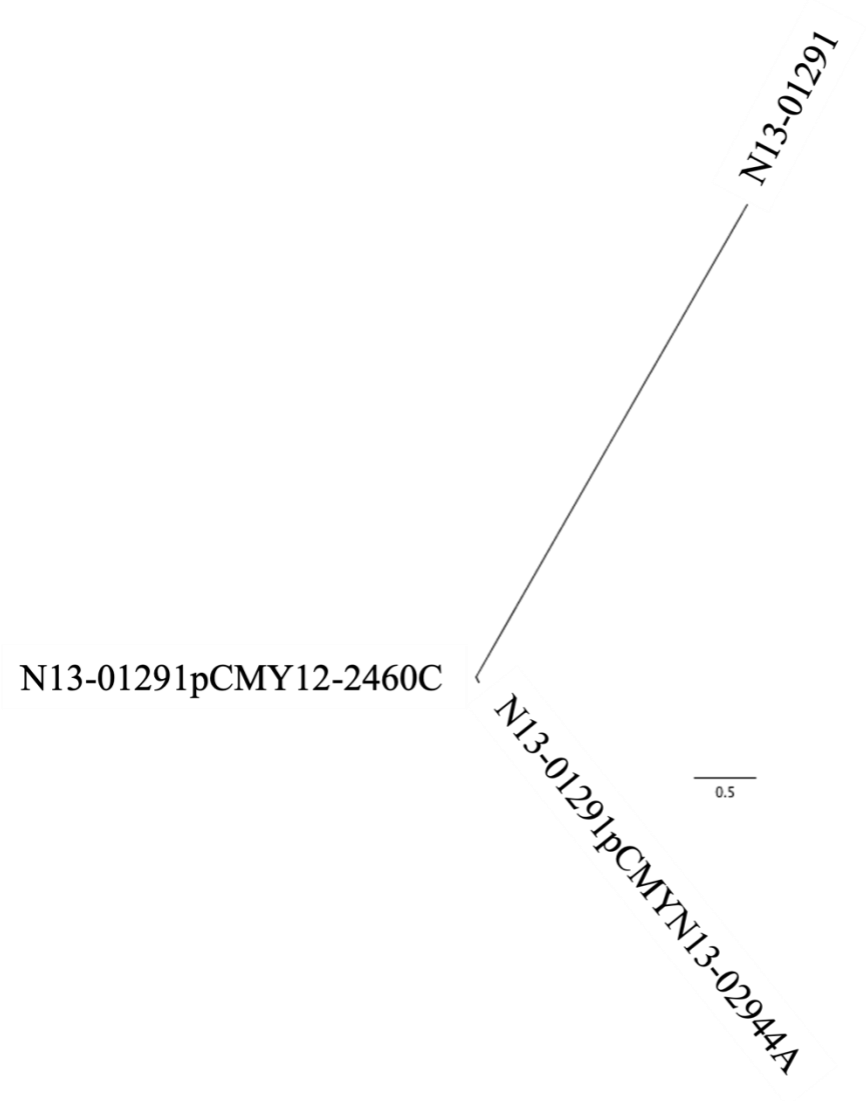


Figure 3.2. Minimum spanning phylogenetic tree of core genome SNVs between *S.* Heidelberg isolates N13-01291/pCMYN13-02944A and N13-01291/pCMY12-2460C. SNVs were generated using Figtree v1.4.4[112]. The IncI1 plasmid-free parent isolate N13-01291 was used as the reference genome[88,89].

3.3.2 Antimicrobial Gene Detection

The staramr v0.5.1 tool was used to determine and predict the presence of any AMR genes in isolates N13-01291, N13-01291/pCMYN13-02944A, and N13-01291/pCMY12-2460C[90]. The results from this analysis are summarized in Table 3.3[90]. All strains including the CMY-2 plasmid-free N13-01291 were found to contain the fosfomycin resistance gene *fosA7*. In the CMY-2 plasmid-containing isogenic strain pairs the β-lactamase resistance gene $bla_{\text{CMY-2}}$ was detected, confirming the presence of the IncI1 plasmid DNA within N13-01291. The staramr tool predicted that the detected $bla_{\text{CMY-2}}$ gene would confer resistance to ampicillin, amoxicillin/clavulanic acid, cefoxitin, and ceftriaxone.

Table 3.3. Predicted AMR genotypes and phenotypes of the three isolates using staramr[90].

Isolate ID	Genotype	Predicted Resistance Phenotype*	Plasmids Present in Sample	Sequence Type	Genome Length
N13-01291	*fosA7*	fosfomycin	ColpVC, IncX1	15	4759549
N13-01291/pCMYN13-02944A	*bla*$_{CMY-2}$, *fosA7*	ampicillin, amoxicillin/clavulanic acid, cefoxitin, ceftriaxone, fosfomycin	ColpVC, IncI1, IncX1	15	4856415
N13-01291/pCMY12-2460C	*bla*$_{CMY-2}$, *fosA7*	ampicillin, amoxicillin/clavulanic acid, cefoxitin, ceftriaxone, fosfomycin	ColpVC, IncI1, IncX1	15	4858846

*Average sensitivity for the prediction of these AMR phenotypes using staramr is 91.2% and average specificity is 99.7%. Positive predictive value is 99.1% and negative predictive value is 99.1%[113].

3.3.3 Plasmid Identification and Characterization

Plasmids from whole genome sequencing were detected and analyzed using the Galaxy platform in order to characterize the plasmids of interest and confirm the absence of non-CMY-2 AMR plasmids[79]. The MOB-recon and MOB-typer tools v1.4.9.1 were used to extract plasmid contigs and characterize any plasmids present in the isolates N13-01291, N13-01291/pCMYN13-02944A, or N13-01291/pCMY12-2460C; these results are summarized in Table 3.4[94]. The extracted IncI1 plasmid contigs obtained using the MOB-suite can be visualized in Figures 3.3 and 3.4[94].

In order to further characterize the IncI1 plasmids analyzed in this study, the TRAMS tool was used to annotate SNVs in the IncI1 plasmids using the characterized plasmid pCVM_29188_101 from *S.* Kentucky (GenBank accession CP001121.1) as a reference; these annotation results can be found in Tables 3.5 and 3.6[80,96].

Table 3.4. Replicon typing and characterization of plasmids identified using MOB-recon[94].

Plasmid Replicon Type	Length	Relaxase Type	MPF Type	oriT Type	Predicted Mobilization	Isolated from
IncI1	95570	MOBP	MPF_I	MOBP	Conjugative	N13-01291/pCMYN13-02944A
IncI1	99573	MOBP	MPF_I	MOBP	Conjugative	N13-01291/pCMY12-2460C
IncX1	37808	MOBP	MPF_T	N/A	Conjugative	N13-01291, N13-01291/pCMYN13-02944A, N13-01291/pCMY12-2460C
ColpVC	2207	N/A	N/A	MOBP	Mobilizable	N13-01291, N13-01291/pCMYN13-02944A, N13-01291/pCMY12-2460C

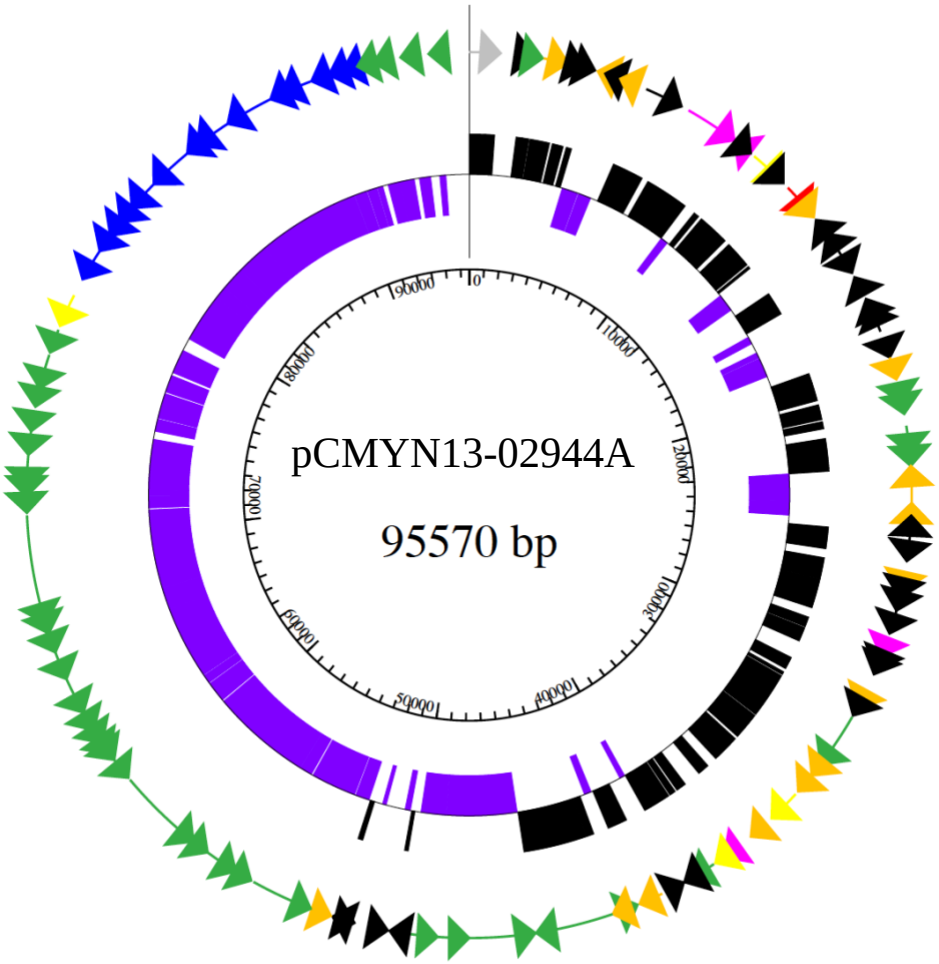


Figure 3.3. Visualization of Group A IncI1 plasmid "pCMYN13-02944A" isolated from sample N13-02944. The innermost circle represents the plasmid size in base pairs, the middle circle represents the strand that the coding sequence exists on the forward strand (black) and the reverse strand (purple) indicated, and the outermost circle indicates the identified coding sequences which are colour-coded according to function: grey; replication initiation, pink; colicin biosynthesis and immunity, green; plasmid transfer and maintenance, yellow; transposition/recombination, red; antimicrobial resistance, blue; pilus, black; hypothetical, and orange; other.

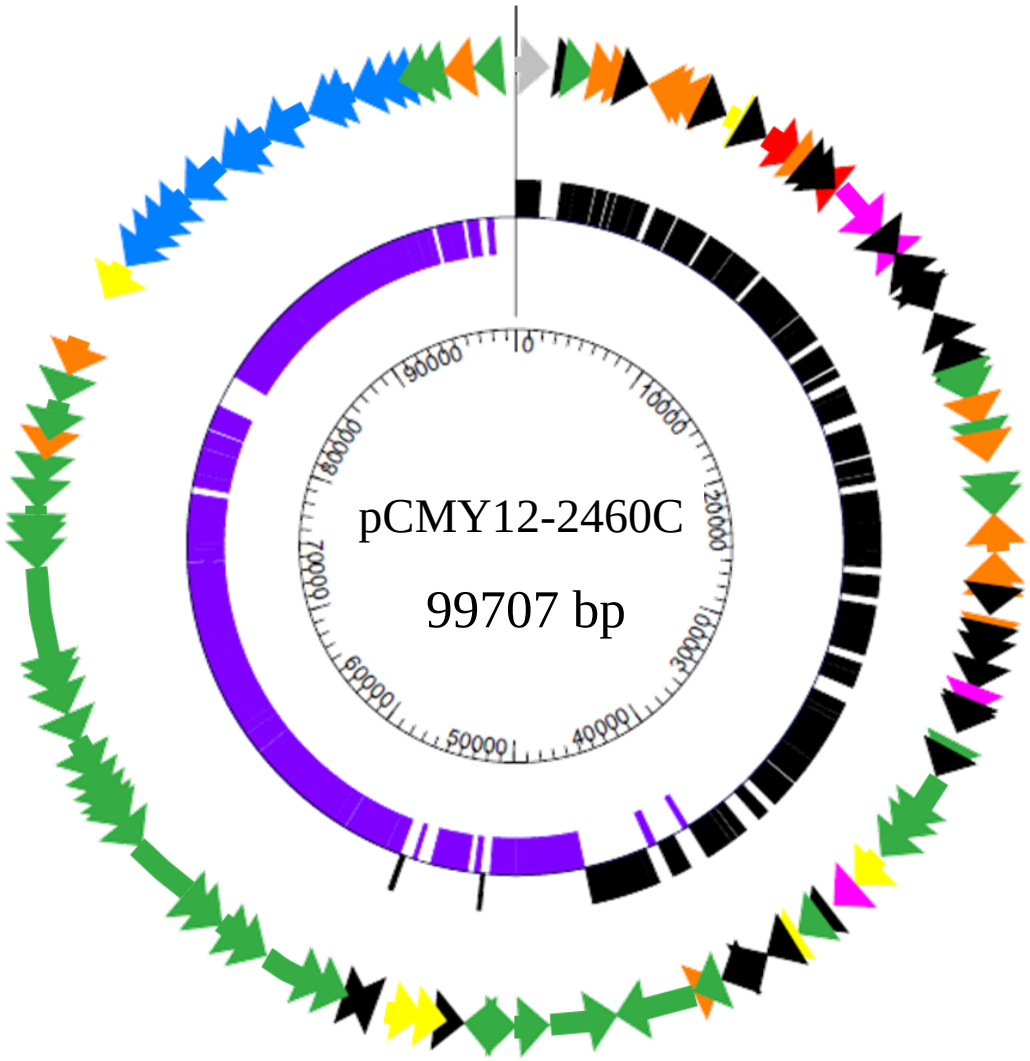


Figure 3.4. Visualization of Group C IncI1 plasmid "pCMY12-2460C" isolated from sample 12-2460. The innermost circle represents the plasmid size in base pairs, the middle circle represents the strand that the coding sequence exists on with the forward strand (black) and the reverse strand (purple) indicated, and the outermost circle indicates the identified coding sequences which are colour-coded according to function: grey; replication initiation, pink; colicin biosynthesis and immunity, green; plasmid transfer and maintenance, yellow; transposition/recombination, red; antimicrobial resistance, blue; pilus, black; hypothetical, and orange; other.

Table 3.5. TRAMS results for isolate N13-01291/pCMYN13-02944A using pCVM_29188_101 as a reference[46,80].

Position	Feature[a]	Gene	Product	Ref. base	Ref. codon	Ref. result	SNP type	New base	New codon	New result
10701	intergenic			T				a		
16541	CDS	*sucA*	2-oxoglutarate dehydrogenase E1 component	A	CTG	L	synonymous	t	tTG	L
18901	CDS	*sdhA*	Succinate dehydrogenase flavoprotein subunit	C	GAA	E	nonsynonymous	a	aAA	K
71101	CDS	*glnS*	Glutamine--tRNA ligase	A	ACG	T	synonymous	t	ACt	T
187101	CDS	*dgaR_1*	Transcriptional regulatory protein DagR	T	AAT	N	nonsynonymous	a	AAa	K
336801	CDS	*phnT*	Putative 2-aminoethylphosphonate import ATP-binding protein PhnT	A	AAA	K	nonsynonymous	t	AtA	I
432253	CDS		hypothetical protein	T	ATC	I	nonsynonymous	g	ATg	M

[a]CDS; coding sequence

Table 3.6. TRAMS results for isolate N13-01291/pCMY12-2460C using pCVM_29188_101 as a reference[80].

Position	Feature[a]	Gene	Product	Ref. base	Ref. codon	Ref. result	SNP type	New base	New codon	New result
10701	intergenic			T				a		
18901	CDS	*sdhA*	Succinate dehydrogenase flavoprotein subunit	C	GAA	E	nonsynonymous	a	aAA	K
64390	CDS	*ifcA*	Fumarate reductase flavoprotein subunit	A	GCG	A	synonymous	c	GCc	A
71101	CDS	*glnS*	Glutamine--tRNA ligase	A	ACG	T	synonymous	t	ACt	T
187101	CDS	*dgaR_1*	Transcriptional regulatory protein DagR	T	AAT	N	nonsynonymous	a	AAa	K
336801	CDS	*phnT*	Putative 2-aminoethylphosphonate import ATP-binding protein PhnT	A	AAA	K	nonsynonymous	t	AtA	I
432253	CDS		hypothetical protein	T	ATC	I	nonsynonymous	g	ATg	M

[a]CDS; coding sequence

3.3.4 IncI1 Plasmid Comparisons

Plasmids pCMYN13-02944A and pCMY12-2460C were aligned using the EasyFig tool v2.2.2 to compare genomic differences; this alignment can be found in Figure 3.5[95]. As shown in Figure 3.5, there are four main regions of difference. Region 1 contains a sequence that is identical between the two plasmids but inverted relative to one another, with an insertion of two additional genes between the inversion on pCMY12-2460C which encodes the quaternary ammonium compound resistance protein SugE and *blc* gene which encodes for an outer membrane lipoprotein. Region 2 is a unique region in each plasmid; for pCMY12-2460C, this region contains the genes for the two-component Ccd plasmid addiction system, c*cdA* and *ccdB.* This same region on pCMYN13-02944A contains a gene encoding a hypothetical protein which potentially encodes for a shufflon protein. Region 3 shows an insertion of two additional genes on pCMY12-2460C encoding insertion sequences IS5376 and IS100. Region 4 shows a region encoding insertion sequences that are similar in content but variable in order between the two plasmids. Insertion sequences are highly repetitive which makes it difficult for short-read sequencers such as Illumina to accurately analyze these regions and therefore any differences here are of minute significance. In summary, regions of difference include two unique coding sequences found on pCMYN13-02944A; a gene encoding a hypothetical protein and a putative insertion sequence, and seven unique coding sequences on pCMY12-2460C; *sugE*, *blc*, *ccdA, ccdB,* a region encoding a hypothetical protein, and coding sequences for IS5376 and IS100.

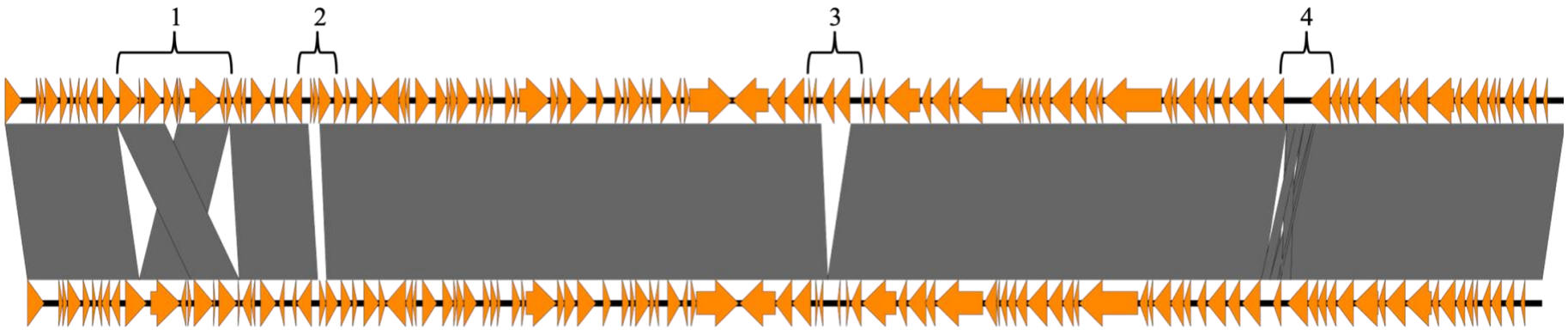


Figure 3.5. Plasmid alignment generated using EasyFig v2.2.2[95]. Plasmid pCMY12-2460C is seen on the top and pCMYN13-02944A is seen on the bottom. Arrows indicate coding sequences oriented in their transcribed direction.

3.4 Plasmid Maintenance Assays

3.4.1 Determination of Plasmid Retention

Determination of plasmid maintenance throughout the growth cycle of *S.* Heidelberg was performed to confirm the maintenance of the plasmids of interest in the absence of selective pressure. Maintenance was determined using the PMAxx™ viability dye and comparing the amount of plasmid template to the chromosomal template during different phases of the growth cycle in viable cells. A reference curve was generated in triplicate for the amplification of *invA* fragments from 10 ng, 1 ng, 100 pg, and 1 pg of *S. enterica* serotype Heidelberg N13-01291 and a melt curve was generated using 1 ng of sample; these results can be found in Figures A21 and A22 of the appendix. The plasmid maintenance results for pCMYN13-02944A and pCMY12-2460C can be found in Figures 3.6-3.7 respectively. For these experiments, the positive controls were N13-01291 containing either pCMYN13-02944A or pCMY12-2460C grown in the presence of 10 μg/mL cefoxitin and harvested at log phase. This was done to determine the ratio of plasmid copies to chromosome copies in viable cells under selective pressure as these growth conditions would only be survivable for a host containing the plasmid of interest. The sample being analyzed was harvested during the stationary phase without selective pressure to determine if the ratio of plasmid copies to chromosome copies was similar to the positive control – indicating plasmid maintenance throughout the growth cycle and in the absence of selective pressure via cefoxitin. As shown in both Figures 3.6 and 3.7, plasmids pCMYN13-02944A and pCMY12-2460C were maintained throughout the growth cycle of their host and in the absence of cefoxitin.

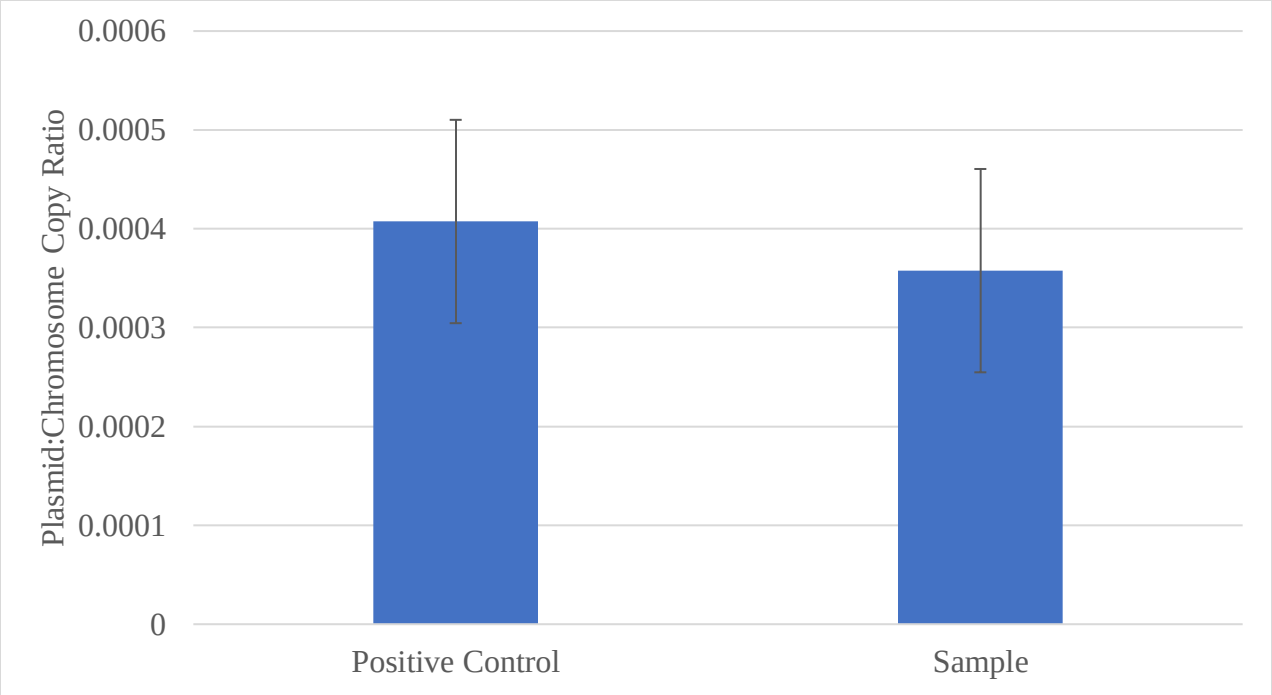


Figure 3.6. Plasmid maintenance assay results for pCMYN13-02944A performed in biological triplicate and technical duplicate using PMAxx™ to isolate DNA from viable cells through qPCR. Error bars indicate standard deviation of replicates.

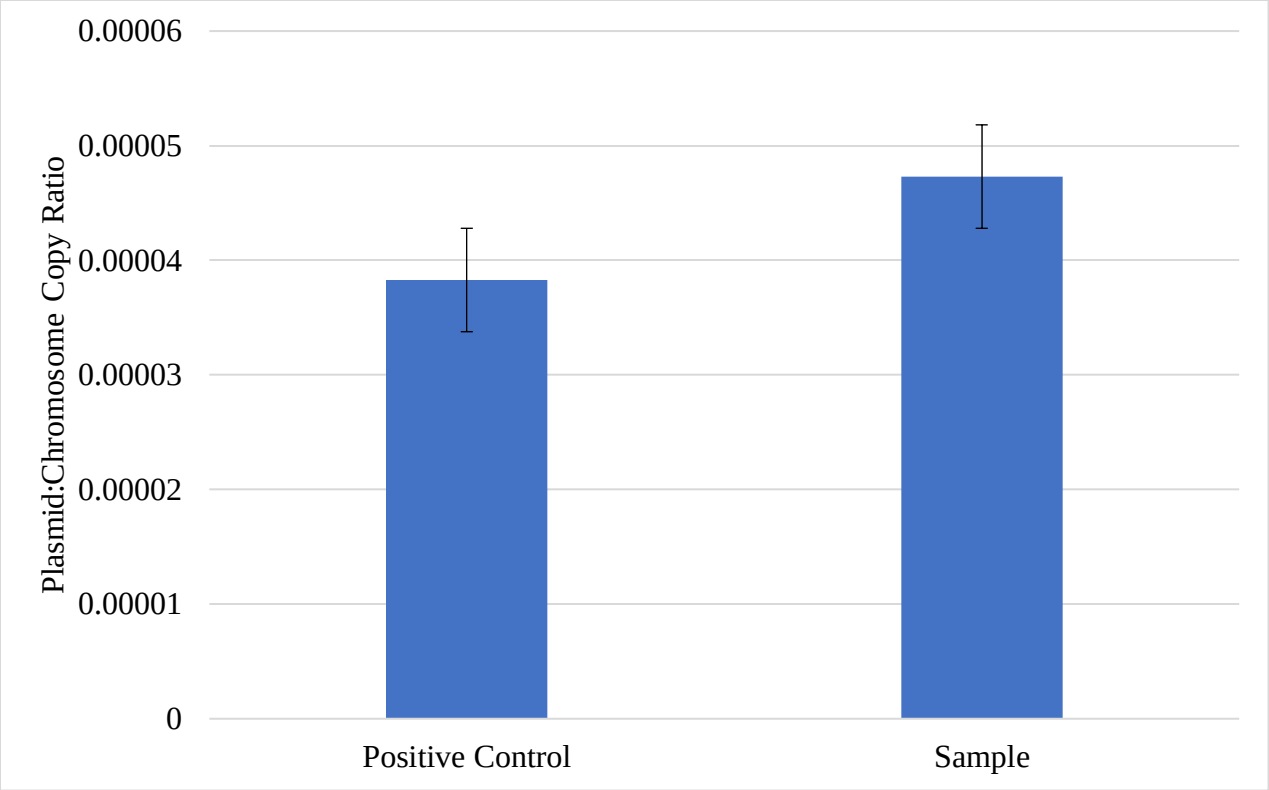


Figure 3.7. Plasmid maintenance assay for pCMY12-2460C performed in biological triplicate and technical duplicate using PMAxx™ to isolate DNA from viable cells through qPCR. Error bars indicate standard deviation of replicates.

3.5 Growth Assays

Analysis of changes in the growth patterns of *S.* Heidelberg in the presence or absence of a CMY-2 plasmid was performed to determine the effects of the CMY-2 plasmids on host fitness. Growth assays were performed in biological triplicate and technical duplicate under various conditions both manually as well as by the Epoch™ 2 Microplate Spectrophotometer (BioTek Instruments, Winooski, VT, USA). Manual readings were performed by removing 1 mL of sample periodically for single cuvette readings of optical density in a spectrophotometer. Conditions analyzed include growth in LB at 30ºC, 37ºC, 42ºC, and growth in M9 minimal salts media at 37ºC. Depending on the instrumentation used, growth was also analyzed in either 20 mL or 100 µL of broth. The results from the growth assays performed at 30ºC and 37ºC that were performed manually in 20 mL of broth show the same growth patterns as those performed using the Epoch™ 2 Microplate Spectrophotometer so the results of these assays will be discussed concurrently based on temperature and media conditions examined; the rest of the results will be discussed individually. The growth curves obtained from the manual assays can be found in Figure 3.8 and the growth curves obtained using the Epoch™ 2 (BioTek Instruments, Winooski, VT, USA) can be found in Figure 3.9. Growth curves of isogenic strain pairs showed that there was variation in growth at different temperatures for each isolate depending on the presence or absence of specific CMY-2 plasmids. Figure 10 was also generated to compare differences in growth at different temperatures for individual isolates.

At 37ºC in LB, the CMY-2-plasmid-free parent isolate reached the log phase at an earlier time interval and reached a higher optical density at the stationary phase than isolates containing a CMY-2 plasmid at an OD600 ≅ 0.62/3.2. The isolate containing pCMYN13-02944A displayed a similarly shaped growth curve to the plasmid-free parent with a delay in reaching the

logarithmic phase of growth and plateaued at a lower maximum optical density than the plasmid-free parent at an OD600 ≅ 0.60/2.9. The isolate containing pCMY12-2460C displayed a more gradual logarithmic growth phase that was nearly biphasic and reached a much lower maximum optical density during the stationary phase at an OD600 ≅ 0.45/2.1.

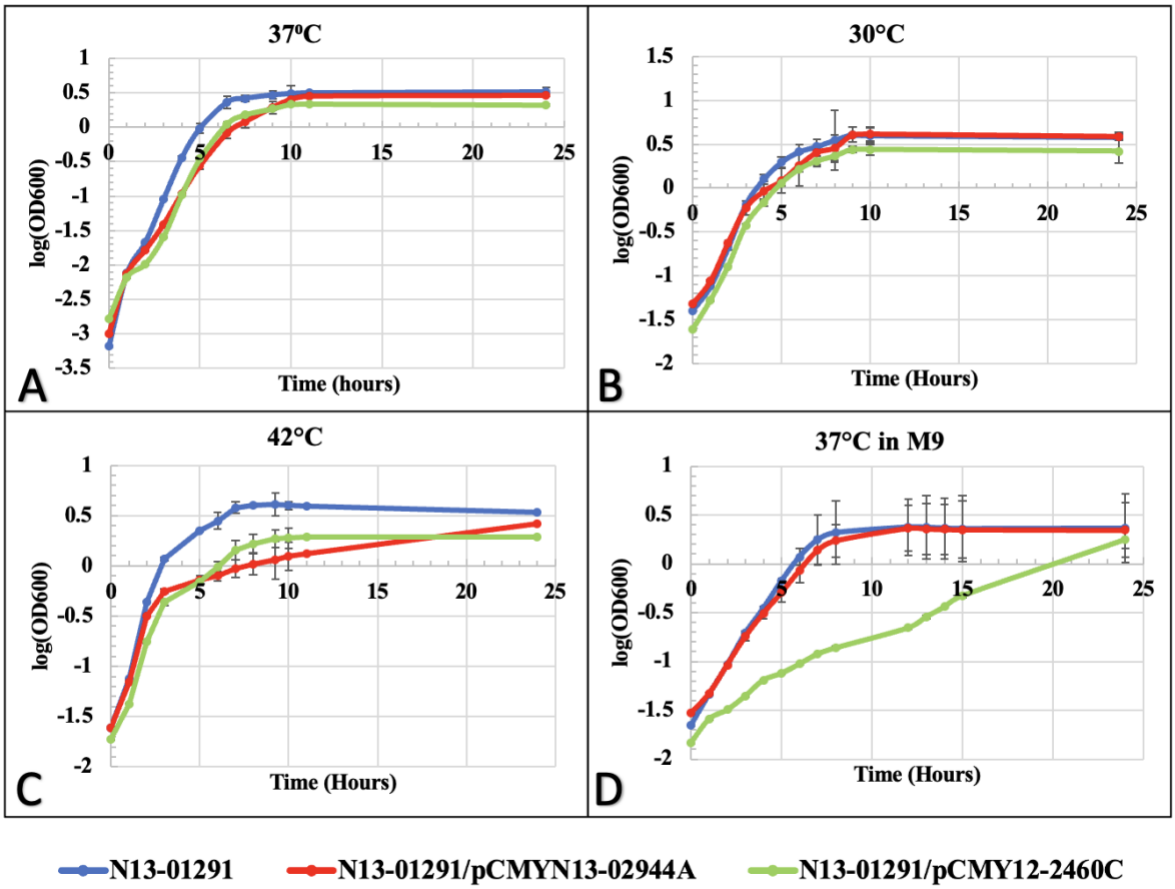


Figure 3.8. Growth curves of *S.* Heidelberg isogenic strain pairs for 24 hours at various temperatures in 20 mL LB broth or M9 minimal salts media with 250 rpm shaking. OD at 600nm was measured approximately every hour using an Eppendorf BioPhotometer spectrophotometer. Error bars represent standard deviation of measurements between replicates of isogenic strain pairs.

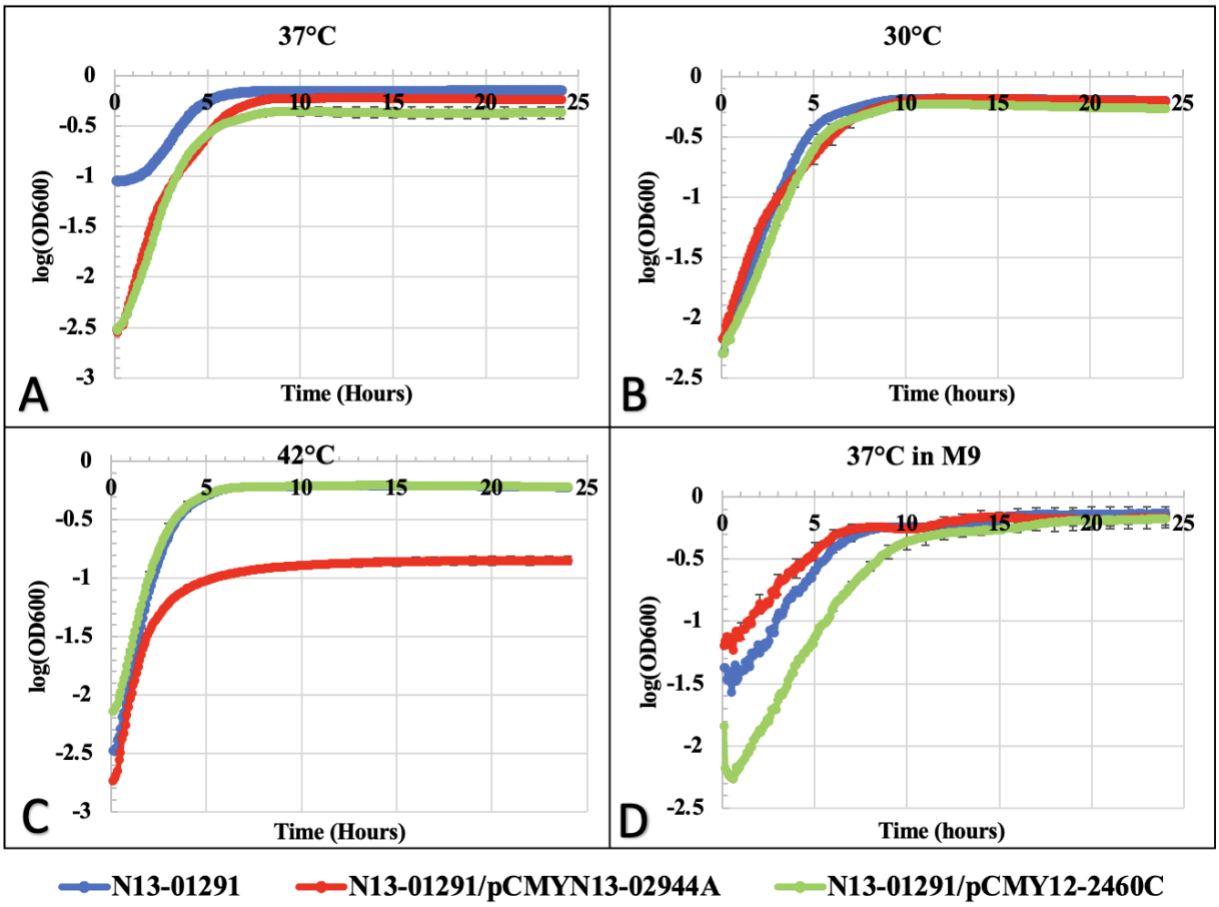


Figure 3.9. Growth curves of S. Heidelberg isogenic strain pairs for 24 hours at various temperatures in 100 µL LB broth or M9 minimal salts media with 280 cpm shaking. OD readings at 600nm were measured every minute in the Epoch™ 2 Microplate Spectrophotometer. Error bars represent standard deviation of measurements between replicates of isogenic strain pairs.

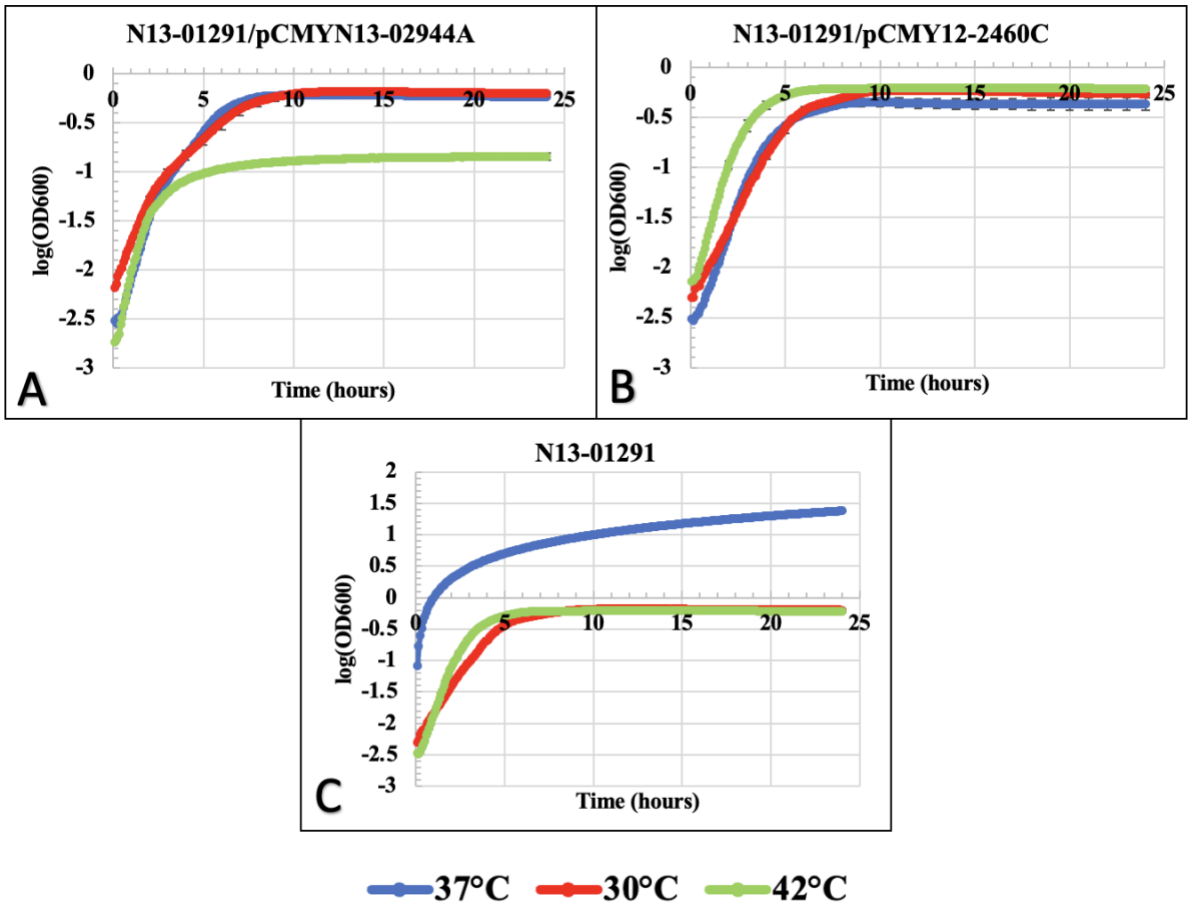


Figure 3.10. Growth curves of *S.* Heidelberg isogenic strain pairs performed in biological triplicate and technical duplicate for 24 hours at various temperatures in 100 µL LB broth with 280 cpm shaking in Epoch™ 2 Microplate Spectrophotometer. Error bars represent standard deviation of measurements between replicates of isogenic strain pairs.

At 30ºC in LB, the CMY-2-plasmid-free parent isolate reached the log phase at an earlier time interval than the other isolates but reached a maximum optical density at the stationary phase that was nearly equivalent to the isolate containing pCMYN13-02944A at an OD600 ≅ 0.63/4.1. The isolate containing pCMYN13-02944A displayed a similarly shaped growth curve to the plasmid-free parent with a delay in reaching the logarithmic phase. The isolate containing pCMY12-2460C displayed a more gradual logarithmic growth phase and reached a much lower maximum optical density during the stationary phase at an OD600 ≅ 0.59/2.7.

At 42ºC in LB via manual reading, the CMY-2-plasmid-free parent isolate displayed a growth curve that was distinct from the plasmid-containing isolates with a much earlier and steep logarithmic growth phase, and a higher maximum optical density at stationary phase at an OD600 ≅ 4.0 that appeared to be decreasing over time. The isolate containing pCMYN13-02944A displayed a linear growth pattern with a maximum optical density that could not be confirmed due to the absence of a plateau in the growth curve. The isolate containing pCMY12-2460C displayed a biphasic growth curve that reached a maximum OD at the stationary phase at an OD600 ≅ 1.9. Due to the manual method of measurement, it appeared that there may have been potential errors or the loss of visualization of distinguishable phases in growth between the last two measurements that were taken approximately 12 hours apart. Due to the automatic nature and serial measuring of the Epoch™ 2 device, this growth curve was repeated with more accurate results and will be described below.

At 42ºC in LB on the Epoch™ 2, the CMY-2-plasmid-free parent isolate displayed a growth curve nearly identical to the isolate containing pCMY12-2460C and both isolates reach a maximum optical density at stationary phase at an OD600 ≅ 0.61. The isolate containing pCMYN13-02944A displayed an extremely flattened growth curve without a distinguishable

logarithmic phase or transition into stationary phase with a maximum optical density at stationary phase at an OD600 ≅ 0.13.

At 37ºC in M9 minimal media via manual reading, the CMY-2-plasmid-free parent isolate displayed a similar growth pattern to the isolate containing pCMYN13-02944A but reached the logarithmic growth phase approximately one hour earlier. These two isolates reached a maximum optical density at the stationary phase at an OD600 ≅ 2.3. The isolate containing pCMY12-2460C displayed an extended lag phase before exhibiting a flattened logarithmic phase and a maximum optical density at stationary phase at an OD600 ≅ 1.8. Due to the delayed growth of the isolate containing pCMY12-2460C and the lack of visualization of an extended stationary phase, this growth assay was repeated using the Epoch™ 2 for 48 hrs instead of 24 and is discussed below.

At 37ºC in M9 minimal media on the Epoch™ 2, all isolates displayed biphasic growth curves with a variable stationary phase. The CMY-2-plasmid-free parent displayed a growth curve that was similar to the isolate containing pCMYN13-02944A, with the latter beginning the log phase marginally earlier. All isolates reached a maximum optical density at the stationary phase at an OD600 ≅ 0.65-0.75 with variability over time.

Isolate N13-01291 displayed a similar growth pattern under all temperatures in LB, with growth at 30ºC displaying a slightly delayed start to the logarithmic growth phase. The isolate containing pCMYN13-02944A displayed similar growth patterns at 30ºC and 37ºC in LB but displayed drastically reduced growth at 42ºC. The isolate containing pCMY12-2460C displayed the most varied growth in the presence of different temperatures with the earliest log phase and highest maximum optical density reached during growth at 42ºC. At 30ºC and 37ºC, this isolate

reached the log phase at the same time but displayed a more biphasic log phase at 30ºC with a higher maximum optical density compared to growth at 37ºC.

3.6 Phenotypic Microarrays

Phenotypic microarrays using the Biolog Omnilog® were performed to examine the effects of pCMYN13-02944A and pCMY12-2460C presence in *S.* Heidelberg N13-01291 on growth under various conditions.

3.6.1 Metabolic Assays

3.6.1.1 N13-01291 vs N13-01291/pCMYN13-02944A

The kinetic data for the metabolic tests (PM 1-10) performed using the Biolog Omnilog® is shown in Figure 3.11 for isolate N13-01291 vs N13-01291/pCMYN13-02944A. The first two phenotypic microarray plates contained kinetic assays that examined growth in the presence of various carbon sources. Overall, the plasmid-free isolate N13-01291 displayed a greater growth rate in the majority of the carbon sources that were tested and had growth. There were five carbon-utilization conditions where the isolate containing the plasmid was able to grow and the plasmid-free parent was not; these conditions were in the presence of formic acid, D-mannitol, L-glutamic acid, a-hydroxyl glutaric acid-y-lactone, and glycolic acid.

Phenotypic microarrays 3, 6, 7, and 8 all tested growth kinetics in the presence of nitrogen sources. In each of these conditions the growth kinetics between isolates was nearly identical with the exception of the presence of L-asparagine where isolate N13-01291/pCMYN13-02944A was not able to grow and isolate N13-01291 grew well.

Phenotypic microarray plate 4 tested growth kinetics in the presence of phosphorus and sulfur. The plasmid-free isolate N13-01291 grew with a slightly greater growth rate in all conditions but overall, both isolates had very similar growth kinetic patterns.

Phenotypic microarray plate 5 tested biosynthetic pathways. The growth pattern for both isolates was identical for the entire plate with plasmid-free isolate N13-01291 having a slightly greater growth rate in all conditions. Both isolates were able to grow in all conditions tested on this plate.

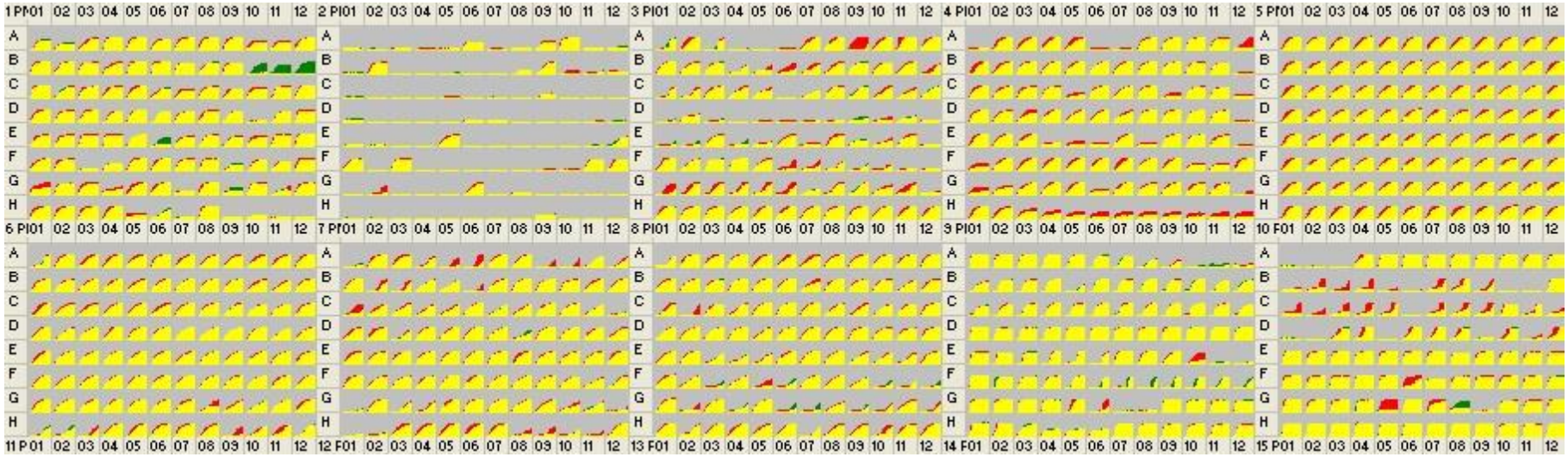


Figure 3.11. Metabolic assays (PM 1-10) comparing the growth kinetics of isolates N13-01291 indicated in red and N13-01291/pCMYN13-02944A indicated in green. Areas where the growth curves of the two isolates overlap are shown in yellow.

Phenotypic microarray plate 9 tested growth kinetics with osmotic and ionic effects. This plate was unique because it tested multiple conditions in the presence of the same solutions but at different concentrations and with different additives. Wells in row A tested growth in the presence of 1%-10% w/v NaCl (including 5.5% and 6.5% NaCl) for 12 concentrations tested total. Growth between both isolates was very similar in all NaCl concentrations with growth diminishing for both isolates as the concentration of salt increased. The contents of the rest of this plate can be found in Figure A9 of the appendix. Growth in these wells was not particularly significant as the growth between isolates was nearly identical.

Phenotypic microarray plate 10 tested the effect of increasing pH, where row A contained a range pHs from increasing from 3.5 to 10. Both isolates were able to grow starting at a pH of 5 and growth was very similar between isolates at pHs 5-10. Rows B, C, and D of plate 10 tested growth kinetics at a pH of 4.5 plus various compounds. Overall, plasmid-free isolate N13-01291 was able to grow at a greater rate and in more conditions than isolate N13-01291/ pCMYN13-02944A. Rows E, F, and G, of plate 10 tested growth kinetics at a pH of 9.5 combined with various compounds such as amino acids; specific contents can be found in Figure A10 of the appendix. Growth in these wells was extremely similar between both isolates aside from three conditions. At a pH of 9.5 in the presence of i) L-tryptophan and ii) cadaverine, the plasmid-free isolate N13-01291 had a significantly greater growth rate compared to the isolate containing pCMYN13-02944A and iii) a pH of 9.5 with phenylethylamine isolate N13-01291/pCMYN13-02944A had a greater growth rate than N13-01291.

3.6.1.2 N13-01291 vs N13-01291/pCMY12-2460C

The kinetic data for the metabolic tests (PM 1-10) is shown in Figure 3.12 for isolate N13-01291 versus N13-01291/pCMY12-2460C. The first two phenotypic microarray plates

contained kinetic assays that examined growth in the presence of a total of 190 various carbon sources; a comprehensive list of carbon sources tested are listed in Figures A1 and A2 of the appendix. Overall, on carbon sources where the plasmid-free isolate N13-01291 was able to grow, this isolate displayed a greater growth rate than N13-01291/pCMY12-2460C. Carbon-utilization conditions where the plasmid-free isolate N13-01291 was able to grow but isolate N13-01291/pCMY12-2460C was not able to grow include growth in glyoxylic acid, 5-keto-D-gluconic acid, L-tartaric acid, L-alaninamide, and L-histidine. There were three carbon-utilization conditions where the isolate containing pCMY12-2460C was able to grow and the plasmid-free parent was not; these conditions were in the presence of formic acid, D-mannitol, and L-glutamic acid.

Phenotypic microarrays 3, 6, 7, and 8 all tested growth kinetics in the presence of nitrogen sources. In each of these conditions, the plasmid-free isolate N13-01291 grew with a greater growth rate, aside from Cys-Gly and Glu-Val where the growth was nearly identical between both isolates.

Phenotypic microarray plate 4 tested growth kinetics in the presence of phosphorus and sulfur. The plasmid-free isolate N13-01291 grew with a greater growth rate in all conditions and grew in conditions where isolate N13-01291/pCMY12-2460C was not able to grow. Conditions where isolate N13-01291 could grow and isolate N13-01291/pCMY12-2460C could not grow included adenosine-3'-5'-cyclic monophosphate, D,L-α-glycerol phosphate, phosphorylcholine, O-phosphoryl-ethanolamine, phosphono acetic acid, methylene diphosphonic acid, D,L-ethionine, taurocholic acid, taurine, hypotaurine, p-amino benzene sulfonic acid, butane sulfonic acid, 2-hydroxyethane sulfonic acid, methane sulfonic acid, tetramethylene sulfone, Lys-Met, Val-Lys, Met- β -Ala, and Leu-β-Ala. Phosphorus and sulfur conditions where neither isolate

could grow included triethyl phosphate, hypophosphite, guanosine-3’-5’-cyclic monophosphate, cytidine-3’-5’-cyclic monophosphate, and thymidine 3’-5’-cyclic monophosphate.

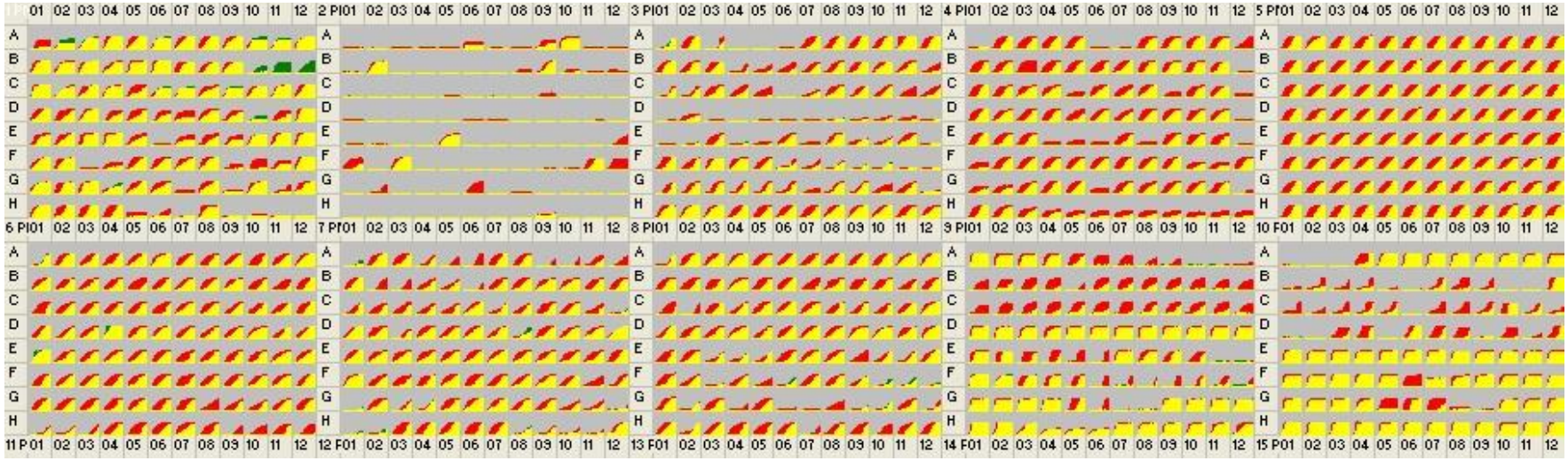


Figure 3.12. Metabolic assays (PM 1-10) comparing the growth kinetics of isolates N13-01291 indicated in red and N13-01291/pCMY12-2460C indicated in green. Areas where the growth curves of the two isolates overlap are shown in yellow.

Phenotypic microarray plate 5 tested biosynthetic pathways. The growth pattern for both isolates was identical for the entire plate for the plasmid-free isolate N13-01291, showing a greater growth rate compared to CMY-2-containing strains in all conditions. Both isolates were able to grow in all conditions tested on this plate.

Phenotypic microarray plate 9 tested growth kinetics with osmotic and ionic effects. This plate was slightly unique because it tested multiple conditions in the presence of the same solutions but at different concentrations and with different additives. Wells in row A tested growth in the presence of 1%-10% w/v NaCl (including 5.5% and 6.5% w/v NaCl for 12 concentrations tested total. Growth between both isolates was very similar from 1-4% w/v NaCl with isolate N13-01291 growing slightly better and better as the concentration increased. Isolate N13-01291/pCMY12-2460C ceased to be able to grow at 5-7% w/v NaCl and neither isolate could grow at NaCl contents greater than 7% w/v. Wells B1-C12 tested 6% w/v NaCl plus various compounds. Plasmid-free isolate N13-01291 was able to grow in all of these conditions and at a greater growth rate than isolate N13-01291/pCMY12-2460C. Row D tested four increasing concentrations of potassium chloride, sodium sulfate, and ethylene glycol respectively. Growth between isolates was nearly identical in these growth conditions with isolate N13-01291 having a slightly greater growth rate. A comprehensive list of well contents and concentrations can be found in Figure A9 of the appendix. Growth in these wells was not particularly noteworthy aside from the fact that plasmid-free isolate N13-01291 was able to grow at higher concentrations than isolate N13-01291/pCMY12-2460C.

Phenotypic microarray plate 10 tested pH effects. Row A contained pHs from 3.5-10. The lowest pH that plasmid-free isolate N13-01291 was able to grow at was a pH of 5 while the lowest pH that isolate N13-01291/pCMY12-2460C was able to grow at was a pH of 5.5. Growth

comparison between isolates N13-01291 and N13-01291/pCMY12-2460C at pH 5.5-10 showed very similar kinetic patterns. Rows B, C, and D of plate 10 tested growth kinetics at a pH of 4.5 plus various compounds. Overall, plasmid-free isolate N13-01291 was able to grow at a greater rate and in more conditions than isolate N13-01291/pCMY12-2460C. Rows E, F, and G, of plate 10 tested growth kinetics at a pH of 9.5 plus various compounds. Growth in these wells was extremely similar between both isolates aside from four conditions. At a pH of 9.5 and in the presence of L-tryptophan, N13-01291 was able to grow and isolate N13-01291/pCMY12-2460C was not able to grow. At a pH of 9.5 and in the presence of cadaverine, putrescine, and histamine, isolate N13-01291 had a much greater growth rate than N13-01291/pCMY12-2460C.

3.6.1.3 N13-01291/pCMYN13-02944A vs N13-01291/pCMY12-2460C

The kinetic data for the metabolic tests (PM 1-10) is shown in Figure 3.13 for isolate N13-01291/pCMYN13-02944A vs N13-01291/pCMY12-2460C. The first two phenotypic microarray plates contained kinetic assays that examined growth in the presence of various carbon sources. The isolate containing pCMYN13-02944A displayed a greater growth rate than the isolate containing pCMY12-2460C in many carbon sources including but not limited to D-aspartic acid, sucrose, glycolic acid, dextrin, D-lactic acid, and tartaric acid. The isolate containing pCMY12-2460C displayed a greater growth rate in the presence of L-arabinose, D-trehalose, D-mannose, L-rhamnose, lactulose, glycyl-L-glutamic acid, and L-threonine. However, under the majority of carbon sources tested, both isolates demonstrated similar growth patterns.

Phenotypic microarrays 3, 6, 7, and 8 all tested growth kinetics in the presence of nitrogen sources. In the majority of conditions tested, the isolate containing pCMYN13-02944A displayed a greater growth rate than the isolate containing pCMY12-2460C. Exceptions to this

included the following: L-asparagine, guanine, xanthine, cystine-glycine, glutamine-valine, methionine-isoleucine, valine-isoleucine, valine-leucine, D-leucine-glycine, and γ-D-glutamate-glycine.

Phenotypic microarray plate 4 tested growth kinetics in the presence of phosphorus and sulfur. The isolate containing pCMYN13-02944A displayed a greater growth rate than the isolate containing pCMY12-2460C in all conditions tested in these plates. One notable difference in growth kinetics was demonstrated in the presence of D, L-α-glycerol phosphate where the isolate containing pCMY12-2460C was unable to grow and the isolate containing pCMYN13-02944A did not display any inhibition to growth.

Phenotypic microarray plate 5 tested biosynthetic pathways. The growth pattern for both isolates was identical for the entire plate with plasmid-free isolate N13-01291/pCMYN13-02944A having a slightly greater growth rate in all conditions. Both isolates were able to grow in all conditions tested on this plate.

Phenotypic microarray plate 9 tested growth kinetics with osmotic and ionic effects. This plate was slightly unique because it tested multiple conditions in the presence of the same solutions but at different concentrations and with different additives. Wells in row A tested growth in the presence of 1%-10% w/v NaCl (including 5.5% and 6.5% w/v NaCl for 12 concentrations tested total. Beginning at a concentration of about 4% NaCl, the isolate containing pCMY12-2460C began to display decreases in growth while the isolate containing pCMYN13-02944A continued to be able to grow until a concentration of 7% w/v NaCl was reached. The isolate containing pCMYN13-02944A also demonstrated greater growth in the

presence of increasing concentrations of sodium lactate and continued to grow past 6% w/v sodium lactate whereas the isolate containing pCMY12-2460C ceased to grow.

Phenotypic microarray plate 10 tested pH effects. Row A contained pH's from 3.5-10. Both isolates demonstrated similar growth throughout the plate, with the main notable difference indicating that the isolate containing pCMYN13-02944A was able to demonstrate some growth in a pH of 4.5 whereas the isolate with pCMY12-2460C demonstrated lesser growth. Both isolates demonstrated equivocal growth starting at a pH of 5. Rows B, C, and D of plate 10 tested growth kinetics at a pH of 4.5 plus various compounds.

Overall, N13-01291/pCMYN13-02944A was able to grow with a greater rate and in more conditions than isolate N13-01291/ pCMY12-2460C. Rows E, F, and G, of plate 10 tested growth kinetics at a pH of 9.5 plus various compounds. Growth in these wells was extremely similar between both isolates aside from four conditions. At a pH of 9.5 in the presence of L-tryptophan, putrescine, histamine, and phenylethylamine, isolate N13-01291/pCMYN13-02944A had a significantly greater growth rate compared to the isolate containing pCMY12-2460C.

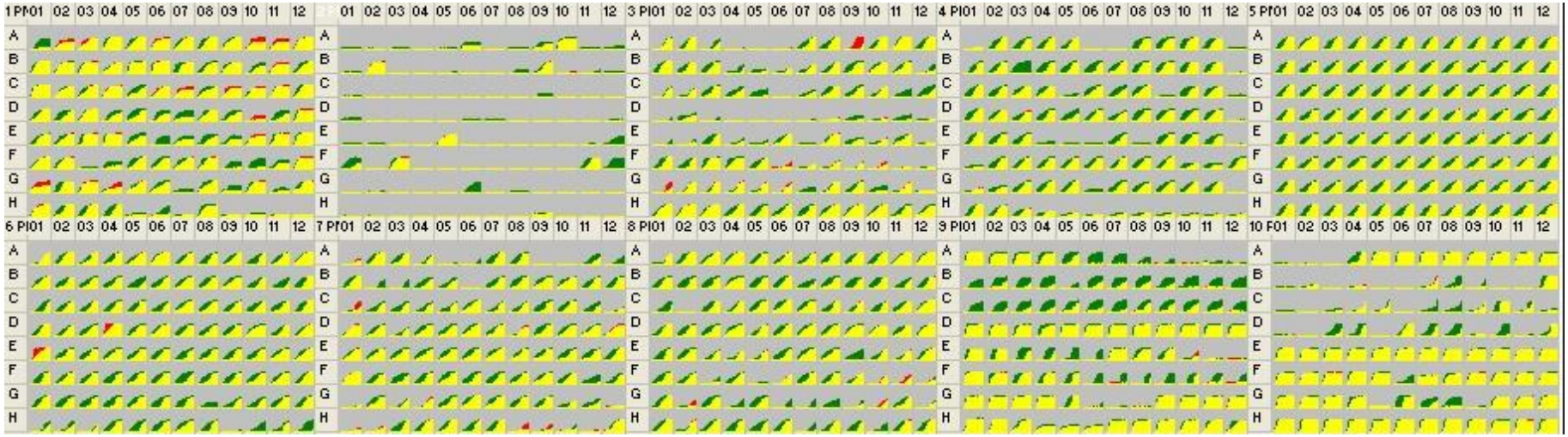


Figure 3.13. Metabolic assays (PM 1-10) comparing the growth kinetics of isolates N13-01291/pCMYN13-02944A indicated in green and N13-01291/pCMY12-2460C indicated in red. Areas where the growth curves of the two isolates overlap are shown in yellow.

3.6.2 Chemical Sensitivity Assays and Comparisons to Sensititre®

Biolog Omnilog® phenotypic microarray plates 11-20 contained various chemical sensitivity assays. The kinetic data for these chemical sensitivity tests (PM11-20) is shown in Figure 3.14 for isolate N13-01291 vs N13-01291/pCMYN13-02944A, in Figure 3.15 for isolate N13-01291 vs. N13-01291/pCMY12-2460C, and in Figure 3.16 for isolate N13-01291/pCMYN13-02944A vs. N13-01291/pCMY12-2460C. Overall, plasmid-containing strains had a greater growth rate during log phase in the presence of lactam, cephalosporin, aminoglycoside, and tetracycline drugs, as well as phleomycin. There were 14 drugs that were tested in both the phenotypic microarrays and with the Sensititre® assays. Sensititre® is an automated system that detects fluorescence liberated by bacterial enzymes that cleave fluorogenic substrates in the growth media and then converts the detected fluorescent signal to a MIC using a computer algorithm to determine measures of antimicrobial susceptibility or resistance[114]. Comparisons of antimicrobial susceptibility interpretations between the Biolog Omnilog® phenotypic microarray plates and the Sensititre® assays are shown in Table 3.7.

When comparing notable differences between the two plasmids, N13-01291/pCMYN13-02944A demonstrated more growth in the presence of higher concentrations of polymyxins and most quinolones. Isolate N13-01291/pCMYN13-02944A also demonstrated greater growth at increased concentrations of many penicillins and other β-lactam drugs including cefotaxime. Isolate N13-01291/pCMY12-2460C demonstrated greater growth at higher concentrations of antimicrobials that inhibit protein synthesis such as chloramphenicol.

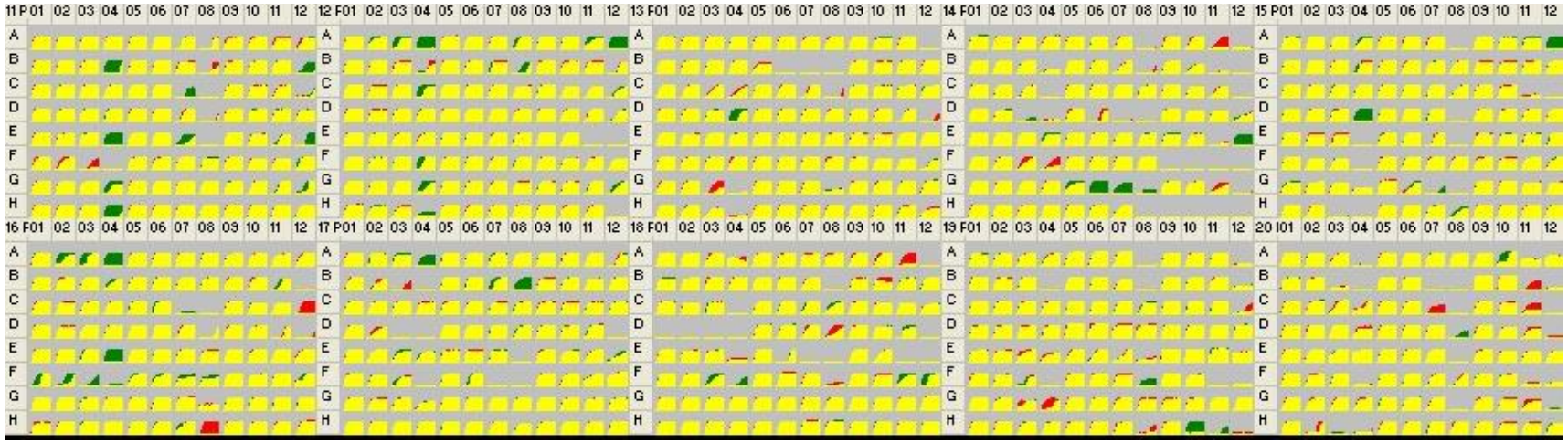


Figure 3.14. Chemical sensitivity assays (PM 11-20) comparing the growth kinetics of isolates N13-01291 indicated in red and N13-01291/pCMYN13-02944A indicated in green. Areas where the growth curves of the two isolates overlap are shown in yellow.

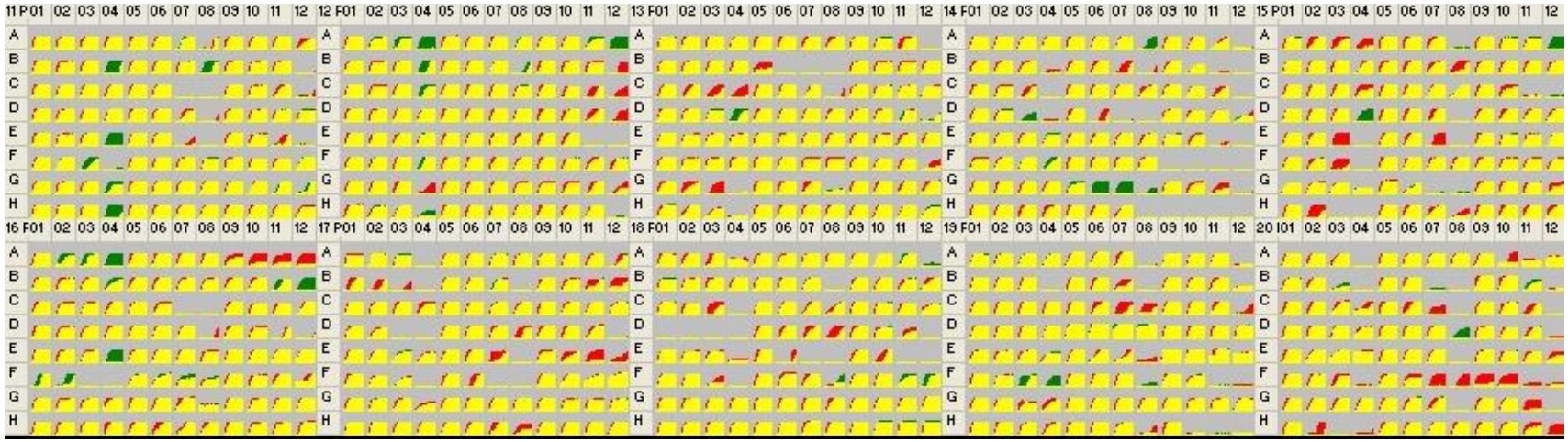


Figure 3.15. Chemical sensitivity assays (PM 11-20) comparing the growth kinetics of isolates N13-01291 indicated in red and N13-01291/pCMY12-2460C indicated in green. Areas where the growth curves of the two isolates overlap are shown in yellow.

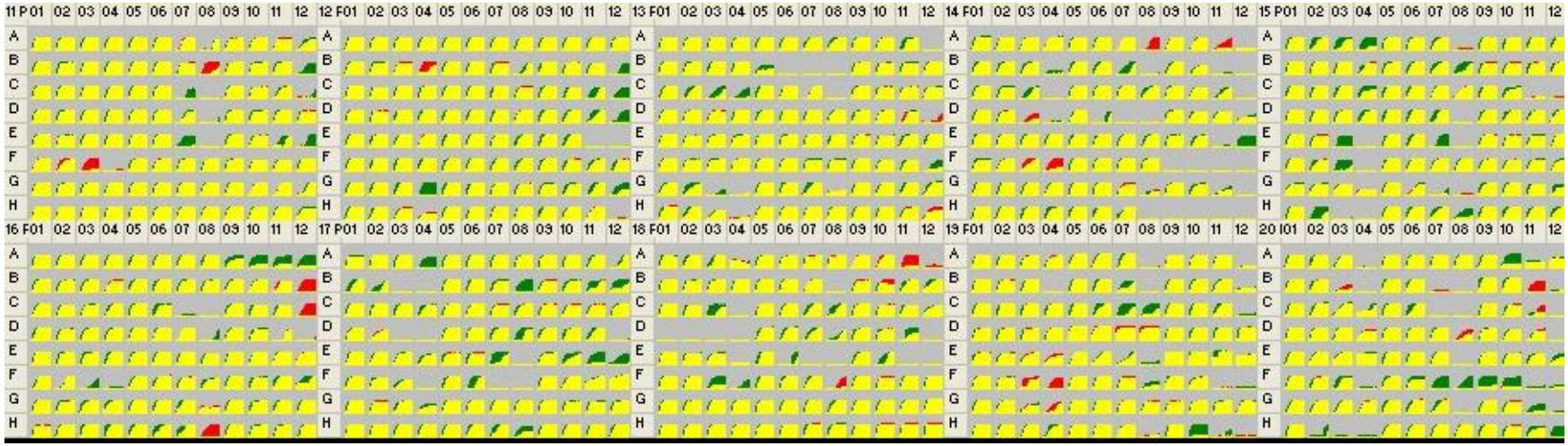


Figure 3.16. Chemical sensitivity assays (PM 11-20) comparing the growth kinetics of isolates N13-01291/pCMYN13-02944A indicated in green and N13-01291/pCMY12-2460C indicated in red. Areas where the growth curves of the two isolates overlap are shown in yellow.

Table 3.7. Antimicrobial susceptibility testing results from the Sensititre® analyses as compared to the results from the Biolog Omnilog® phenotypic microarray plates*. There were no sensitivity results that were found to be concordant between these two methods of AST.

Drug	N13-01291		N13-01291/pCMYN13-02944A		N13-01291/pCMY12-2460C	
	Sensititre® Result	**PM Result**	**Sensititre® Result**	**PM Result**	**Sensititre® Result**	**PM Result**
Amoxicillin/Clavulanic Acid	1 S	R 1-3, S 4	32 R	R 1-4	32 R	R 1-4
Ampicillin	1 S	R 1-4	32 R	R 1-4	32 R	R 1-4
Azithromycin	4 NI	N/A	8 S	N/A	8 S	N/A
Cefoxitin	2 S	R 1-4	32 R	R 1-4	32 R	R 1-4
Ceftriaxone	0.25 S	R 1-3, I 4	64 R	R 1-4	32 R	R 1-4
Chloramphenicol	8 S	R 1-2, I 3, S 4	8 S	R 1-2, I 3, S 4	16 I	R 1-3, S 4
Ciprofloxacin	0.03 S	R 1-3, S 4	0.06 S	R 1-3, I 4	0.06 S	R 1-4
Gentamicin	0.5 S	R 1-4	4 S	R 1-4	2 S	R 1-4
Meropenem	0.06 S	N/A	0.06 S	N/A	0.06 S	N/A

Nalidixic Acid	4 S	R 1-3, S 4	32 R	R 1-3, I 4	32 R	R 1-2, I 3, S 4
Streptomycin	32 R	R 1-3, S 4	64 R	R 1-4	64 R	R 1-4
Sulfisoxazole	32 S	R 1-4	32 S	R 1-4	64 S	R 1-4
Tetracycline	4 S	R 1-4	4 S	R 1-4	4 S	R 1-4
Trimethoprim/Sulfamethoxazole	0.12 S	R 1-2, I 3, S 4 / R 1-4	0.12 S	R 1-3, S4 / R1-4	0.25 S	R 1-4 / R 1-4

*S = susceptible, I = intermediate, R = resistant

3.7 Biofilm Assays

Biofilm formation was quantified by growing the isogenic strain pairs at 37°C for 24 hours, rinsing loose cells away, and staining remaining biomass using 0.1% CV (w/w) for 30 minutes. After overnight drying of the biofilm assay plates, CV was solubilized with 30% acetic acid in water (w/v) and absorbance of each well was measured at 600nm. The absorbance of each well was measured at 600 nm using 30% acetic acid as a blank. This experiment was performed to determine the incidence of biofilm formation in various strains of *S.* Heidelberg. The strain information for the isolates tested can be found in Table 3.8 and the results of the biofilm formation assays can be found in Figure 3.17. There were 18 strains of *S.* Heidelberg tested against the controls in this experiment, some of which contained group A, B, or C CMY-2 plasmids. Of those 18, all were found to be poor biofilm producers when compared to the positive control (*E. coli* ATCC 9522). Due to the overall lack of biofilm formation, any potential variations in biofilm formation between isolates due to the presence of various IncI1 plasmids could not be analyzed.

Table 3.8. *S.* Heidelberg isolates tested for biofilm formation; these isolates were previously described by Edirmanasinghe et al., 2017[46].

Strain ID	Province	Year	Source	Resistance phenotypes	Resistance genotypes	ST	Plasmid(s)	Size of blaCMY2 contig	ST of blaCMY2 plasmid	Group of Plasmid
12-1195	QC	2012	Human stool	AMC, AMP, FOX, TIO, CRO	*bla CMY2*	15	IncI1, IncX1, ColpVC	48418; 28410; 23779	12	
12-2460	QC	2012	Human stool	AMC, AMP, FOX, TIO, CRO	*bla CMY2*	15	IncI1, IncX1, ColRNAI	99125	12	C
12-4585	QC	2012	Human stool	AMC, AMP, FOX, TIO, CRO	*bla CMY2*	15	IncI1, IncX1, ColpVC, IncFII	96616	12	A
12-6245	QC	2012	Human stool	AMC, AMP, FOX, TIO, CRO	*bla CMY2*	15	ColRNAI	Plasmid integrated into Chromosome		NA
12-1016	QC	2012	Human stool	AMC, AMP, FOX, TIO, CRO, (CHL)	*bla CMY2*	15	IncI1, IncX1, ColpVC, ColRNAI	96047; 1108	12	A
12-3327	QC	2012	Human stool	Susceptible	*None*	15	IncX1	NA	NA	NA

12-3461	QC	2012	Human stool	Susceptible	*none*	15	IncX1, ColpVC	NA	NA	NA
12-7730	QC	2012	Human stool	Susceptible	*None*	15	IncX1, ColpVC	NA	NA	NA
12-5335	QC	2012	Human blood	AMC, AMP, FOX, TIO, CRO	*bla CMY2*	15	IncI1, IncX1, ColRNAI	99577	12	C
12-7092	QC	2012	Human blood	AMC, AMP, FOX, TIO, CRO	*bla CMY2*	15	IncI1	99675	12	C
12-3792	QC	2012	Human (unknown)	AMC, AMP, FOX, TIO, CRO	*bla CMY2*	15	IncI1, IncX1	100625; 1219	12	A
N13-02944	NB	2012	Animal cecal content (chicken)	AMC, AMP, FOX, TIO, CRO	*bla CMY2*	15	IncI1, IncX1, ColpVC	96280	12	A
N13-01291	QC	2012	Animal cecal content (chicken)	Susceptible	*None*	15	IncX1, ColpVC	NA	NA	NA
N13-01313	QC	2012	Food aliquot (turkey)	AMC, AMP, FOX, TIO,	*aadA1, blaCMY2, blaTEM-*	15	IncI1, ColpVC, ColRNAI,	82151; 12485; 5833	25	

				CRO, STR, SUL, TET	*1B, straA, strB, sul1, tetB*		Col156, IncHI2, IncHI2A			
N13-01323	QC	2012	Animal cecal content (chicken)	Susceptible	*None*	15	IncX1, ColpVC, ColRNAI	Na	NA	NA
N13-01326	QC	2012	Food aliquot (turkey)	AMP	*blaTEM-1B*	15	IncI1, IncX1, ColRNAI	NA	NA	NA
N13-01366	QC	2012	Food aliquot (turkey)	TET	*tetB*	15	IncI1	NA	NA	NA
N13-01304	QC	2012	Food prepackaged (chicken)	AMC, AMP, FOX, TIO, CRO	*blaCMY2*	15	IncI1, IncX1	73672; 20599; 5280; 1108	12	A
N13-01318	QC	2012	Food prepackaged (chicken)	AMC, AMP, FOX, TIO, CRO	*blaCMY2*	15	IncI1, IncX1	103897	12	B
N13-01342	QC	2012	Food aliquot (chicken)	AMC, AMP, FOX, TIO, CRO	*blaCMY2*	15	IncI1, IncX1, ColpVC, Col156	98725	12	C

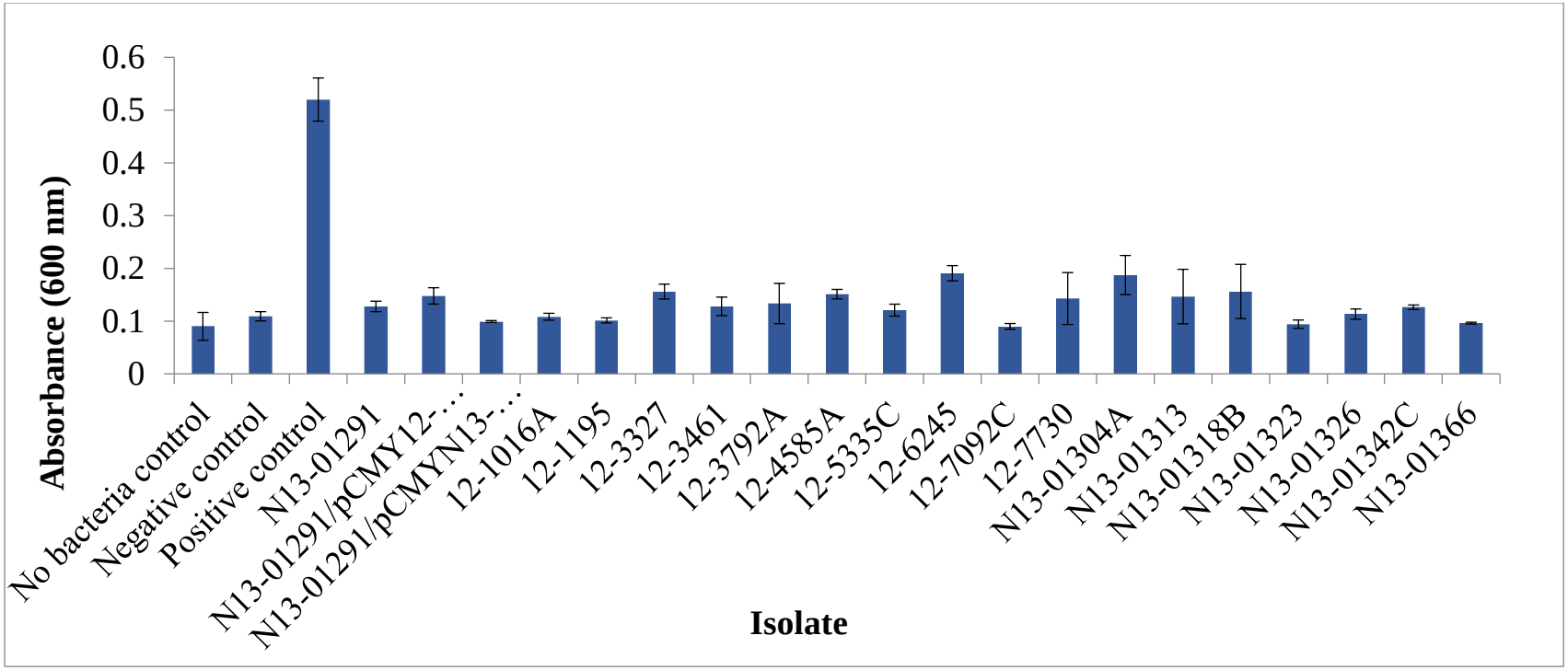


Figure 3.17. Biofilm content determination was based on absorbance readings at 600nm after staining with crystal violet. Negative control used was Salmonella Typhimurium LT2 and the positive control used was E. coli ATCC 9522.

3.8 Proteomics

3.8.1 General

To analyze the effects that plasmids may have upon chromosomal expression of proteins, a proteomic analysis of *S.* Heidelberg in the presence of two similar IncI1 plasmids was performed. Samples were run in parallel, meaning that isogenic strain pairs (one containing the IncI1 plasmid and one without the IncI1 plasmid) were analyzed at the same time.

In total, 2752 proteins were detected by LC/MS/MS for the run comparing isolates N13-01291 and N13-01291/pCMYN13-02944A. Of these, 2295 proteins were detected with a Mann-Whitney significance of $p < 0.05$. There were 341 significantly detected proteins that had a $\log_2$-fold-change ≥ 1 (2-fold change) and 72 that had a $\log_2$-fold-change ≥ 2 (4-fold change).

There were 2940 proteins detected by LC/MS/MS for the run comparing isolates N13-01291 and N13-01291/pCMY12-2460C. Of these, 2215 proteins were detected with a Mann-Whitney significance of $p < 0.05$. There were 415 significantly detected proteins that had a $\log_2$-fold-change ≥ 1 (2-fold) and 96 had a $\log_2$-fold-change ≥ 2 (4-fold). When comparing the proteins that had changes in expression in the presence of either plasmid, there were 87 chromosomally derived proteins that were altered in the presence of both pCMYN13-02944A and pCMY12-2460C; these proteins can be found in Table A2 of the appendix.

3.8.2 Functional Annotation

The GhostKOALA v2.0 tool was used to group the results of the proteomic analysis based on functional pathways. The functional annotation for the 341 proteins that were significantly ($p<0.05$) detected for isolate N13-01291/pCMYN13-02944A can be found in Figure 3.18. Of these 341 proteins, 32.0% were unable to be annotated, 11.7% belonged to carbohydrate metabolism pathways, 7.0% belonged to environmental information processing pathways, 6.2% belonged to various unclassified metabolism pathways, 5.9% belonged to amino acid metabolism pathways, 5.3% of proteins belonged to cellular processes, 5.0% belong to protein families involved with genetic information processing, 4.7% of proteins were able to be annotated but had unclassified functions, 4.4% were involved in energy metabolism, and 4.4% of these proteins belonged to protein families involved with signalling and cellular processes. The remaining 13.7% of proteins were classified into various groups with no more than 2.3% of proteins belonging to a single functional category.

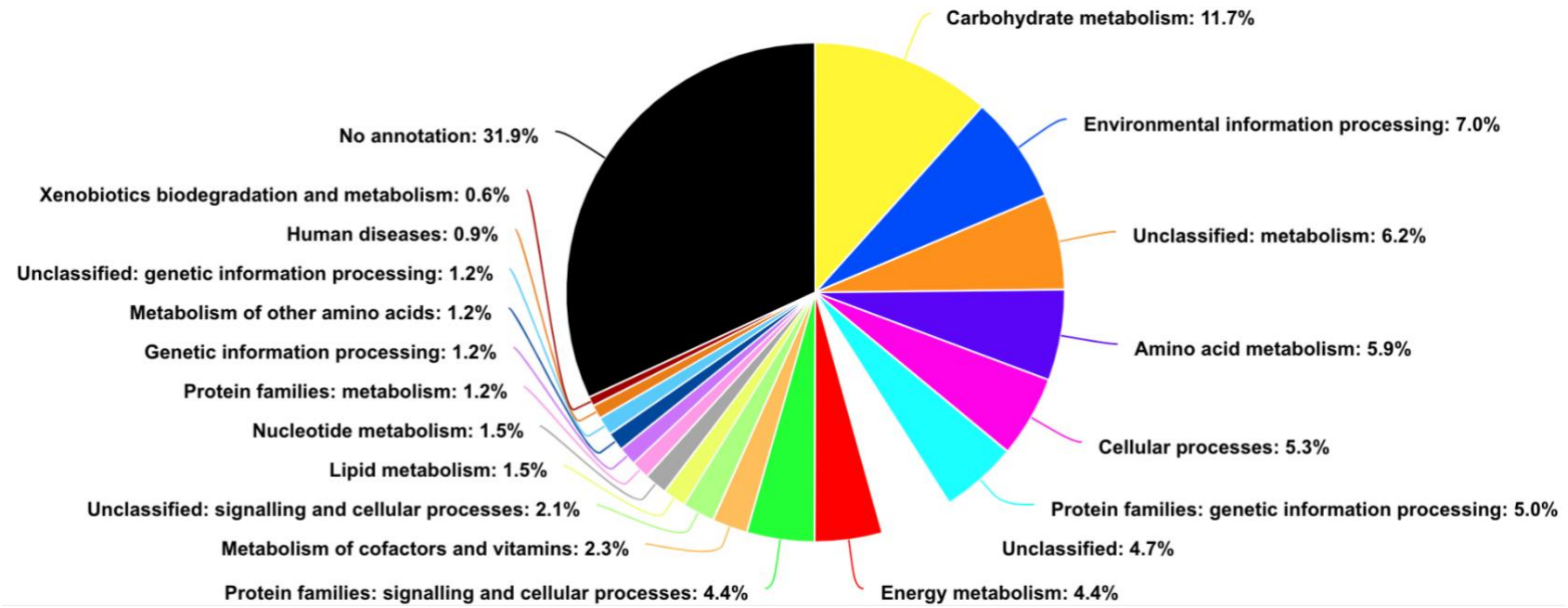


Figure 3.18. Functional annotation of 341 significantly ($p<0.05$) detected proteins with a 2-fold or greater change in regulation in the presence of pCMYN13-02944A.

The functional annotation for the 415 proteins that were significantly ($p<0.05$) detected for isolate N13-01291/pCMY12-2460C can be found in Figure 3.19. Of these 415 proteins, 28.0% were unable to be annotated, 12.0% belonged to environmental information processing pathways, 10.8% belonged to protein families involved with signalling and cellular processing, 8.2% belonged to carbohydrate metabolism pathways, 6.0% belonged to energy metabolism pathways, 5.8% belonged to various unclassified metabolism pathways, 4.1% belonged to amino acid metabolism pathways, 3.9% belonged to protein families involved with genetic information processing, and 3.4% were involved in the metabolism of cofactors and vitamins. The remaining 17.8% of proteins were classified into various groups with no more than 2.7% of proteins belonging to a single functional category.

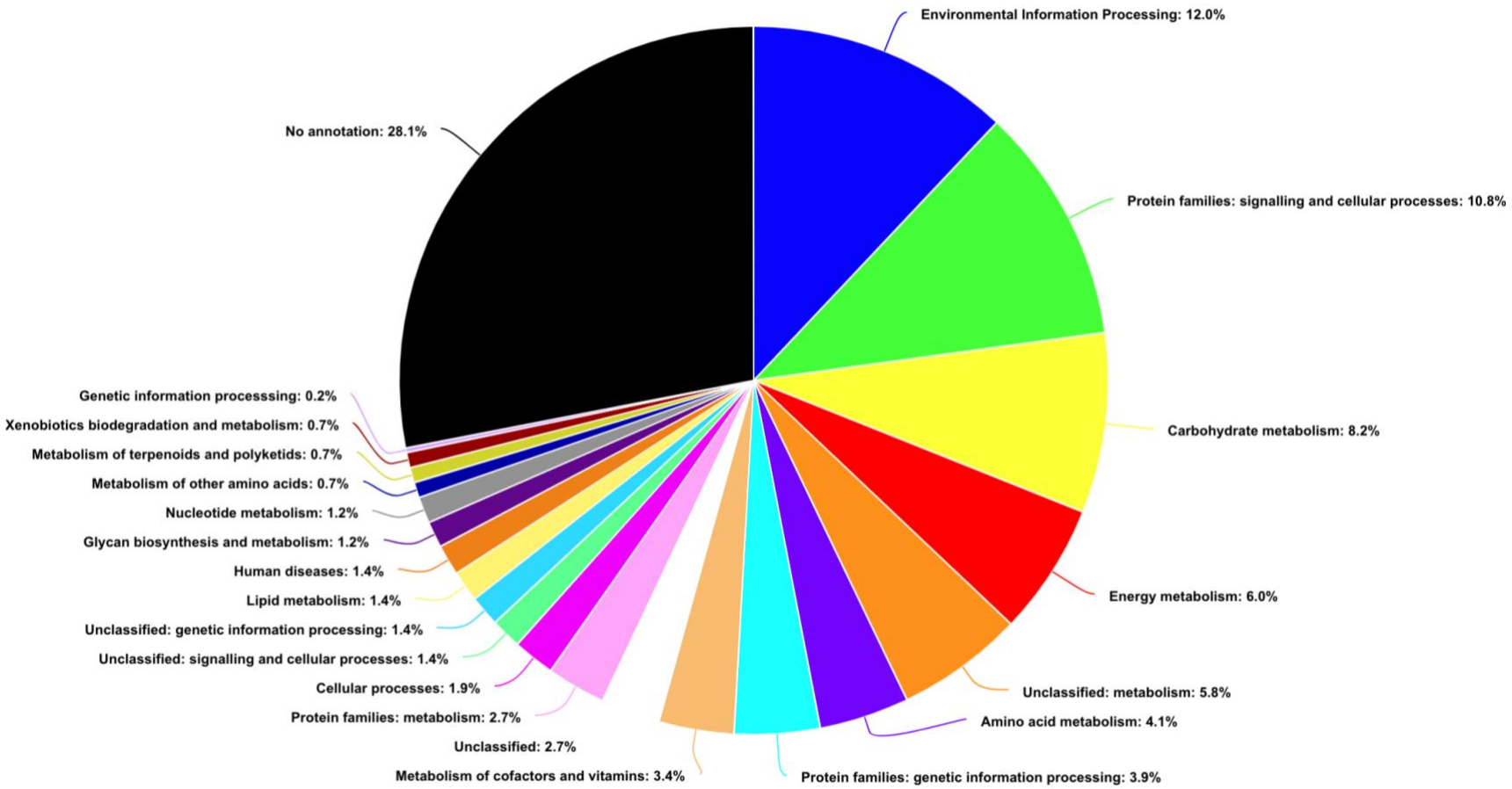


Figure 3.19. Functional annotation of 415 significantly ($p<0.05$) detected proteins with a 2-fold or greater change in regulation in the presence of pCMY12-2460C.

3.8.3 Protein Structures

The Phyre2 (Protein Homology/analogY Recognition Engine v2.0) was used to model the three proteins modified by core-genome SNVs in the presence of the CMY-2 plasmids; i) MshA_1, ii) UbiB, iii) CpxA, these results are displayed in figures 3.20-3.22[106]. This analysis was performed to identify any obvious changes in protein structure due to the presence of the identified SNVs.

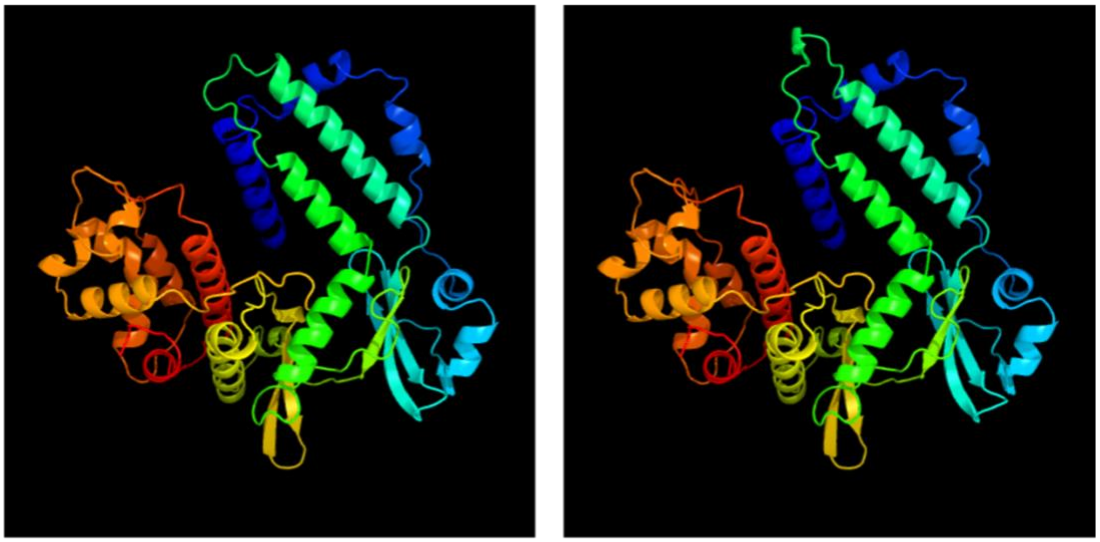


Figure 3.20. 3D model of UbiB designed using the Phyre2 server. (A) UbiB structure from CMY-2-plasmid-free isolate N13-01291. (B) UbiB structure from N13-01291/pCMYN13-2944A containing glutamine to leucine mutation. Images are coloured by rainbow N to C terminus.

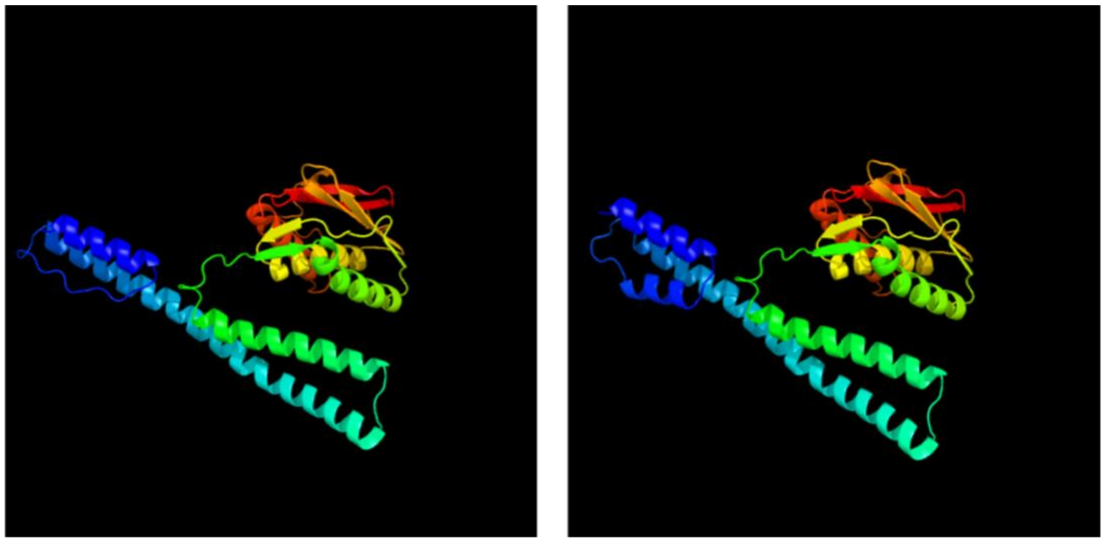


Figure 3.21. 3D model of CpxA designed using the Phyre2 server. (A) CpxA structure from CMY-2-plasmid-free isolate N13-01291. (B) CpxA structure from N13-01291/pCMY12-2460C containing leucine to arginine mutation. Images are coloured by rainbow N to C terminus.

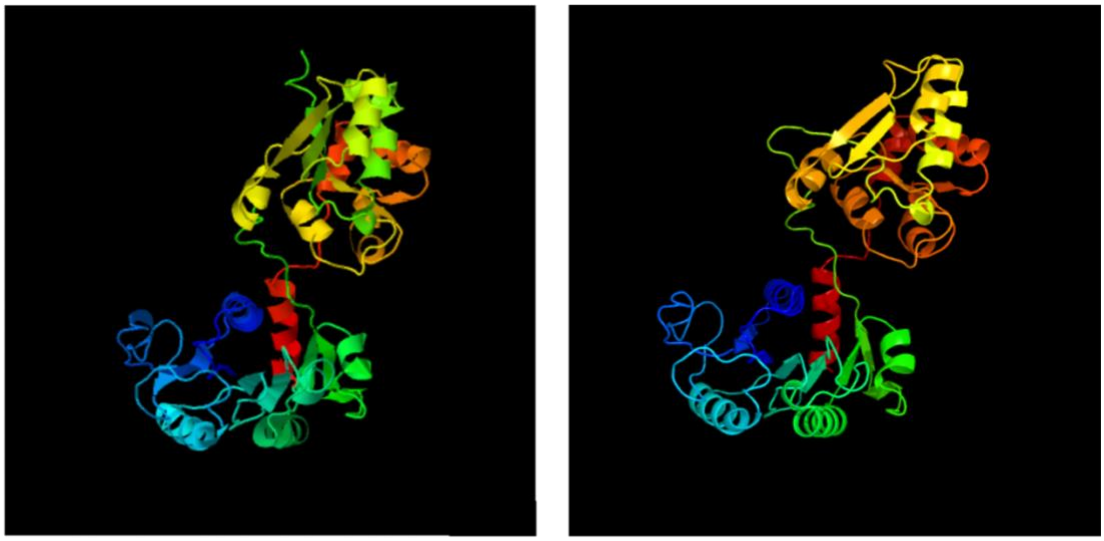


Figure 3.22. 3D model of MshA_1 designed using the Phyre2 server. (A) MshA_1 structure from CMY-2-plasmid-free isolate N13-01291. (B) CpxA structure from N13-01291/pCMY12-2460C containing leucine to arginine mutation. Images are coloured by rainbow N to C terminus.

4. Discussion

This study was performed to determine if an isolate, labelled N13-01291, combined with a specific IncI1 plasmid variant, pCMYN13-02944A or pCMY12-2460C, leads to heightened bacterial fitness or virulence through the alteration of chromosomal gene expression and proteomic expression. To examine this hypothesis, isogenic strain pairs were generated containing either plasmid and analyzed for genomic and proteomic changes in expression when compared to the susceptible plasmid-free parent isolate.

4.1 Comparison of pCMYN13-02944A and pCMY12-2460C

The CMY-2 plasmids analyzed in this study belong to incompatibility group I1 (IncI1), a group that is widely found in *Salmonella* from food animal sources such as chickens[115]. These plasmids are known for their potential to carry AMR genes such as the ones in this study which carry *bla*$_{\text{CMY-2}}$[115]. The plasmids analyzed in this study share a large portion of identical coding regions, approximately half of which is dedicated to plasmid transfer such as genes for the formation of pilus and conjugative transfer mechanisms. These plasmids also contain genes for colicin biosynthesis and immunity as well as various insertion sequences and coding sequences that do not yet have an identified or confirmed function.

A comparison of the two IncI1 plasmids used in this study showed that pCMYN13-02944A contains one unique region compared to the similar plasmid pCMY12-2460C. This region encodes for a hypothetical protein. Plasmid pCMY12-2460C contains three unique regions compared to plasmid pCMYN13-02944A. The first region encodes for 2 hypothetical proteins with similarities to insertion sequences and the SugE protein responsible for tolerance to quaternary ammonium compounds, the second region encodes for the toxin and antitoxin

components of the *ccd* addiction system (*ccdA* and *ccdB*), and the third region encodes two insertion sequences. Further differences include an inversion of the area containing the $bla_{\text{CMY-2}}$ gene and a region of variable repeat sequences that appears to encode insertion sequences. A BLAST analysis of these two plasmids indicates a 99.55% identity on the DNA level between the two[110]. Despite this large similarity, the isolate harbouring these plasmids show significant differences in their growth dynamics and phenotypes as well as their proteomic expression when compared to each other as well as their CMY-plasmid-free parent isolate N13-01291.

4.2 Phylogenomics

Phylogenomic analysis of isolates N13-01291/pCMYN13-2944A and N13-01291/pCMY12-2460C was performed to examine the relatedness and isogenicity of the strain pairs formed in this study. This analysis indicated that the addition of either CMY-2 plasmid resulted in 2 core-genome SNVs, one of which was identical between the isogenic pairs. There is no defined value for the allowable number of SNVs between *S.* Heidelberg isolates that can still be deemed "related"; however, a study by Bekal *et al.* determined that a maximum number of 4 SNVs between isolates could be used to cluster isolates to the same outbreak[111]. Using this definition of relatedness, these pairs can be defined as closely related or isogenic since there is a maximum of two SNVs differentiating each isolate[116].

4.2.1 Shared SNV in the Presence of Either pCMYN13-02944A or pCMY12-2460C

The addition of either plasmid resulted in a cytosine to adenine change that led to an aspartate to tyrosine amino acid in the chromosomal *mshA_1*. The *mshA_1* gene encodes for the protein D-inositol 3-phosphate glycosyltransferase which catalyzes a reaction in the biosynthesis of mycothiol, which has the ability to detoxify antibiotics[117,118]. While mycothiol in *Salmonella* is not well characterized, mycothiol has been shown to act as an antioxidant that can maintain the

reducing environment of the bacterial cell in *Mycobacterium tuberculosis* and *Actinobacteria*[118,119]. In *Salmonella* Derby, *mshA* has been identified as an essential gene for survivability under acid stress, which helps to enhance the pathogenesis of its host[120]. *Salmonella* infection requires surviving stressful conditions such as the low pH of the gastric environment within an acidified macrophage that may have an external pH of 4-5[120]. Acidic conditions have been theorized to induce the expression of virulence genes, and therefore this could be a possible effect that pCMYN13-02944A is exerting on its host by affecting this pathway via SNP in *mshA_1*[120].

4.2.2 Unique SNV in the Presence of Plasmid pCMY-N13-02944A

In the presence of pN13-02944A, there was a thymine-to-adenine base pair change that resulted in a glutamine-to-leucine amino acid change in UbiB. The *ubiB* gene encodes for a putative protein kinase that is hypothesized to act as a regulator for the ubiquinone biosynthesis pathway [121]. Ubiquinone, also known as coenzyme Q, is located in the bacterial plasma membrane and plays an important role in energy-generating processes[121]. These energy-generating processes are important as they play a role in aerobic respiratory growth, the import of nutrients, oxidative stress adaptation, protein secretion, and cell motility[122]. A 2014 study by Aussel *et al.* demonstrated that UbiB is essential for *Salmonella* intracellular proliferation in macrophages and therefore plays an important role in virulence[122]. This study indicated that *ubiB* mutants did not synthesize coenzyme Q under anaerobic conditions and showed changes in growth in the presence of various carbon sources such as fumarate, nitrate, and TMAO[122]. While the specific role of UbiB remains unclear, it is possible that alterations in this gene could lead to alterations in the survivability of the host in various conditions as well as affecting virulence pathways.

4.2.3 Unique SNV in the presence of plasmid pCMY-12-2460C

In the presence of p12-2460C, there was a thymine-to-guanine base pair change that resulted in a leucine-to-arginine amino acid change in CpxA at position 38. The *cpxA* gene encodes for a sensor histidine kinase which is a member of a two-component regulatory system involved in the bacterial response to envelope stress and is essential for surviving acid stress[123,124]. As well, the CpxRA system has shown that this two-component system also plays a role in multidrug resistance, particularly to aminoglycosides and β-lactams in *S.* Typhimurium[124]. A 2020 study by Jing *et al* investigated the effect of the L38F mutation in CpxA and discovered that this variant constitutively induced activation of the Cpx system, resulting in increased resistance to antimicrobials[125]. Furthermore, in a 2021 study by Jing *et al* that investigated the role of *cpxA* mutants in *Salmonella*, it was found that all tested *cpxA* mutations resulted in conferred resistance to aminoglycosides and β-lactams as determined by CLSI guidelines[124]. A possible mechanism for this finding was that *cpxA* mutants can help to confer AMR by reducing the production of reactive oxygen species, which is a common mechanism of action for bactericidal antibiotics[124].

Proteomic analysis of N13-01291 with and without p12-2460C indicated that in the presence of p12-2460C, CpxA had a $\log_2$-fold change of 1.63. This observation indicates that the addition of this antimicrobial-resistance-conferring plasmid not only affects host AMR through the direct addition of the *bla*$_{\text{CMY-2}}$ gene but also through the regulation of host proteins that play a role in AMR. The upregulation and mutation of this histidine kinase may increase resistance to aminoglycosides and β-lactams, which would confer an additional benefit to the host of p12-2460C.

4.3 Plasmid Effects on Fitness and Pathogenicity

4.3.1 Plasmid Viability and Maintenance

An important consideration while studying changes in growth and proteomic expression in the presence of a plasmid is to ensure that any possible confounding factors that could cause changes are removed. In the case of this study, the presence of an antimicrobial that would select for the presence of certain plasmids could possibly cause changes in growth kinetics. However, without the selective pressure of an antimicrobial, there is a concern that the plasmid will no longer be maintained by the host throughout the growth cycle. For this reason, plasmid maintenance during growth in the absence of a selective antibiotic was analyzed. These maintenance experiments were able to confirm that the CMY-2 plasmids are maintained throughout the growth cycle with or without selective pressure from cefoxitin. This result allowed us to infer that any changes in growth or proteomic expression that were seen in further experiments were due to the presence of the plasmids of interest alone, or the chromosomal point mutations described above.

The results seen in the plasmid maintenance experiments were expected due to the presence of addiction systems on each plasmid; the sequence of pCMYN13-02944A contains only the PndAC addiction system while pCMY12-2460C contains both the PndAC addiction system and the CcdAB addiction system. As described in the introduction, addiction systems work through a toxin-antitoxin system that will kill the host if the plasmid is ejected[29]. The presence of these addiction systems on the CMY-2 plasmids is likely the reason that these plasmids are maintained in the absence of selective pressure.

4.3.2 Growth Curves

Growth assays can be used as an observable indicator to predict underlying changes in genomic or proteomic expression due to the presence of a plasmid. In this study, growth assays were performed using various temperatures, mediums, volumes, and machinery. The goal of these experiments was to determine differences that occurred due to the presence of either pCMYN13-02944A or pCMY12-2460C, however, it is important to note that there are many variables at play that can be difficult to control. All growth assays were performed both manually at a volume of 20 mL in Erlenmeyer flasks and mechanically at a volume of 100 µL in a 96-well microplate. While assays may have been performed with the same isolates, media, and temperatures, the differences between the growth kinetics seen in the manually performed assays and the mechanically performed assays can likely be attributed to factors such as aeration, evaporation, and media volume.

4.3.2.1 Comparison of Growth Kinetics in the Presence of pCMYN13-012944A vs pCMY12-2460C

In most of the tested growth conditions, the isolates containing either CMY-2 plasmid display decreased growth kinetics when compared to the plasmid-free parent. Fitness changes associated with the presence of various plasmids have been well described, and theories as to the underlying mechanism of this fitness cost include increased metabolic burden to the host and alterations in host gene expression[126]. It has been theorized however, that despite the apparent negative effect on growth kinetics, that AMR plasmids confer a net fitness advantage to their host through providing greater survivability and promoting networking among other microbes[127]. It has been shown that plasmid-mediated AMR actually carries a lower fitness cost than

chromosomally-mediated AMR and therefore can be the best option to promote survival of the host[128].

The theory of net fitness advantage would indicate that the presence of these plasmids would only be necessary under conditions with selective pressure, otherwise, the host would be undertaking a net disadvantage. When a bacterium is not in need of a plasmid, it is possible that this material will be deleted or not copied during replication[129]. In this study, the growth assays were performed without the presence of a selective antimicrobial, yet the plasmids seem to be paradoxically maintained by the host despite conferring a net fitness disadvantage. There have been many hypotheses as to why plasmid persistence such as this occurs, including the possibility of some unknown fitness advantages being conferred by these plasmids outside of AMR to encourage retention[126]. However, in this case, it is most likely the presence of addiction systems that ensure that the plasmid is maintained. The presence of one or more addiction system on these CMY-2 plasmids provides another simple explanation as to why a decrease in growth kinetics caused by the presence of these plasmids is tolerated by the host bacterium.

Another interesting point that can be noted from these growth curves is that there are grossly distinguishable differences in growth between the isolates containing either pCMYN13-02944A or pCMY12-2460C despite their vast similarities. This likely indicates that the small regions of genetic difference between these two plasmids confer key changes to growth kinetics or host benefits. One possible explanation is that since pCMY12-2460C contains over 4kbp more genetic material than pCMYN13-02944A, the metabolic burden of expressing these additional regions leads to slower growth as seen in the majority of growth conditions tested. A possible explanation for the difference in growth kinetics between pCMY12-2460C and pCMYN13-02944A seen at 42℃ might lie within the additional coding sequences found on pCMY12-

2460C. One of the additional regions found only on pCMY12-2460C is the coding sequence for bacterial lipocalin Blc, an outer membrane lipoprotein with a binding preference for lysophospholipids that is expressed under conditions that exert stress on the cell envelope[130,131]. It has been shown in *E. coli* that the modification of lipid expression is used to adapt to changes in temperature, while it has not yet been explored it could be theorized that Blc might be playing a similar role[132].

4.3.2.2 Notable Changes in Growth Kinetics in the Presence of pCMYN13-02944A

The most notable change in growth kinetics that occurred in the presence of pCMYN13-02944A was the delay in reaching the mid-log phase. In nearly all conditions tested, N13-01291/pCMYN13-02944A demonstrated a similar pattern of growth and reached a maximum optical density that was equal to or slightly less than N13-01291. However, the isolate containing pCMYN13-02944A would take 1-3 hrs longer to reach the mid-log phase of growth. It is possible that the addition of the genetic material from the plasmid is the cause of this observation, as it would impose a greater metabolic burden during each replication. Another possible explanation would be due to changes in proteomic expression that are induced in the presence of pCMYN13-02944A. During the lag phase of bacterial growth, gene expression prioritizes carbon source utilization enzymes to maximize growth[133]. As indicated by the functional annotation of the proteins with a 2-fold or greater change in regulation in the presence of pCMYN13-02944A, 11.7% of proteins affected were those that play a role in carbohydrate metabolism. As well, the phenotypic microarray data comparing N13-01291 and N13-01291/pCMYN13-02944A indicated that the plasmid-free isolate displayed a greater growth rate in the majority of carbon sources tested. Together, this data suggests that the changes in proteomic expression induced by pCMYN13-02944A likely do not prioritize carbon source

utilization which therefore would not maximize growth in the same way as the plasmid-free isolate.

4.3.2.3 Notable Changes in Growth Kinetics in the Presence of pCMY12-2460C

It is interesting to note that while the CMY-2 plasmids appear to result in a fitness cost in the form of decreased growth kinetics in the majority of conditions, there is a notable change in this pattern that is seen at 42ºC. At this temperature, the isolate containing pCMY12-2460C displayed a growth pattern equivalent to the plasmid-free host despite any additional fitness cost that this plasmid is adding to its host. Interestingly, the body temperature of a chicken is approximately 42ºC, which is where this serotype-plasmid combination is most commonly found[46,134]. The lack of decreased growth kinetics suggests that it is possible this plasmid is conferring an advantage or compensation for growth at this temperature to improve plasmid uptake during growth in chickens. A possible mechanism for the apparent pCMY12-2460C-mediated growth at greater temperatures was found in the proteomic studies.

Heat stress can lead to protein instability and the aggregation of misfolded proteins[135]. In the presence of heat stress, the protease FtsH is recruited to degrade unstable or misfolded proteins to prevent their accumulation[136]. The proteolytic activity of FtsH is modulated through the formation of a complex with the membrane proteins HflK and HflC, and if there is any disruption in the function of FtsH, the Cpx stress response pathway is activated[136,137]. Once the Cpx heat stress pathway is activated, Cpx targets the *htpX* gene which leads to the production of HtpX, a zinc metalloprotease which aids in the proteolytic quality control of misfolded proteins caused by heat stress[138]. Proteomic studies indicated ≥2-fold upregulation of CpxA, CpxP, HflK, HflC, and HtpX in the presence of pCMY12-2460C; all of which play important roles in the cellular response to heat stress. These changes in proteomic expression combined with the

growth kinetics indicate that the presence of this plasmid is likely conferring a fitness advantage in conditions like the gastrointestinal tract of a chicken where these CMY-2-plasmid-containing *Salmonella* are commonly found[115].

4.4 Proteomic Changes in the Presence of CMY-2 Plasmids

4.4.1 Changes in Protein Expression Found in the Presence of Either Plasmid

There were 87 chromosomally derived proteins that had a ≥2-fold change in expression in the presence of either CMY-2 plasmid. Functional annotation of these 87 proteins indicated that 50% of annotatable proteins were involved in one of three categories: amino acid metabolism, carbohydrate metabolism, and energy metabolism.

4.4.1.1 Proteins Regulated in the Same Direction

There were 50 proteins that were regulated in the same direction in the presence of either plasmid; of these, only 7 were upregulated. The main functional pathways that were affected were involved in energy metabolism, with 23.1% of annotatable proteins found to be downregulated in the presence of either pCMYN13-02944A or pCMY12-2460C.

Throughout their life, bacteria may find themselves exposed to various environments with changes in the flow of nutrients and available substrates[139]. The ability to optimize cellular processes to adapt to environmental changes is crucial to ensuring bacterial survival, which suggests that these processes could be an important regulatory target for plasmids that depend on host survival for their own persistence[139]. The modulation of amino acid metabolism, carbohydrate metabolism, and energy metabolism pathways in *Salmonella* can lead to benefits such as energy preservation and substrate substitution, which can both enhance and optimize survivability[139–141]. For example, there were 6 proteins involved in nitrate/nitrite metabolism that

were downregulated in the presence of either CMY-2 plasmid. In *S.* Typhimurium, nitrate is a metabolite that plays an important role in virulence as it is abundantly produced during gut infection, it plays a central role in promoting fitness in the gut, and it can be used as an electron acceptor to enhance growth in the intestines[142]. The proteins identified in this investigation were extracted from an environment where the virulence advantages of nitrate metabolism would not have been in use, therefore it is logical that these pathways would be downregulated in this environment to promote energy efficiency[142].

In the proteomic assay performed, there were 7 proteins found to be upregulated in the presence of either plasmid; the protein with the largest increase in expression was hypothetical protein APS45_06820, also known as Spy. In 2011, Quan *et al* identified Spy as a small periplasmic chaperone that facilitates protein stabilization through protein refolding in an ATP-independent manner[143]. Spy expression is modulated through the BaeRS and CpxRA stress response systems and is induced in conditions that cause protein unfolding[143]. Protein stability has been linked to AMR[143]. Specifically, it has been shown that unstable proteins can negatively affect β-lactamase activity and decrease penicillin resistance[143]. The protein refolding activity of Spy plays an important role in reducing the presence of unstable proteins, and in this way, it can inhibit reductions in β-lactamase activity. The upregulation of the Spy protein in the presence of the *bla*$_{\text{CMY-2}}$-containing plasmids pCMYN13-02944A and pCMY12-2460C suggests that this may be an evolutionary mechanism developed by these plasmids to promote the effectiveness of β-lactamase activity and provides an interesting question for further investigations.

4.4.1.2 Proteins Regulated in Opposite Directions

An unexpected finding observed in this study was that 37 proteins were regulated in opposite directions in the presence of each plasmid; however, this finding could offer a possible

clue as to an explanation for the differences in growth kinetics and fitness that were observed between the CMY-2-plasmid-containing isolates.

The isolates analyzed in this study were grown at 37℃ in LB broth before proteomic extraction; growth curves performed under the same conditions are shown in Figure 19A. LB broth is a peptone-based broth that offers amino acids as the carbon source for bacterial growth[144]. In these growth conditions, isolate N13-01291/pCMYN13-02944A shows an ~3-hour delay in reaching the mid-log phase compared to the plasmid-free isolate and reaches a lower maximum optical density at $OD_{600} \cong 2.9$. Isolate N13-01291/pCMY12-2460C shows an ~2-hour delay in reaching the mid-long phase and reaches an even lower maximum optical density at $OD_{600} \cong 2.1$. The differences in the patterns of these growth kinetics are puzzling as pCMYN13-2944A and pCMY12-2460C are identical outside of the 4 genomic regions outlined in Figure 12. Functional annotation of the proteins regulated in opposite directions revealed two proteins that reveal clues to a possible mechanism of this observable difference.

The carbon starvation-induced protein CsiD was found to be upregulated in the presence of pCMYN13-02944A and downregulated in the presence of pCMY12-2460C. CsiD is a 2OG-dependent glutarate L-2-hydroxylase that enables bacteria to utilize lysine as an energy source, particularly in carbon starvation conditions[145]. The carbon source provided for energy in LB broth is amino acids, including lysine[144]. The ability to upregulate the utilization of lysine as an energy source as carbon sources diminish throughout the growth phase could provide a possible advantage to growth and could partially explain the improved growth seen by the isolate containing pCMYN13-02944A.

The second protein of interest is the DppA-like peptide ABC transporter substrate-binding protein which was also found to be upregulated in the presence of pCMYN13-02944A and downregulated in the presence of pCMY12-2460C. DppA is a periplasmic protein that works as part of an osmotic shock transport system responsible for the uptake of oligopeptides[146]. The ability of DppA to transport dipeptides is altered as the nutritional environment changes, specifically when it senses a need for amino acids[146]. The upregulation of the DppA-like protein may be playing a similar role in cellular transport, increasing the ability for isolate N13-0129/pCMYN13-02944A to uptake and utilize amino acids for growth and metabolic process whereas N13-01291/pCMY12-2460C does not have this advantage.

4.4.2 Changes in Protein Expression Found in the Presence of pCMYN13-02944A

Analysis of the changes in proteomic expression in the presence of pCMYN13-02944A indicated that the majority of annotatable proteins that had a 2-fold change or greater were involved in metabolism and environmental information processing pathways. This included 13 proteins involved in flagellar assembly as shown in Figure 4.1, 8 proteins involved in quorum sensing as shown in Figure 4.2, and 16 proteins involved in ABC transporter systems as shown in Figure 4.3. These pathways are particularly important for pathogenesis and virulence, therefore the changes in expression of these pathways in the presence of pCMYN13-02944A likely play a role in the changes in growth kinetics seen in the presence of this plasmid due to the metabolic burden of expressing these pathways[147–149].

Flagella are important motility factors involved in host colonization and pathogenicity[147,150]. *Salmonella* adapts to various environments during infection and responds to varying inputs to determine whether it will need to be motile or non-motile and regulate the flagellar biosynthesis pathways accordingly[147]. Flagella are also important targets for immune

recognition, and therefore the downregulation of these pathways can be important for immune evasion[150]. In the presence of pCMYN13-02944A, many members of the flagellar synthesis pathway were found to be downregulated. The growth conditions that these changes in proteomic expression were identified were conditions where virulence factors such as flagella would not be needed for pathogenicity.

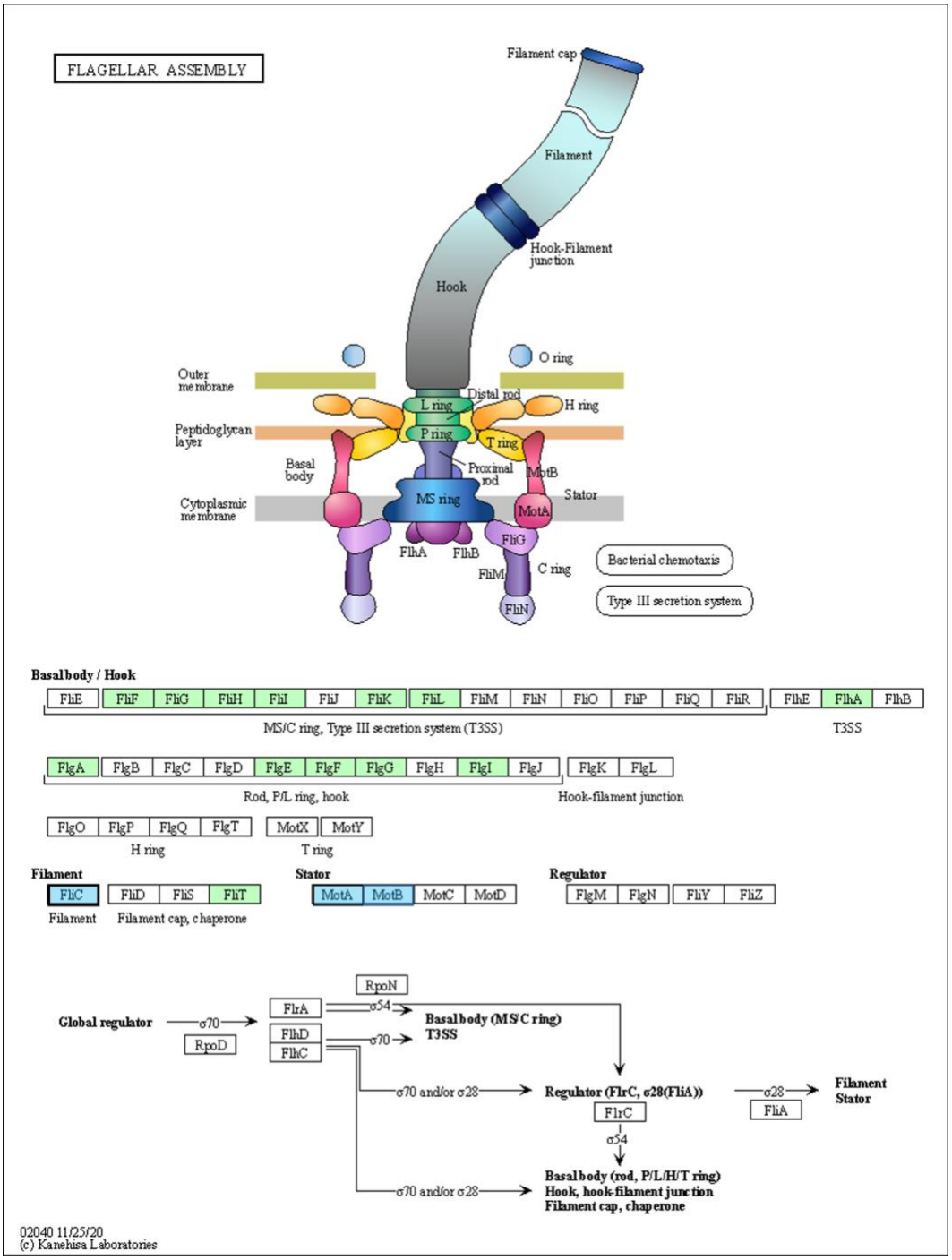


Figure 4.1. Flagellar assembly proteins that had changes in regulation in the presence of pCMYN13-02944A (green) and pCMY12-2460C (blue) as indicated by inputting GhostKOALA v2.0 annotation data into the KEGG PATHWAY database via KEGG Mapper[151,152].

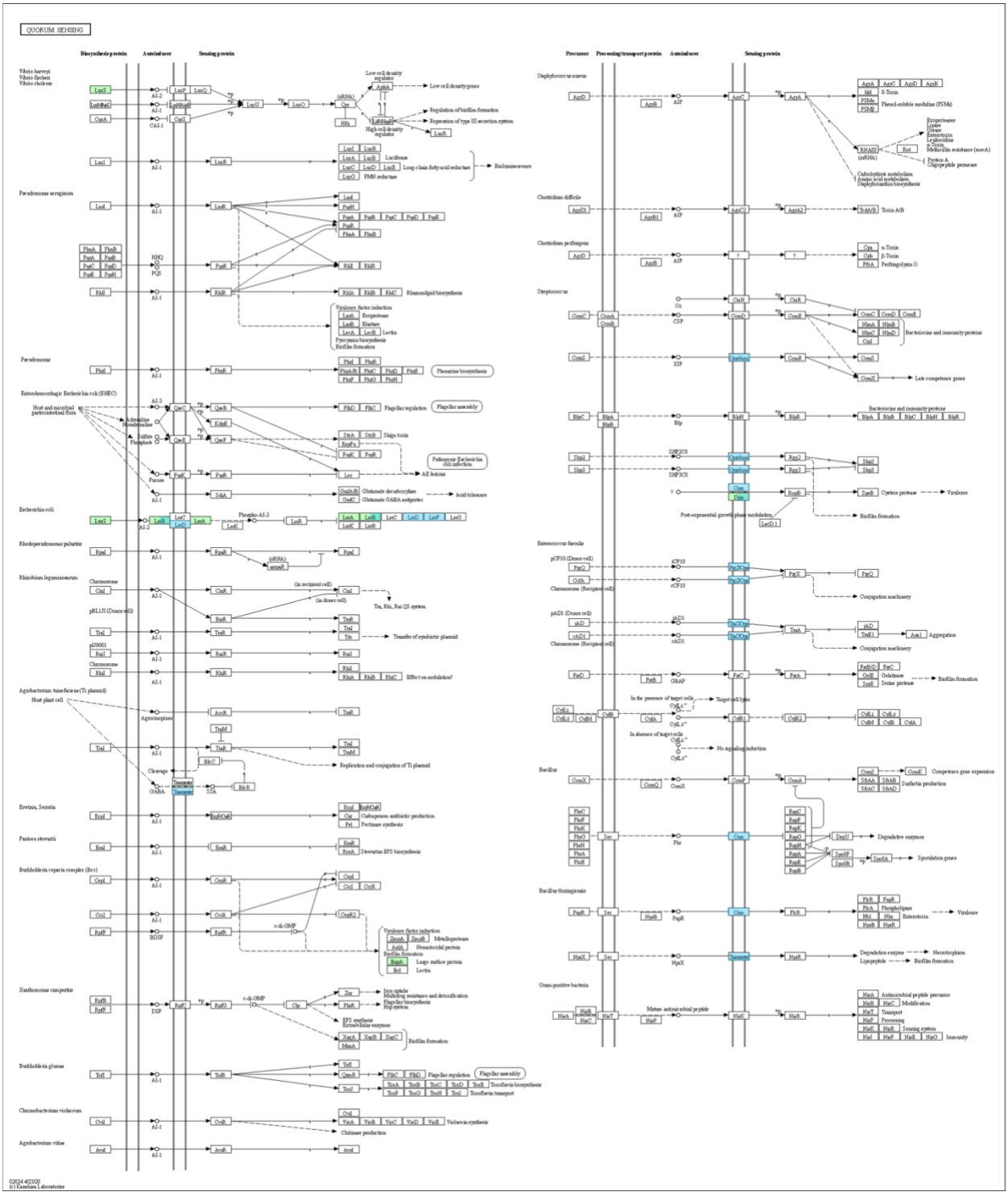


Figure 4.2. Quorum sensing proteins that had changes in regulation in the presence of pCMYN13-02944A (green) and pCMY12-2460C (blue) as indicated by inputting GhostKOALA v2.0 annotation data into the KEGG PATHWAY database via KEGG Mapper[151,152].

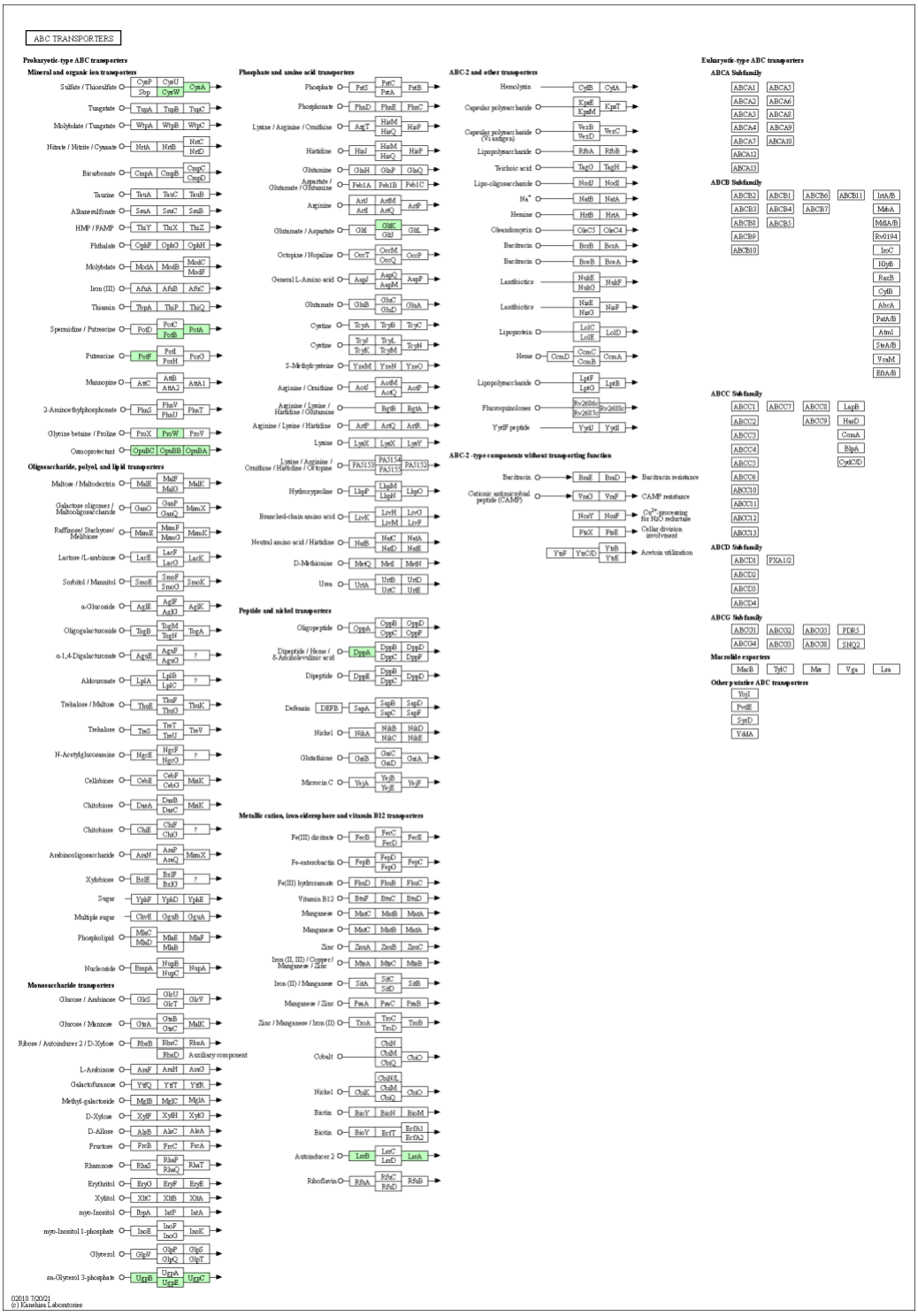


Figure 4.3. ABC transporter proteins that had changes in regulation in the presence of pCMYN13-02944A (green) as indicated by inputting GhostKOALA v2.0 annotation data into the KEGG PATHWAY database via KEGG Mapper[151,152].

The downregulation of flagellar biosynthesis in these conditions would reduce the metabolic burden of producing these factors, without providing any unnecessary disadvantages to the pathogenicity of the host. As well, the resultant reduction in metabolic burden through this regulation could also offer a partial explanation for the lessened decrease in growth kinetics when comparing this isolate to N13-01291/pCMY12-2460C.

The ability to adapt to changes in the environment including heat, nutrients, or antimicrobials is often due to the work of quorum sensing[149]. Quorum sensing is a mechanism of signal transduction or cell-cell communication that works through extracellular signalling molecules known as autoinducers[149,153]. A well-known quorum sensing pathway involved in *Salmonella* pathogenicity island 1 (SPI-1) expression is the LuxS protein which acts as an autoinducer (AI) for the AI-2 transporter complex LsrABCD[153]. Together, these proteins are involved in the expression of flagellar invasion genes through reduced expression of *fliC* and *invF*, respectively[153]. The value in up- or down-regulating flagellar biosynthesis pathways has already been described, and regulation of InvF has similar benefits. InvF is involved in the expression of a type III secretion system required for invasion of the intestinal epithelium during infection[154]. The induction of virulence factors under various growth conditions has been studied, and it has been shown that induction of SPI-1 in preparation to invade, or in "pre-invasion" conditions can be beneficial[155]. The induction of virulence factors in pre-invasion conditions can aid the ability of *Salmonella* to survive and replicate, thus preparing it for invasion and infection[155]. The upregulation of this quorum-sensing pathway seen in N13-01291/pCMYN13-02944A could be a mechanism for improving growth kinetics, as seen in the growth assays performed in this study.

ATP-binding cassette (ABC) transporters are a very important transport family involved in the transport of many varied substrates and are found in all domains of life[148]. In this study, the osmoprotectant import system composed of OpuBA, OpuBB, and OpuBC was found to be upregulated in the presence of pCMYN13-02944A. The Opu system is important in the protection of a bacterium from changes in osmolarity through detecting and adapting to environmental changes[156]. The improved ability to grow in various osmolarities was demonstrated through the Biolog Omnilog® (Biolog, Hayward, CA, USA) phenotypic microarrays, where the isolate containing pCMYN13-02944A showed a greater ability to grow in higher concentrations of NaCl when compared to the isolate containing pCMY12-2460C. The regulation of this pathway and improved adaptability involved with the upregulation of this pathway demonstrates a possible regulatory mechanism used by this plasmid to promote survivability.

4.4.3 Changes in Proteomic Expression Found in the Presence of pCMY12-2460C

Analysis of the changes in proteomic expression in the presence of pCMY12-2460C indicated that the majority of annotatable proteins with a 2-fold change or greater were involved in environmental information processing and signalling pathways (Fig. 3.19) which included proteins important for flagellar assembly, bacterial invasion, and chemotaxis shown in Figures 4.1, 4.4, and 4.5, respectively. The changes in proteomic expression of these pathways that are induced by pCMY12-2460C may accentuate the AMR benefits conferred by the *bla*$_{\text{CMY-2}}$ gene and provide additional survivability benefits to the plasmid host, however, they may also explain the growth deficits observed.

The function of flagellar motility involves multiple components including the basal body, hook, filament, motor, and interactions with membrane proteins[157]. In the presence of

pCMYN13-02944A, flagellar body/hook elements were found to have changes in expression, however in the presence of pCMY12-2460C, it was motor proteins and membrane proteins that were found to have alterations in protein expression. The MotA and MotB proteins form a complex to act as both a transmembrane proton channel and an anchor for the flagella to attach to the cellular membrane[157,159]. The upregulation of these motility proteins could partially explain the decreases in growth kinetics seen by N13-01291/pCMY12-2460C as the expression of these biosynthetic pathways carry a large energy burden. These growth kinetics were observed in assays performed *in vitro* at 37℃ in the absence of antimicrobials. These conditions do not require the expression of flagellar motility factors to aid in growth or pathogenicity and therefore provide an unnecessary metabolic cost to the host bacterium.

Another pathway found to have multiple proteins that were downregulated in the presence of pCMY12-2460C was a type III secretion system (TTSS) that is part of SPI-1. These systems work through the secretion of protein effectors and translocating them into host cells to stimulate the uptake of bacteria to facilitate bacterial invasion[154,160]. A TTSS is also referred to as an injectisome, as they are composed of a basal body that crosses the bacterial outer membrane and a needle-like complex that is used to secrete or inject effectors[161]. SipB is an effector protein that promotes cellular apoptosis and necrosis of host cells such as macrophages, SipD is a component of the needle-tip protein complex, and SopB has phosphatase activity that plays a role in fluid secretion and delaying apoptosis to allow *Salmonella* to establish a niche in intestinal epithelium before cell death[160–162]. The ability to regulate these virulence factors could provide an additional fitness and pathogenic advantage to the persistence of pCMY12-2460C, and the downregulation of these factors in growth conditions where virulence is not required could help to reduce the energy burden of expressing this pathway.

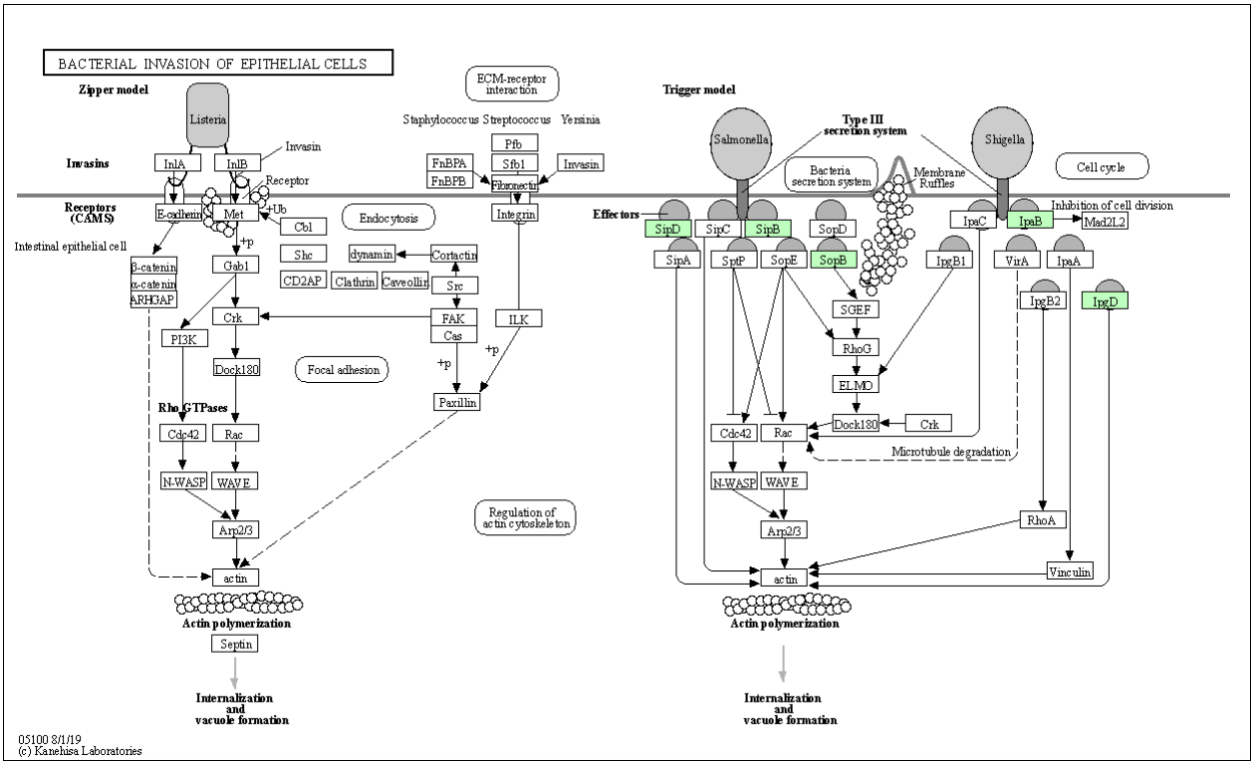


Figure 4.4. Bacterial invasion proteins that had changes in regulation in the presence of pCMY12-2460C (green) as indicated by inputting GhostKOALA v2.0 annotation data into the KEGG PATHWAY database via KEGG Mapper[151,158].

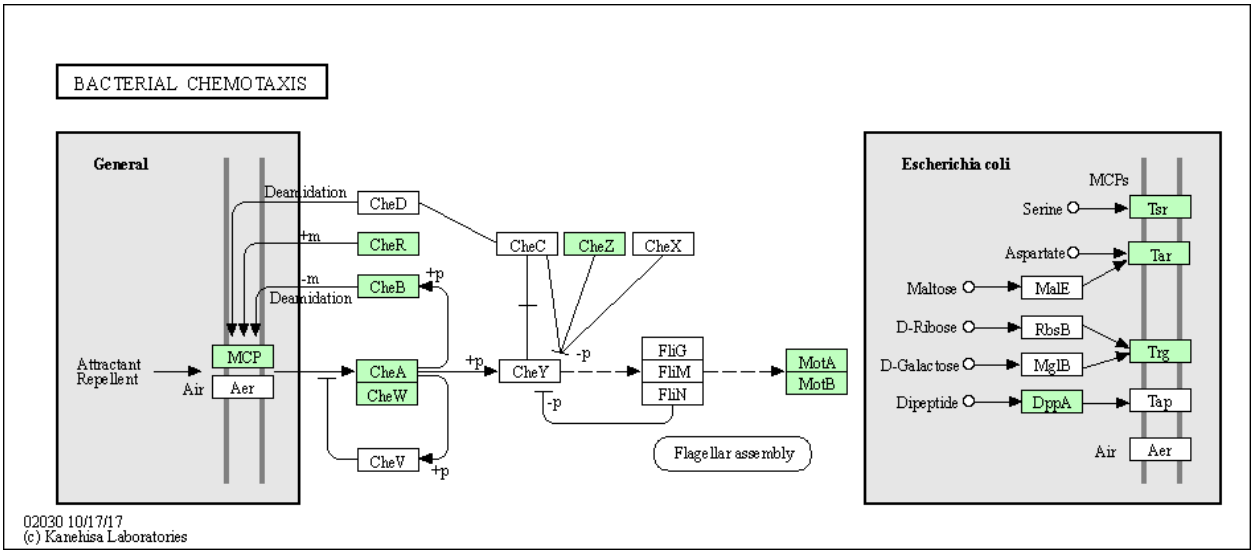


Figure 4.5. Bacterial chemotaxis proteins that had changes in regulation in the presence of pCMY12-2460C (green) as indicated by inputting GhostKOALA v2.0 annotation data into the KEGG PATHWAY database via KEGG Mapper[151,152].

Finally, another pathway of interest found to be altered in the presence of pCMY12-2460C was the chemotaxis pathway. Multiple proteins in this pathway were found to be upregulated including Tsr, Trg, and the CheA/CheW complex. Chemotaxis is an important virulence mechanism used by bacteria to sense environmental factors and direct bacterial motility and has been associated with increased antibiotic resistance[163,164]. Chemotaxis works through the detection of methyl-accepting chemotaxis proteins (MCPs) by chemoreceptors[163]. Tsr is an MCP that is sufficient for proper chemotaxis in response to AI-2, an autoinducer discussed previously[165]. Trg is also an MCP, however, it senses galactose and ribose, the detection of which is particularly useful for directing a bacterium toward mucosa for invasion[166]. CheA is a kinase that is coupled to the chemoreceptor adaptor protein CheW to form CheA/CheW, a complex that is important in the regulation of the SOS system which mediates DNA repair[163,164]. Similarly, to other pathways with changes in regulation in the presence of these CMY-2 plasmids, the chemotaxis pathway plays an important role in virulence, and therefore the regulation of this pathway can promote the survivability of both the host and any plasmids it contains.

4.5 Potential Plasmid Gene Targets Influencing Expression of Chromosomal Genes

4.5.1 ProQ/FinO Domain-Containing Protein YafB

WGS analysis of the two plasmids of interest revealed the presence of a gene of particular interest, *yafB,* which encodes an RNA-binding protein (RBP) belonging to the ProQ/FinO protein family. Specifically, the "ProQ/FinO domain" refers to the PFAM04352 domain which has been identified in approximately 7000 proteins, including ProQ and FinO[167]. ProQ and FinO both act as RNA chaperones, however, ProQ acts as more of a global regulator

able to bind large sets of sRNAs and mRNAs, while FinO has a much narrower range with only two ligands identified as binding sites[168,169].

ProQ is a chromosome-encoded protein that was initially identified as an osmoregulatory factor (PROline uptake regulator Q) that was required for optimal expression of the proline channel protein ProP but was later discovered to function as a major small noncoding RNA-binding protein that associates with ~400 transcripts[170–172]. Through modulation of gene expression via its RNA-binding activity, ProQ has been shown to affect the expression of genes involved in amino acid metabolism, biofilm formation, motility, virulence, translation energy production, and osmoregulation[172].

FinO is a plasmid-encoded fertility inhibition protein that represses conjugation of its plasmid through the binding of *traJ* mRNA and is commonly found on plasmids of the IncFI group[172]. A more recent study performed in 2021 identified a second major ligand for FinO, the RepX sRNA of the streptomycin-resistant plasmid pRSF1010[169]. This observation was particularly interesting as FinO and RepX were carried on different plasmids in this study, demonstrating that an RBP encoded by one plasmid can regulate gene expression of another plasmid existing within the same host[169].

Multiple plasmid-encoded proteins belonging to the ProQ/FinO family have been identified, and a common function of many of these proteins involves the modulation of plasmid copy number to decrease the metabolic burden of a plasmid and therefore decrease fitness cost for the host[172]. In 2021, Yang *et al* characterized PcnR (plasmid copy number repressor), a ProQ/FinO family protein found on *mcr-1*-bearing IncI2 plasmids[173]. This study revealed that PcnR aided in balancing the large fitness cost of expressing the colistin-resistance gene *mcr-1*

through interacting with *repR* mRNA resulting in plasmid repression to maintain copy levels at ~1 copy/cell[172,173].

The ProQ/FinO family of proteins regulate gene expression through functioning as RNA chaperones, providing a mechanism to alter bacterial fitness[172]. Figure 4.6 outlines mechanisms that ProQ/FinO proteins use to affect their bacterial hosts, ultimately leading to changes in fitness cost, genome stability, and adaptability[172]. Phenotypically, the presence of plasmids carrying *yafB* demonstrated alterations in fitness and proteomic expression when compared to the plasmid- and *yafB*-free parent N13-01291. In this study, the presence of either CMY-2 plasmid in isolate N13-01291 resulted in changes in fitness, promotion and maintenance of AMR and many changes in proteomic expression. These types of alterations have been demonstrated by other ProQ/FinO family proteins, however, the specific targets of the putative RNA chaperone YafB have not been investigated. The plasmids analyzed in this study are low-copy-number IncI1 plasmids, which have been demonstrated to have replication that is tightly controlled via RNA-mediated negative regulation of *repZ*[174,175].

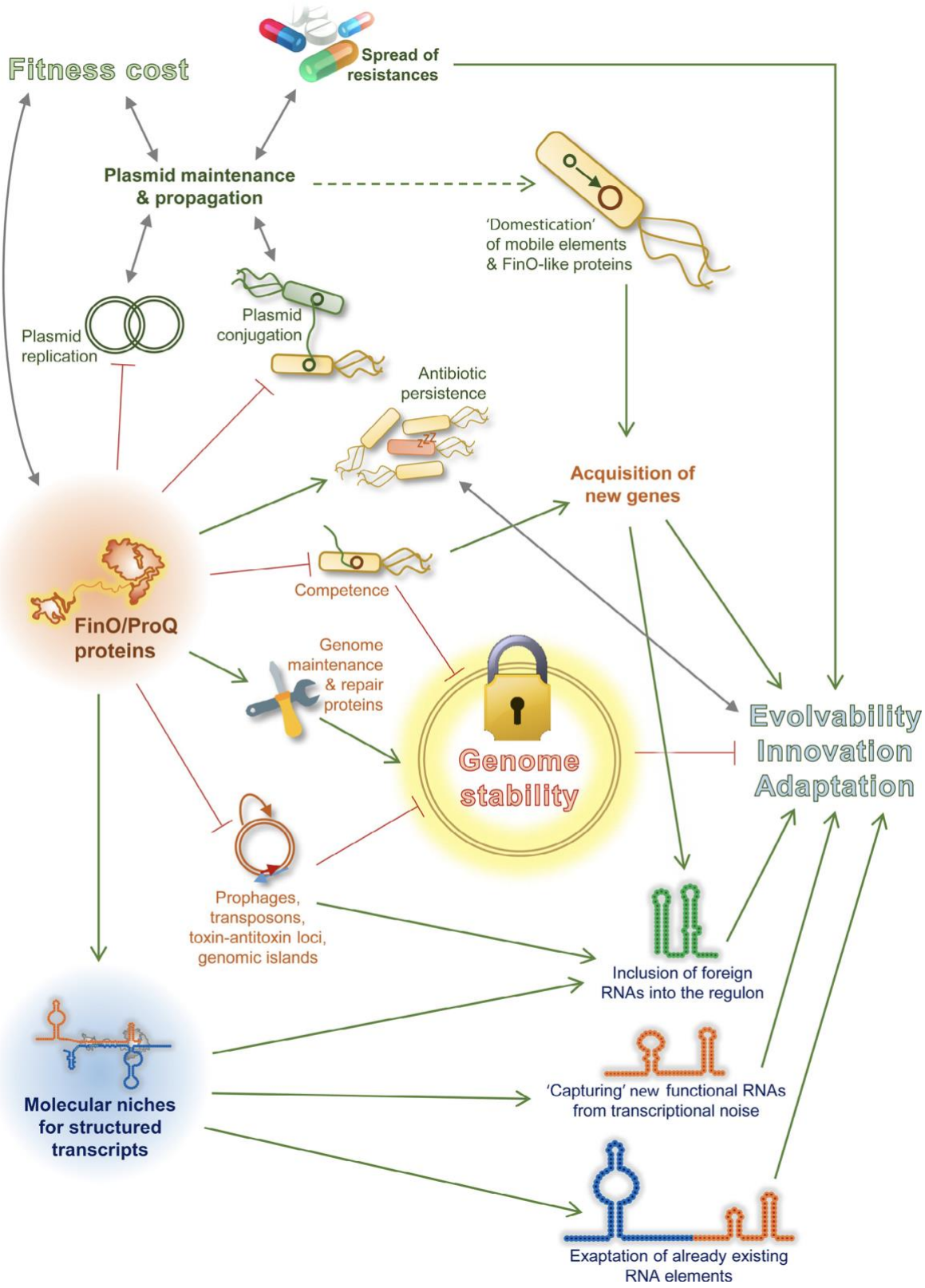


Figure 4.6. Effects of ProQ/FinO family proteins adapted from Liao and Smirnov[172].

In this study, it was demonstrated that there were significant changes in the expression of the plasmid conjugation factor TraF in the presence of both plasmids; an increase in the expression of $\log_2$=3.12 in the presence of pCMYN13-02944A and a decrease in expression of $\log_2$=-1.49 in the presence of pCMY12-2460C. In a similar mechanism to other ProQ/FinO family proteins such as FinO and PcnR, YafB may play a role in maintaining low levels of plasmid replication through RNA-mediated modulation of *repZ* or *tra* genes[172]. In contrast to PcnR however, YafB does not appear to balance the fitness cost of the plasmid to a large extent; this observation may be due to the differences in fitness cost of *mcr-1* and *bla* genes, however, this would need to be investigated further[173].

Another important observation made during this study was that 87 proteins had ≥2-fold changes in expression in the presence of both pCMYN13-02944A and pCMY12-2460C. Functional annotation of these proteins indicated that the majority of annotatable proteins were involved in amino acid metabolism, carbohydrate metabolism, and energy metabolism. A possible explanation for these changes could be the role of YafB as a global regulator able to bind many transcripts in a similar fashion to ProQ; as ProQ has been shown to modulate transcripts with functional categories similar to those identified here[172].

The function of YafB and its putative function as an RNA chaperone has yet to be confirmed. The presence of the ProQ/FinO domain indicates a strong likelihood that YafB can bind RNA and therefore modulate the expression of various proteins that would alter the fitness and adaptability of its host. Further studies regarding the identification of YafB ligands and interactions will help to identify the function and scope of YafB and other ProQ/FinO family proteins.

5. Conclusions

Salmonella Heidelberg is a frequently isolated serotype from Canadian poultry sources[47]. IncI1 plasmids containing *bla*$_{\text{CMY-2}}$ are predominantly responsible for conferring cephalosporin resistance in *S.* Heidelberg[46]. These plasmids are nearly 100 kb in size and carry many coding sequences alongside this AMR gene. Understanding the effects of these plasmids on the changes in chromosomal gene expression, growth kinetics, and proteomic expression may help to further understand why the presence of these plasmids leads to the formation of superbugs.

This study has shown that the presence of either pCMYN13-02944A or pCMY12-2460C results in multiple changes in growth and proteomic expression. One of the most unique findings was that the presence of either plasmid resulted in reproducible chromosomal SNVs in N13-01291. The effect of these specific mutations on the function of their transcripts remains to be investigated further, however, they appear to play a role in virulence, AMR, and survival in stressful conditions[120,122,124]. As well, despite the 99.55% similarity in structure of pCMYN13-02944A and pCMY12-2460C, their presence results in observable differences in growth kinetics in various growth conditions. Additionally, the presence of either plasmid resulted in 87 chromosomally derived proteins showing a ≥2-fold change in expression, indicating that these plasmids share a common regulatory factor affecting chromosomal gene expression. Many of the proteins shown to have changes in regulation in the presence of a CMY-2 plasmid were related to pathways responsible for virulence and adaptability to various environmental conditions. These findings indicate that *bla*$_{\text{CMY-2}}$-containing AMR plasmids may enhance the virulence and survival of their host through the modulation of various pathways.

The observations in this study point to the conclusion that AMR plasmids have a much greater effect on their host than just conferring AMR. This study indicates that pCMYN13-

02944A and pCMY12-2460C play a much larger role in altering the physiology of their host bacterium and that there are factors present on these plasmids that play regulatory roles in protein expression and fitness.

5.1 Future Directions

The findings in this study offer up many questions for further study. The presence of either CMY-2 plasmid was found to result in many changes in proteomic expression. These observed changes raise the question of whether the presence of these plasmids could also result in alterations in transcriptomic expression. To examine this possible effect, eight targets found to have ≥2-fold significant changes in expression in the presence of a CMY-2 plasmid have been chosen for future RT-qPCR experiments; these targets and primers are listed in Table 5.1. These targets could offer insight into the regulatory effects of plasmid-mediated proteins as well as additional fitness changes conferred by AMR plasmids.

One plasmid-mediated protein identified for RT-qPCR experiments was the ProQ/FinO domain-containing protein YafB. This protein garnered special interest because it is an RBP that contains the potential to act as a regulator through binding sRNAs and mRNAs similarly to ProQ and FinO[170–172]. It would be interesting to investigate knockout mutants of YafB to determine if this results in changes in growth kinetics and proteomic expression. Additionally, further analysis to determine the structure, ligands, and interactions of YafB could shed light on the scope of proteins containing a ProQ/FinO domain as well as indicate possible virulence advantages to the presence of this CDS on CMY-2-containing AMR plasmids.

Table 5.1. Targets and primer sequences chosen for future RT-qPCR experiments.

Name	Gene	Sequence (5'-3')	Tm (℃)	Product Size	Efficiency (%)
16S-F	*16S rRNA*	TCGTGTTGTGAAATGTTGGGTTA			
16S-R		TCTTTGTATGCGCCATTGTAGC		323	98.6
16S-P		CCGCAACGAGCGCAACCCTT			
Spy_1-F	*spy*	GGACGCACAGAAGCAACAAA	60.0		
Spy_1-R		GCTGCGCTTCCATTTTCGTA	60.0	161	97.2
Spy_1-P		AAGAGCGTCGCGCCATGC	72.0		
Spy_2-F	*spy*	TGCCGCTGAGACTACCACC	58.4		
Spy_2-R		GCGCTGCGCTTTCATAATG	59.2	155	115.3
Spy_2-P		CGCGCCAGCGGATGCGA	69.8		
NapA-F	*napA*	CAAGGCTGGTTTCCGCTCTA	60.0		
NapA-R		TCGGCCTGCTCAATATCGTC	60.0	132	96.3
NapA-P		AATGCGCGTCACTGCATGGCC	69.5		
YgaU-F	*ygaU*	CGGATATATTTTTTCCGGGCT	58.0		
YgaU-R		AGCAGCGTTGACGATCAGG	58.6	180	105.0

YgaU-P		TCAGCCGCCGGCGTCGT	68.2		
YhjQ-F		GCCTCTTCTTGTCTGCGTGAA	59.2		
YhjQ-R	*yhjQ*	GCAGGCTTTGCAGATATCCG		165	98.3
YhjQ-P		TTGTCGCCTGGCGGCGC	68.7		
FlgG-F		CACGCCGGTACCGATTTG	59.5		
FlgG-R	*flgG*	TAACCTGGCAAACGTCAGCA	58.9	145	97.4
FlgG-P		ACAACAGATCTTCAAATAC	69.0		
Rpos-F		GACCGATTTCACGGCCTACA	59.5		
Rpos-R	*rpos*	CACCACGCAAGATGACGATATG	60.0	146	103.8
Rpos-P		CGGCGCGCCAGCACTTCA	68.7		
YafB_1-F		GCC ACC GTC CTT ATC CGA			
YafB_1-R	*proQ*	GGATATGTGTTTCGACGGCA		110	86.3
YafB_1-P		CG GCA GAA TC AGCCCC CGC			

References

1. Jiang X, Liu X, Law COK, et al. The CTX-M-14 Plasmid pHK01 Encodes Novel Small RNAs and Influences Host Growth and Motility. *FEMS Microbiol Ecol*. 2017;93(7):1-10. doi:10.1093/femsec/fix090

2. Armstrong GL, Conn LA, Pinner RW. Trends in Infectious Disease Mortality in the United States During the 20th Century. *J Am Med Assoc*. 1999;281(1):61-66. doi:10.1001/jama.281.1.61

3. Public Health Agency of Canada. *Handle with Care: Preserving Antibiotics Now and Into the Future*.; 2019.

4. Gould K. Antibiotics: From Prehistory to the Present Day. *J Antimicrob Chemother*. 2016;71(3):572-575. doi:10.1093/jac/dkv484

5. Shellcross LJ. Antibiotic Overuse: A Key Driver of Antimicrobial Resistance. *Br J Gen Pract*. 2014;64(629):604-605. doi:10.1136/bmj.f5806.6.

6. Manyi-Loh C, Mamphweli S, Meyer E, Okoh A. Antibiotic Use in Agriculture and its Consequential Resistance in Environmental Sources: Potential Public Health Implications. *Molecules*. 2018;23(4):795. doi:10.3390/molecules23040795

7. Aslam B, Wang W, Arshad MI, et al. Antibiotic Resistance : A Rundown of a Global Crisis. *Infect Drug Resist*. 2018;11:1645-1658.

8. O'Neill J. *Antimicrobial Resistance: Tackling a Crisis for the Health and Wealth of Nations*.; 2014.

9. Public Health Agency of Canada. Antibiotic-Resistant Illnesses and Bacteria. https://www.canada.ca/en/public-health/services/antibiotic-antimicrobial-resistance/antibiotic-resistant-illnesses-bacteria.html. Published 2014. Accessed June 30, 2020.

10. Iredell J, Brown J, Tagg K. Antibiotic Resistance in *Enterobacteriaceae*: Mechanisms and Clinical Implications. *BMJ*. 2016;352:h6420. doi:10.1136/bmj.h6420

11. Munita JM, Arias CA, Unit AR, Santiago A De. Mechanisms of Antibiotic Resistance. *Microbiology*. 2016;4(2):1-37. doi:10.1128/microbiolspec.VMBF-0016-2015.Mechanisms

12. Soto SM. Role of Efflux Pumps in the Antibiotic Resistance of Bacteria Embedded in a Biofilm. *Virulence*. 2013;4(3):223-229. doi:10.4161/viru.23724

13. Du D, Wang Z, James NR, et al. Structure of the AcrAB-TolC Multidrug Efflux Pump. *Nature*. 2014;509(7501):512-515. doi:10.1038/nature13205.Structure

14. Choi U, Lee CR. Distinct Roles of Outer Membrane Porins in Antibiotic Resistance and Membrane Integrity in *Escherichia coli*. *Front Microbiol*. 2019;10(APR):1-9. doi:10.3389/fmicb.2019.00953

15. Fernández L, Hancock REW. Adaptive and Mutational Resistance: Role of Porins and Efflux Pumps in Drug Resistance. *Clin Microbiol Rev*. 2012;25(4):661-681. doi:10.1128/CMR.00043-12

16. Ipinza F, Collao B, Monsalva D, et al. Participation of the Salmonella OmpD porin in the infection of RAW264.7 macrophages and BALB/c mice. *PLoS One*. 2014;9(10):1-11. doi:10.1371/journal.pone.0111062

17. Poole K. Resistance to β-lactam Antibiotics. *Cell Mol Life Sci*. 2004;61(17):2200-2223. doi:10.1007/s00018-004-4060-9

18. Delcour AH. Outer Membrane Permeability and Antibiotic Resistance. *Biochim Biophys Acta*. 2010;1794(5):808-816. doi:10.1016/j.bbapap.2008.11.005.Outer

19. Li B, Huang Q, Cui A, et al. Overexpression of Outer Membrane Protein X (OmpX) Compensates for the Effect of TolC Inactivation on Biofilm Formation and Curli Production in Extraintestinal Pathogenic *Escherichia coli* (ExPEC). *Front Cell Infect Microbiol*. 2018;8(JUN):1-8. doi:10.3389/fcimb.2018.00208

20. Egorov AM, Ulyashova MM, Rubtsova MY. Bacterial Enzymes and Antibiotic Resistance. *Acta Naturae*. 2018;10(4):33-48.

21. Shaikh S, Fatima J, Shakil S, Rizvi SMD, Kamal MA. Antibiotic Resistance and Extended Spectrum Beta-Lactamases: Types, Epidemiology and Treatment. *Saudi J Biol Sci*. 2015;22(1):90-101. doi:10.1016/j.sjbs.2014.08.002

22. Lambert PA. Bacterial Resistance to Antibiotics: Modified Target Sites. *Adv Drug Deliv Rev*. 2005;57(10):1471-1485. doi:10.1016/j.addr.2005.04.003

23. Frye JG, Jackson CR. Genetic Mechanisms of Antimicrobial Resistance Identified in *Salmonella enterica, Escherichia coli, and Enteroccocus spp*. Isolated from U.S. Food Animals. *Front Microbiol*. 2013;4(MAY):1-22. doi:10.3389/fmicb.2013.00135

24. Annunziato G. Strategies to Overcome Antimicrobial Resistance (AMR) Making use of Non-Essential Target Inhibitors: A Review. *Int J Mol Sci*. 2019;20(23). doi:10.3390/ijms20235844

25. Carattoli A. Resistance Plasmid Families in *Enterobacteriaceae*. *Antimicrob Agents Chemother*. 2009;53(6):2227-2238. doi:10.1128/AAC.01707-08

26. Medema MH, Trefzer A, Kovalchuk A, et al. The Sequence of a 1.8-Mb Bacterial Linear Plasmid Reveals a Rich Evolutionary Reservoir of Secondary Metabolic Pathways. *Genome Biol Evol*. 2010;2(1):212-224. doi:10.1093/gbe/evq013

27. Couturier M, Bex F, Bergquist PL, Maas3 WK. Identification and Classification of Bacterial Plasmids. *Microbiol Rev*. 1988;52(3):375-395.

28. Helinski DR. Introduction to Plasmids: a Selective View of Their History. In: *Plasmid Biology*. ; 2004:1-21. doi:10.1128/9781555817732.ch1

29. Tsang J. Bacterial Plasmid Addiction Systems and Their Implications for Antibiotic Drug Development. *Postdoc J*. 2017;5(5):3-9. doi:10.1177/0963721414541462.Self-Control

30. Rawat D, Nair D. Extended-Spectrum Beta-lactamases in Gram Negative Bacteria. *J Glob Infect Dis*. 2010;2(3):263-274.

31. Lawley T, Wilkins BM, Frost LS. Bacterial Conjugation in Gram-Negative Bacteria. In: *Plasmid Biology*. ; 2004:203-239.

32. Wong JJW, Lu J, Glover JNM. Relaxosome function and conjugation regulation in F-like plasmids - a structural biology perspective. *Mol Microbiol*. 2012;85(4):602-617. doi:10.1111/j.1365-2958.2012.08131.x

33. Venkatesan MM, Borland V. Genome-Scale Analysis of Virulence Plasmids: the Contribution of Plasmid-Borne Virulence Genes to Enterobacterial Pathogenesis. In: *Plasmid Biology*. ; 2004:395-414.

34. Kues U, Stahl U. Replication of Plasmids in Gram-negative Bacteria. *Microbiol Rev*. 1989;53(4):491-516. doi:10.1128/mmbr.53.4.491-516.1989

35. Cheah UE, Weigand WA, Stark BC. Effects of Recombinant Plasmid Size on Cellular Processes in *Escherichia coli*. *Plasmid*. 1987;18(2):127-134. doi:10.1016/0147-619X(87)90040-0

36. San Millan A, Toll-Riera M, Qi Q, et al. Integrative Analysis of Fitness and Metabolic Effects of Plasmids in *Pseudomonas aeruginosa* PAO1. *ISME J*. 2018;12(12):3014-3024. doi:10.1038/s41396-018-0224-8

37. Pilla G, Tang CM. Going Around in Circles: Virulence Plasmids in Enteric Pathogens. *Nat Rev Microbiol*. 2018;16(8):484-495. doi:10.1038/s41579-018-0031-2

38. Vial L, Hommais F. Plasmid-Chromosome Cross-Talks. *Environ Microbiol*. 2020;22(2):540-556. doi:10.1111/1462-2920.14880

39. Harrison E, Guymer D, Spiers AJ, Paterson S, Brockhurst MA. Parallel Compensatory Evolution Stabilizes Plasmids across the Parasitism-Mutualism Continuum. *Curr Biol*. 2015;25(15):2034-2039. doi:10.1016/j.cub.2015.06.024

40. San Millan A. Evolution of Plasmid-Mediated Antibiotic Resistance in the Clinical Context. *Trends Microbiol*. 2018;26(12):978-985. doi:10.1016/j.tim.2018.06.007

41. Harrison E, Dytham C, Hall JPJ, et al. Rapid Compensatory Evolution Promotes the Survival of Conjugative Plasmids. *Mob Genet Elements*. 2016;6(3):1-6. doi:10.1080/2159256X.2016.1179074

42. Loftie-Eaton W, Yano H, Burleigh S, et al. Evolutionary Paths that Expand Plasmid Host-Range: Implications for Spread of Antibiotic Resistance. *Mol Biol Evol*. 2016;33(4):885-897. doi:10.1093/molbev/msv339

43. Andino A, Hanning I. *Salmonella enterica*: Survival, Colonization, and Virulence

Differences Among Serovars. *Sci World J*. 2015;2015:1-16. doi:10.1155/2015/520179

44. Gal-Mor O, Boyle EC, Grassl GA. Same Species, Different Diseases: How and Why Typhoidal and Non-typhoidal Salmonella enterica Serovars Differ. *Front Microbiol*. 2014;5(AUG):1-10. doi:10.3389/fmicb.2014.00391

45. *Salmonella* (non-typhoidal). World Health Organization. http://www.who.int/mediacentre/factsheets/fs139/en/. Published 2018. Accessed January 30, 2018.

46. Edirmanasinghe R, Finley R, Parmley EJ, et al. A Whole-Genome Sequencing Approach To Study Cefoxitin-Resistant *Salmonella enterica* Serovar Heidelberg Isolates From Various Sources. *Antimicrob Agents Chemother*. 2017;61(4):e01919-16.

47. Zhao S, White DG, Friedman SL, et al. Antimicrobial Resistance in *Salmonella enterica* serovar Heidelberg Isolates from Retail Meats, Including Poultry, from 2002 to 2006. *Appl Environ Microbiol*. 2008;74(21):6656-6662. doi:10.1128/AEM.01249-08

48. Scallan E, Hoekstra RM, Angulo FJ, et al. Foodborne Illness Acquired in the United States-Major Pathogens. *Emerg Infect Dis*. 2011;17(1):7-15. doi:10.3201/eid1701.P11101

49. Vugia DJ, Samuel M, Farley MM, et al. Invasive Salmonella Infections in the United States, FoodNet, 1996–1999: Incidence, Serotype Distribution, and Outcome. *Clin Infect Dis*. 2004;38(s3):S149-S156. doi:10.1086/381581

50. Hohmann EL. Nontyphoidal *Salmonella*: Gastrointestinal Infection and Carriage. UptoDate. https://www-uptodate-com.uml.idm.oclc.org/contents/nontyphoidal-salmonella-gastrointestinal-infection-and-carriage?search=salmonella enterica treatment&source=search_result&selectedTitle=1~150&usage_type=default&display_rank=1#H1058721080. Published 2020. Accessed July 3, 2020.

51. Ilaria F, Giusti F. *EM Reconstruction of Adhesins: Future Prospects*. Vol 715.; 2011. doi:10.1007/978-94-007-0940-9_17

52. Dhanani AS, Block G, Dewar K, et al. Genomic Comparison of Non-typhoidal *Salmonella enterica* Serovars Typhimurium, Enteritidis, Heidelberg, Hadar and Kentucky Isolates from Broiler Chickens. *PLoS One*. 2015;10(6):1-24. doi:10.1371/journal.pone.0128773

53. Nakazato G, Campos TA De, Stehling EG, Brocchi M, Silveira WD Da. Virulence Factors of Avian Pathogenic *Escherichia coli* (APEC). *Pesqui Veterinária Bras*. 2009;29(7):479-486. doi:10.1590/S0100-736X2009000700001

54. Haiko J, Westerlund-Wikström B. The Role of the Bacterial Flagellum in Adhesion and Virulence. *Biology (Basel)*. 2013;2(4):1242-1267. doi:10.3390/biology2041242

55. Labbé G, Edirmanasinghe R, Ziebell K, et al. Complete Genome and Plasmid Sequences of Three Canadian Isolates of *Salmonella enterica* subsp. *enterica* Serovar Heidelberg from Human and Food Sources: TABLE 1 . *Genome Announc*. 2016;4(1):e01526-15. doi:10.1128/genomeA.01526-15

56. Varma JK, Mølbak K, Barrett TJ, et al. Antimicrobial-Resistant Nontyphoidal <i>Salmonella<i/> is Associated with Excess Bloodstream Infections and Hospitalizations. *J Infect Dis*. 2005;191(4):554-561. doi:10.1086/427263

57. McCracken M. Characterization of Extended-Spectrum Beta-Lactamases (ESBLs) in North America. 2006.

58. Bauernfeind A, Stemplinger I, Jungwirth R, Giamarellou H. Characterization of the Plasmidic β-lactamase CMY-2, Which is Responsible for Cephamycin Resistance. *Antimicrob Agents Chemother*. 1996;40(1):221-224.

59. Martin LC, Weir EK, Poppe C, Reid-Smith RJ, Boerlin P. Characterization of bla CMY-2 Plasmids in Salmonella and Escherichia coli Isolates from Food Animals in Canada. *Appl Environ Microbiol*. 2012;78(4):1285-1287. doi:10.1128/AEM.06498-11

60. Cejas D, Vignoli R, Quinteros M, et al. First Detection of a CMY-2 Plasmid Mediated β-lactamase in Salmonella Heidelberg in South America. *Rev Argent Microbiol*. 2014;46(1):30-33. doi:10.1016/S0325-7541(14)70044-6

61. Souza AIS, Saraiva MMS, Casas MRT, et al. High Occurrence of β-lactamase-Producing *Salmonella* Heidelberg from Poultry Origin. *PLoS One*. 2020;15(3):1-11. doi:10.1371/journal.pone.0230676

62. Melo RT, Galvão NN, Guidotti-Takeuchi M, et al. Molecular Characterization and Survive Abilities of *Salmonella* Heidelberg Strains of Poultry Origin in Brazil. *Front Microbiol*. 2021;12(June). doi:10.3389/fmicb.2021.674147

63. *Salmonella* Heidelberg - Ceftiofur-Related Resistance in Human and Retail Chicken Isolates. Public Health Agency of Canada. http://www.phac-aspc.gc.ca/cipars-picra/heidelberg/pdf/heidelberg_e.pdf. Published 2006. Accessed January 30, 2018.

64. Andrea Isabel Moreno Switt. *Salmonella* Heidelberg. https://confluence.cornell.edu/display/FOODSAFETY/Salmonella+Heidelberg. Published 2017. Accessed January 30, 2018.

65. Multistate Outbreak of Multidrug-Resistant *Salmonella* Heidelberg Infections Linked to Contact with Dairy Calves. Center for Disease Control. https://www.cdc.gov/salmonella/heidelberg-11-16/index.html. Published 2017.

66. Han J, Lynne AM, David DE, et al. DNA Sequence Analysis of Plasmids from Multidrug Resistant *Salmonella enterica* Serotype Heidelberg Isolates. *PLoS One*. 2012;7(12):1-8. doi:10.1371/journal.pone.0051160

67. Oladeinde A, Cook K, Orlek A, et al. Hotspot mutations and ColE1 Plasmids Contribute to the Fitness of *Salmonella* Heidelberg in Poultry Litter. *PLoS One*. 2018;13(8):1-36. doi:10.1371/journal.pone.0202286

68. Chen CY, Lindsey RL, Strobaugh TP, Frye JG, Meinersmann RJ. Prevalence of ColE1-like Plasmids and Kanamycin Resistance Genes in *Salmonella enterica* serovars. *Appl Environ Microbiol*. 2010;76(20):6707-6714. doi:10.1128/AEM.00692-10

69. Grimont PA, Weill F-X. *Antigenic Formulae of the* Salmonella *Serovars*. 9th ed. WHO Collaborating Centre for Reference and Research on Salmonella; 2007. https://www.pasteur.fr/ip/portal/action/WebdriveActionEvent/oid/01s-000036-089.

70. *Edwards and Ewing's Identification of* Enterobacteriaceae. 4th ed. New York: Elsevier Science Publishing Co.; 1986. doi:10.1177/1748895811401979

71. Binotto J, MacLachlan PR, Sanderson KE. Electrotransformation in *Salmonella typhimurium* LT2. *Can J Microbiol*. 1991;37(6):474-477. doi:10.1139/m91-078

72. How Should I Calculate the Transformation Efficiency (C2992)? New England BioLabs. https://international.neb.com/faqs/0001/01/01/how-should-i-calculate-the-transformation-efficiency-c2992. Accessed July 22, 2021.

73. Alderliesten JB, Duxbury SJN, Zwart MP, De Visser JAGM, Stegeman A, Fischer EAJ. Effect of Donor-Recipient Relatedness on the Plasmid Conjugation Frequency: A Meta-Analysis. *BMC Microbiol*. 2020;20(1):1-10. doi:10.1186/s12866-020-01825-4

74. Mataseje LF, Boyd DA, Willey BM, et al. Plasmid Comparison and Molecular Analysis of *Klebsiella pneumoniae* Harbouring *bla*kpc from New York city and Toronto. *J Antimicrob Chemother*. 2011;66(6):1273-1277. doi:10.1093/jac/dkr092

75. Patel JB, Cockerill FR, Bradford PA, et al. Methods for Dilution Antimicrobial Susceptibility Tests for Bacteria That Grow Aerobically; Approved Standard - Tenth Edition. *Clin Lab Stand Inst*. 2015;35(2):1-15. doi:10.1093/cid/ciw353

76. Weinstein MP, Lewis II JS, Bobenchik AM, et al. Performance Standards for Antimicrobial Susceptibility Testing - 30th Edition. *Clin Lab Stand Inst*. 2020;40(1). doi:10.1016/s0196-4399(01)88009-0

77. National Antimicrobial Resistance Monitoring System for Enteric Bacteria (NARMS). Centers for Disease Control and Prevention.

78. Matthews TC, Bristow FR, Griffiths EJ, et al. The Integrated Rapid Infectious Disease Analysis (IRIDA) Platform. *bioRxiv*. 2018:1-34. doi:10.1101/381830

79. Afgan E, Baker D, Batut B, et al. The Galaxy Platform for Accessible, Reproducible and Collaborative Biomedical Analyses: 2018 Update. *Nucleic Acids Res*. 2018;46(W1):W537-W544. doi:10.1093/nar/gky379

80. Reumerman RA, Tucker NP, Herron PR, Hoskisson PA, Sangal V. Tool for Rapid Annotation of Microbial SNPs (TRAMS): A Simple Program for Rapid Annotation of Genomic Variation in Prokaryotes. *Antonie van Leeuwenhoek, Int J Gen Mol Microbiol*. 2013;104(3):431-434. doi:10.1007/s10482-013-9953-x

81. Andrews Si. FastQC: A Quality Control Tool for High Throughput Sequence Data.

82. Seeman T. Shovill. 2019.

83. Bankevich A, Nurk S, Antipov D, et al. SPAdes: A New Genome Assembly Algorithm

and its Applications to Single-Cell Sequencing. *J Comput Biol*. 2012;19(5):455-477. doi:10.1089/cmb.2012.0021

84. Seemann T. Prokka: Rapid Prokaryotic Genome Annotation. *Bioinformatics*. 2014;30(14):2068-2069. doi:10.1093/bioinformatics/btu153

85. Gurevich A, Saveliev V, Vyahhi N, Tesler G. QUAST: Quality Assessment Tool for Genome Assemblies. *Bioinformatics*. 2013;29(8):1072-1075. doi:10.1093/bioinformatics/btt086

86. Kurtz S, Shumway M, Antonescu C, et al. Versatile and Open Software for Comparing Large Genomes. *Genome Biol*. 2004;5(2):12. http://www.tigr.org/software/mummer.

87. Petkau A, Mabon P, Sieffert C, et al. SNVPhyl: A Single Nucleotide Variant Phylogenomics Pipeline for Microbial Genomic Epidemiology. *Microb genomics*. 2017;3(6):e000116. doi:10.1099/mgen.0.000116

88. Guindon S, Gascuel O. A Simple, Fast, and Accurate Algorithm to Estimate Large Phylogenies by Maximum Likelihood. *Syst Biol*. 2003;52(5):696-704. doi:10.1080/10635150390235520

89. Guindon S, Dufayard J, Lefort V. Guindon et al. - 2010 - New Algorithms and Methods to Estimate Maximim-Likelihood Phylogenies Assessing the Performance of PhyML 3.0. *Syst Biol*. 2010;59(3):307-321.

90. Staramr. GitHub. https://github.com/phac-nml/staramr. Published 2018.

91. Carattoli A, Zankari E, Garciá-Fernández A, et al. In Silico Detection and Typing of Plasmids Using Plasmidfinder and Plasmid Multilocus Sequence Typing. *Antimicrob Agents Chemother*. 2014;58(7):3895-3903. doi:10.1128/AAC.02412-14

92. Zankari E, Hasman H, Cosentino S, et al. Identification of Acquired Antimicrobial Resistance Genes. *J Antimicrob Chemother*. 2012;67(11):2640-2644. doi:10.1093/jac/dks261

93. Zankari E, Allesøe R, Joensen KG, Cavaco LM, Lund O, Aarestrup FM. PointFinder: A Novel Web Tool for WGS-Based Detection of Antimicrobial Resistance Associated with Chromosomal Point Mutations in Bacterial Pathogens. *J Antimicrob Chemother*. 2017;72(10):2764-2768. doi:10.1093/jac/dkx217

94. Robertson J, Nash JHE. MOB-suite: software tools for clustering, reconstruction and typing of plasmids from draft assemblies. *Microb genomics*. 2018;4(8). doi:10.1099/mgen.0.000206

95. Sullivan MJ, Petty NK, Beatson SA. Easyfig: A genome comparison visualizer. *Bioinformatics*. 2011;27(7):1009-1010. doi:10.1093/bioinformatics/btr039

96. Fricke WF, McDermott PF, Mammel MK, et al. Antimicrobial resistance-conferring plasmids with similarity to virulence plasmids from avian pathogenic Escherichia coli strains in Salmonella enterica serovar Kentucky isolates from poultry. *Appl Environ*

Microbiol. 2009;75(18):5963-5971. doi:10.1128/AEM.00786-09

97. Fey A, Eichler S, Flavier S, Christen R, Höfle MG, Guzmán CA. Establishment of a Real-Time PCR-based Approach for Accurate Quantification of Bacterial RNA Targets in Water, Using *Salmonella* as a Model Organism. *Appl Environ Microbiol*. 2004;70(6):3618-3623. doi:10.1128/AEM.70.6.3618-3623.2004

98. Merritt JH, Kadouri DE, O'Toole GA. Growing and Analyzing Static Biofilms. *Curr Protoc Microbiol*. 2005;July(1):248-254. doi:10.1002/9780471729259.mc01b01s00

99. Adkins JN, Mottaz HM, Norbeck AD, et al. Analysis of the *Salmonella typhimurium* Proteome Through Environmental Response Toward Infectious Conditions. *Mol Cell Proteomics*. 2006;5(8):1450-1461. doi:10.1074/mcp.M600139-MCP200

100. Liebler DC, Ham AJL. Spin Filter-Based Sample Preparation for Shotgun Proteomics. *Nat Methods*. 2009;6(11):785. doi:10.1038/nmeth1109-785a

101. Wisniewski JR, Zougman A, Nagaraj N, Mann M. Universal Sample Preparation Method for Proteome Analysis. *Nat Methods*. 2009;6(5):359-363.

102. Orsburn BC. Proteome discoverer-a community enhanced data processing suite for protein informatics. *Proteomes*. 2021;9(1). doi:10.3390/proteomes9010015

103. Cox J, Mann M. MaxQuant enables high peptide identification rates, individualized p.p.b.-range mass accuracies and proteome-wide protein quantification. *Nat Biotechnol*. 2008;26(12):1367-1372. doi:10.1038/nbt.1511

104. Sayers EW, Bolton EE, Brister JR, et al. Database resources of the national center for biotechnology information. *Nucleic Acids Res*. 2022;50(D1):D20-D26. doi:10.1093/nar/gkab1112

105. Tyanova S, Temu T, Sinitcyn P, et al. The Perseus computational platform for comprehensive analysis of (prote)omics data. *Nat Methods*. 2016;13(9):731-740. doi:10.1038/nmeth.3901

106. Kelley LA, Mezulis S, Yates CM, Wass MN, Sternberg MJ. The Phyre2 Web Portal for Protein Modeling, Prediction and Analysis. *Nat Protoc*. 2015;10:845-858.

107. Jiang Y, Chen B, Duan C, Sun B, Yang J, Yang S. Multigene editing in the Escherichia coli genome via the CRISPR-Cas9 system. *Appl Environ Microbiol*. 2015;81(7):2506-2514. doi:10.1128/AEM.04023-14

108. ThermoFisher Scientific. Competent Cell Selection-6 General Considerations.

109. Aune TEV, Aachmann FL. Methodologies to increase the transformation efficiencies and the range of bacteria that can be transformed. *Appl Microbiol Biotechnol*. 2010;85(5):1301-1313. doi:10.1007/s00253-009-2349-1

110. Altschul SF, Gish W, Miller W, Meyers EW, Lipman DJ. Basic Local Alignment Search Tool. *J Mol Biol*. 1990;215(3):403-410. doi:10.1016/S0022-2836(05)80360-2

111. Bekal S, Berry C, Reimer AR, et al. Usefulness of High-Quality Core gGnome Single-Nucleotide Variant Analysis for Subtyping the Highly Clonal and the Most Prevalent *Salmonella enterica* Serovar Heidelberg Clone in the Context of Outbreak Investigations. *J Clin Microbiol*. 2016;54(2):289-295. doi:10.1128/JCM.02200-15

112. Rambaut A. Figtree v1.4.4. 2018. http://tree.bio.ed.ac.uk/software/figtree/.

113. Bharat A, Petkau A, Avery BP, et al. Correlation between Phenotypic and In Silico Detection of Antimicrobial Resistance in Salmonella enterica in Canada Using Staramr. *Microorganisms*. 2022;10(2):1-10. doi:10.3390/microorganisms10020292

114. Chapin KC, Musgnug MC. Evaluation of Sensititre Automated Reading and Incubation System for Automated Reading of Sensititre Broth Microdilution Susceptibility Plates. *J Clin Microbiol*. 2004;42(2):909-911. doi:10.1128/JCM.42.2.909-911.2004

115. Kaldhone PR, Carlton A, Aljahdali N, et al. Evaluation of Incompatibility Group I1 (IncI1) Plasmid-Containing Salmonella enterica and Assessment of the Plasmids in Bacteriocin Production and Biofilm Development. *Front Vet Sci*. 2019;6(September):1-13. doi:10.3389/fvets.2019.00298

116. Sekse C, Holst-Jensen A, Dobrindt U, et al. High Throughput Sequencing for Detection of Foodborne Pathogens. *Front Microbiol*. 2017;8(OCT):1-26. doi:10.3389/fmicb.2017.02029

117. Newton GL, Koledin T, Gorovitz B, Rawat M, Fahey RC, Av-Gay Y. The Glycosyltransferase Gene Encoding the Enzyme Catalyzing the First Step of Mycothiol Biosynthesis (*mshA*). *J Bacteriol*. 2003;185(11):3476-3479. doi:10.1128/JB.185.11.3476-3479.2003

118. Buchmeier NA, Newton GL, Fahey RC. A Mycothiol Synthase Mutant of *Mycobacterium tuberculosis* has an Altered Thiol-Disulfide Content and Limited Tolerance to Stress. *J Bacteriol*. 2006;188(17):6245-6252. doi:10.1128/JB.00393-06

119. Newton GL, Buchmeier N, Fahey RC. Biosynthesis and Functions of Mycothiol, the Unique Protective Thiol of Actinobacteria. *Microbiol Mol Biol Rev*. 2008;72(3):471-494. doi:10.1128/mmbr.00008-08

120. Gu D, Xue H, Yuan X, et al. Genome-Wide Identification of Genes Involved in Acid Stress Resistance of *Salmonella* Derby. *Genes (Basel)*. 2021;12(4). doi:10.3390/genes12040476

121. Aussel L, Pierrel F, Loiseau L, Lombard M, Fontecave M, Barras F. Biosynthesis and Physiology of Coenzyme Q in Bacteria. *Biochim Biophys Acta - Bioenerg*. 2014;1837(7):1004-1011. doi:10.1016/j.bbabio.2014.01.015

122. Aussel L, Loiseau L, Chehade H, Pocachard B, Fontecave M, Pierrel F. *ubiJ* a New Gene Required for Aerobic Growth and Proliferation in Macrophage , Is Involved in Coenzyme Q Biosynthesis in *Escherichia coli* and *Salmonella enterica* Serovar Typhimurium. 2014;196(1):70-79. doi:10.1128/JB.01065-13

123. Batchelor E, Walthers D, Kenney LJ, Goulian M. The *Escherichia coli* CpxA-CpxR Envelope Stress Response System Regulates Expression of the Porins OmpF and OmpC. *J Bacteriol*. 2005;187(16):5723-5731. doi:10.1128/JB.187.16.5723-5731.2005

124. Jing W, Liu J, Wu S, Li X, Liu Y. Role of *cpxA* Mutations in the Resistance to Aminoglycosides and β-Lactams in *Salmonella enterica* Serovar Typhimurium. *Front Microbiol*. 2021;12(February):1-12. doi:10.3389/fmicb.2021.604079

125. Jing W, Liu J, Wu S, Chen Q, Li X, Liu Y. Development of a Method for Simultaneous Generation of Multiple Genetic Modification in <i>Salmonella enterica</ii> Serovar Typhimurium. *Front Genet*. 2020;11(September):1-14. doi:10.3389/fgene.2020.563491

126. Carroll AC, Wong A. Plasmid Persistence: Costs, Benefits, and the Plasmid Paradox. *Can J Microbiol*. 2018;64(5):293-304. doi:10.1139/cjm-2017-0609

127. Newbury A, Dawson B, Klumper U, et al. Fitness Effects of Plasmids Shape the Structure of Bacteria–Plasmid Interaction Networks. *Proc Natl Acad Sci U S A*. 2022;119(22):1-8. doi:10.1073/pnas.2118361119

128. Vogwill T, Maclean RC. The Genetic Basis of the Fitness Costs of Antimicrobial Resistance: A Meta-Analysis Approach. *Evol Appl*. 2015;8(3):284-295. doi:10.1111/eva.12202

129. Trevors JT. Plasmid Curing in Bacteria. *FEMS Microbiol Lett*. 1986;32(3-4):149-157. doi:10.1016/0378-1097(86)90286-7

130. Schiefner A, Chatwell L, Breustedt DA, Skerra A. Structural and biochemical analyses reveal a monomeric state of the bacterial lipocalin Blc. *Acta Crystallogr Sect D Biol Crystallogr*. 2010;66(12):1308-1315. doi:10.1107/S0907444910039375

131. Campanacci V, Bishop RE, Blangy S, Tegoni M, Cambillau C. The membrane bound bacterial lipocalin Blc is a functional dimer with binding preference for lysophospholipids. *FEBS Lett*. 2006;580(20):4877-4883. doi:10.1016/j.febslet.2006.07.086

132. Dong H, Cronan JE. Temperature regulation of membrane composition in the Firmicute, Enterococcus faecalis, parallels that of Escherichia coli. *Environ Microbiol*. 2021;23(5):2683-2691. doi:10.1111/1462-2920.15512

133. Schultz D, Kishony R. Optimization and control in bacterial lag phase. *BMC Biol*. 2014;11(1):2-4. doi:10.1186/1741-7007-11-120

134. Troxell B, Petri N, Daron C, et al. Poultry Body Temperature Contributes to Invasion Control Through Reduced Expression of *Salmonella* Pathogenicity Island 1 Genes in *Salmonella enterica* Serovars Typhimurium and Enteritidis. *Appl Environ Microbiol*. 2015;81(23):8192-8201. doi:10.1128/AEM.02622-15

135. Chen P, Shakhnovich EI. Thermal adaptation of viruses and bacteria. *Biophys J*. 2010;98(7):1109-1118. doi:10.1016/j.bpj.2009.11.048

136. Kihara A, Akiyama Y, Ito K. Different pathways for protein degradation by the

FtsH/HflKC membrane-embedded protease complex: An implication from the interference by a mutant form of a new substrate protein, YccA. *J Mol Biol*. 1998;279(1):175-188. doi:10.1006/jmbi.1998.1781

137. Shimohata N, Chiba S, Saikawa N, Ito K, Akiyama Y. The Cpx stress response system of Escherichia coli senses plasma membrane proteins and controls HtpX, a membrane protease with a cytosolic active site. *Genes to Cells*. 2002;7(7):653-662. doi:10.1046/j.1365-2443.2002.00554.x

138. Sakoh M, Ito K, Akiyama Y. Proteolytic activity of HtpX, a membrane-bound and stress-controlled protease from Escherichia coli. *J Biol Chem*. 2005;280(39):33305-33310. doi:10.1074/jbc.M506180200

139. Zampieri M, Hörl M, Hotz F, Müller NF, Sauer U. Regulatory Mechanisms Underlying Coordination of Amino Acid and Glucose Catabolism in *Escherichia coli*. *Nat Commun*. 2019;10(1):1-13. doi:10.1038/s41467-019-11331-5

140. Akashi H, Gojobori T. Metabolic Efficiency and Amino Acid Composition in the Proteomes of *Escherichia coli* and *Bacillus subtilis*. *Proc Natl Acad Sci U S A*. 2002;99(6):3695-3700. doi:10.1073/pnas.062526999

141. Lyubetskaya A V., Rubanov LI, Gelfand MS. Use of the Flux Model of Amino Acid Metabolism of *Escherichia coli*. *Biochem*. 2006;71(11):1256-1260. doi:10.1134/S0006297906110113

142. Li W, Li L, Yan X, et al. Nitrate Utilization Promotes Systemic Infection of *Salmonella* Typhimurium in Mice. *Int J Mol Sci*. 2022;23(13). doi:10.3390/ijms23137220

143. Quan S, Koldewey P, Tapley T, et al. Genetic Selection Designed to Stabilize Proteins Uncovers a Chaperone Called Spy. *Nat Struct Mol Biol*. 2011;18(3):262-269. doi:10.1038/nsmb.2016

144. Sezonov G, Joseleau-Petit D, D'Ari R. *Escherichia coli* Physiology in Luria-Bertani Broth. *J Bacteriol*. 2007;189(23):8746-8749. doi:10.1128/JB.01368-07

145. Herr CQ, Macomber L, Kalliri E, Hausinger RP. Glutarate L-2-Hydroxylase (CsiD/GlaH) is an Archetype Fe(II)/2-Oxoglutarate-Dependent Dioxygenase. *Adv Protein Chem Struct Biol*. 2019;117:63-90. doi:10.1016/bs.apcsb.2019.05.001

146. Olson ER, Dunyak DS, Jurss LM, Poorman r. A. Identification and Characterization of *dppA*, an *Escherichia coli* Gene Encoding a Periplasmic Dipeptide Transport Protein. *J Bacteriol*. 1991;173(1):234-244. doi:10.1128/jb.173.1.234-244.1991

147. Das C, Mokashi C, Mande SS, Saini S. Dynamics and control of flagella assembly in *Salmonella typhimurium*. *Front Cell Infect Microbiol*. 2018;8(FEB):1-13. doi:10.3389/fcimb.2018.00036

148. Akhtar AA, Turner DP. The Role of Bacterial ATP-Binding Cassette (ABC) Transporters in Pathogenesis and Virulence: Therapeutic and Vaccine Potential. *Microb Pathog*. 2022;171(August):105734. doi:10.1016/j.micpath.2022.105734

149. Sholpan A, Lamas A, Cepeda A, Franco CM. *Salmonella spp.* Quorum Sensing: An Overview from Environmental Persistence to Host Cell Invasion. *AIMS Microbiol*. 2021;7(2):238-256. doi:10.3934/microbiol.2021015

150. Spöring I, Felgner S, Preuße M, et al. Regulation of Flagellum Biosynthesis in Rsponse to Cell Envelope Stress in *Salmonella enterica* Serovar Typhimurium. *MBio*. 2018;9(3). doi:10.1128/mBio.00736-17

151. Kanehisa M, Sato Y, Morishima K. BlastKOALA and GhostKOALA: KEGG Tools for Functional Characterization of Genome and Metagenome Sequences. *J Mol Biol*. 2016;428(4):726-731. doi:10.1016/j.jmb.2015.11.006

152. Kanehisa M, Sato Y. KEGG Mapper for Inferring Cellular Functions from Protein Sequences. *Protein Sci*. 2020;29(1):28-35. doi:10.1002/pro.3711

153. Choi J, Shin D, Ryu S. Implication of Quorum Sensing in *Salmonella enterica* Serovar Typhimurium Virulence: The *luxS* Gene is Necessary for Expression of Genes in Pathogenicity Island 1. *Infect Immun*. 2007;75(10):4885-4890. doi:10.1128/IAI.01942-06

154. Darwin KH, Miller VL. Type III Secretion Chaperone-Dependent Regulation: Activation of Virulence Genes by SicA and InvF in Salmonella typhimurium</i>. *EMBO J*. 2001;20(8):1850-1862. doi:10.1093/emboj/20.8.1850

155. Antonio Ibarra J, Knodler LA, Sturdevant DE, et al. Induction of Salmonella Pathogenicity Island 1 Under Different Growth Conditions can Affect Salmonella-Host Cell Interactions *in vitro*. *Microbiology*. 2010;156(4):1120-1133. doi:10.1099/mic.0.032896-0

156. Kempf B, Bremer E. OpuA, an Osmotically Regulated Binding Protein-Dependent Transport System for the Osmoprotectant Glycine Betaine in *Bacillus subtilis*. *J Biol Chem*. 1995;270(28):16701-16713. doi:10.1074/jbc.270.28.16701

157. Garza AG, Harris-Haller LW, Stoebner RA, Manson MD. Motility Protein Interactions in the Bacterial Flagellar Motor. *Proc Natl Acad Sci U S A*. 1995;92(6):1970-1974. doi:10.1073/pnas.92.6.1970

158. Kanehisa M, Goto S. KEGG: Kyoto Encyclopedia of Genes and Genomes. *Nucleic Acids Res*. 2000;28(1):27-30. doi:10.1093/nar/28.1.27

159. Nguyen CC, Saier MH. Structural and Phylogenetic Analysis of the MotA and MotB Families of Bacterial Flagellar Motor Proteins. *Res Microbiol*. 1996;147(5):317-332. doi:10.1016/0923-2508(96)84707-3

160. Asakura H, Ekawa T, Sugimoto N, et al. Membrane Topology of *Salmonella* Invasion Protein SipB Confers Osmotolerance. *Biochem Biophys Res Commun*. 2012;426(4):654-658. doi:10.1016/j.bbrc.2012.09.012

161. Jneid B, Moreau K, Plaisance M, Rouaix A, Dano J, Simon S. Role of T3SS-1 SipD Protein in Protecting Mice Against Non-typhoidal *Salmonella* Typhimurium. *PLoS Negl Trop Dis*. 2016;10(12):1-19. doi:10.1371/journal.pntd.0005207

162. Knodler LA, Finlay B, Steele-Mortimer O. The *Salmonella* Effector Protein SopB Protects Epithelial Cells from Apoptosis by Sustained Activation of Akt. *J Biol Chem*. 2005;280(10):9058-9064. doi:10.1074/jbc.M412588200

163. Frutos-Grilo E, Marsal M, Irazoki O, Barbé J, Campoy S. The Interaction of RecA With Both CheA and CheW Is Required for Chemotaxis. *Front Microbiol*. 2020;11(April):1-15. doi:10.3389/fmicb.2020.00583

164. Irazoki O, Mayola A, Campoy S, Barbé J. SOS System Induction Inhibits the Assembly of Chemoreceptor Signaling Clusters in *Salmonella enterica*. *PLoS One*. 2016;11(1):1-22. doi:10.1371/journal.pone.0146685

165. Hegde M, Englert DL, Schrock S, et al. Chemotaxis to the Quorum-sensing Signal AI-2 Requires the Tsr Chemoreceptor and the Periplasmic LsrB AI-2-binding Protein. *J Bacteriol*. 2011;193(3):768-773. doi:10.1128/JB.01196-10

166. Rivera-Chávez F, Winter SE, Lopez CA, et al. *Salmonella* Uses Energy Taxis to Benefit from Intestinal Inflammation. *PLoS Pathog*. 2013;9(4). doi:10.1371/journal.ppat.1003267

167. Blum M, Chang HY, Chuguransky S, et al. The InterPro protein families and domains database: 20 years on. *Nucleic Acids Res*. 2021;49(D1):D344-D354. doi:10.1093/nar/gkaa977

168. Olejniczak M, Storz G. ProQ/FinO-domain proteins: another ubiquitous family of RNA matchmakers? *Mol Microbiol*. 2017;104(6):905-915. doi:10.1111/mmi.13679

169. El Mouali Y, Gerovac M, Mineikaite R, Vogel J. In vivo targets of Salmonella FinO include a FinP-like small RNA controlling copy number of a cohabitating plasmid. *Nucleic Acids Res*. 2021;49(9):5319-5335. doi:10.1093/nar/gkab281

170. Gonzalez GM, Hardwick SW, Maslen SL, et al. Structure of the *Escherichia coli* ProQ RNA-binding protein. *Rna*. 2017;23(5):696-711. doi:10.1261/rna.060343.116

171. Smirnov A, Förstner KU, Holmqvist E, et al. Grad-seq Guides the Discovery of ProQ as a Major Small RNA-Binding Protein. *Proc Natl Acad Sci U S A*. 2016;113(41):11591-11596. doi:10.1073/pnas.1609981113

172. Liao Z, Smirnov A. FinO / ProQ-family proteins : an evolutionary perspective. 2023;0(March):1-21.

173. Yang J, Wang HH, Lu Y, et al. A ProQ/FinO family protein involved in plasmid copy number control favours fitness of bacteria carrying mcr-1-bearing IncI2 plasmids. *Nucleic Acids Res*. 2021;49(7):3981-3996. doi:10.1093/nar/gkab149

174. Foley SL, Kaldhone PR, Ricke SC, Han J. Incompatibility Group I1 (IncI1) Plasmids: Their Genetics, Biology, and Public Health Relevance. *Microbiol Mol Biol Rev*. 2021;85(2):1-24. doi:10.1128/mmbr.00031-20

175. Asano K, Mizobuchi K. Copy number control of Inclα plasmid ColIb-P9 by competition between pseudoknot formation and antisense RNA binding at a specific RNA site. *EMBO*

J. 1998;17(17):5201-5213. doi:10.1093/emboj/17.17.5201

176. CLSI. *M100 - Performance Standards for Antimicrobial Susceptibility Testing*. 30th ed. Wayne, PA: Clinical and Laboratory Standards Institute; 2023.

Appendix

Table A1. CLSI M100-ED33:2023 and NARMS acceptable quality control ranges for E. coli ATCC 25922 on MIC plates and recommended broths[176].

Antimicrobial	MIC QC Ranges, ug/mL
Amoxicillin-clavulanate (2:1)	2/1-8/4
Ampicillin	2-8
Azithromycin*	0.25-32
Cefoxitin	2-8
Ceftriaxone	0.03-0.12
Chloramphenicol	2-8
Ciprofloxacin	0.004-0.015
Gentamicin	0.25-1
Meropenem	0.008-0.06
Nalidixic acid	1-4
Streptomycin*	2-64
Sulfisoxazole	8-32
Tetracycline	0.5-2
Trimethoprim-sulfamethoxazole (1:19)	≤0.5/9.5

*CLSI breakpoints not established; interpretive standards used are NARMS-established breakpoints for resistance monitoring and should not be used to predict clinical efficacy

Plate 1	1	2	3	4	5	6	7	8	9	10	11	12
A	Negative Control	L-arabinose	N-Acetyl-D-Glucosamine	D-Saccharic Acid	Succinic Acid	D-Galactose	L-Aspartic Acid	L-Proline	D-Alanine	D-Trehalose	D-Mannose	Duicitol
B	D-Serine	D-Sorbitol	Glycerol	L-Fucose	D-Glucuronic Acid	D-Gluconic Acid	D,L-a-Glyverol-Phosphate	D-Xylose	L-Lactic Acid	Formic Acid	D-Mannitol	L-Glutamic Acid
C	D-Glucose-6-Phophate	D-Galactonic Acid-y-Lactone	D,L-Malic Acid	D-Ribose	Tween 20	L-Rhamnose	D-Fructose	Acetic Acid	a-D-Glucose	Maltose	D-Melibiose	Thymidine
D	L-Asparagine	D-Aspartic Acid	D-Glucosaminic Acid	1,2-Propanediol	Tween 40	a-Keto-Glutaric Acid	a-Keto-Butyric Acid	a-Methyl-D-Galactoside	a-D-Lactose	Lactulose	Sucrose	Uridine
E	L-Glutamine	m-Tartaric Acid	D-Glucose-1-Phosphate	D-Fructose-6-Phophate	Tween 80	a-Hydroxyl Glutaric Acid-y-Lactone	a-Hydroxy Butyric Acid	B-Methyl-D-Glucoside	Adonitol	Maltotriose	2-Deoxy Adenosine	Adenosine
F	Glycyl-L-Aspartic Acid	Citric Acid	m-Inositol	D-Threonine	Fumaric Acid	Bromo Succinic Acid	Propionic Acid	Mucic Acid	Glycolic Acid	Glyoxylic Acid	D-Cellobiose	Inosine
G	Glycyl-L-Glutamic Acid	Tricarbailylic Acid	L-Serine	L-Threonine	L-Alanine	L-Alanyl-Glycine	Acetoacetic Acid	N-Acetyl-β-D-Mannosamine	Mono Methyl Succinate	Methyl Pyruvate	D-Malic Acid	L-Malic Acid
H	Glycyl-L-Proline	p-Hydroxy Phenyl Acetic Acid	m-Hydroxy Phenyl Acetic Acid	Tyramine	D-Psicose	L-Lyxose	Glucuronamide	Pyruvic Acid	L-Galactonic Acid-γ-Lactone	D-Galacturonic Acid	Phenylethyl-amine	2-Aminoethanol

Figure A1. Biolog Omnilog® PM plate 1 layout and contents.

Plate 2A	1	2	3	4	5	6	7	8	9	10	11	12
A	Negative Control	Chondroitin Sulfate C	α-Cyclodextrin	β-Cyclodextrin	γ-Cyclodextrin	Dextrin	Gelatin	Glycogen	Inulin	Laminarin	Mannan	Pectin
B	N-Acetyl-D-Galactosamine	N-Acetyl-Neuraminic Acid	β-D-Allose	Amygdalin	D-Arabinose	D-Arabitol	L-Arabitol	Arbutin	2-Deoxy-D-Ribose	i-Erythritol	D-Fucose	3-0-β-D-Galacto-pyranosyl-D-Arabinose
C	Gentiobiose	L-Glucose	Lactitol	D-Melezitose	Maltitol	a-Methyl-D-Glucoside	β-Methyl-D-Glucoside	3-Methyl-Glucose	β-Methyl-D-Glucuronic Acid	α-Methyl-D-Mannoside	β-Methyl-D-Xyloside	Palatinose
D	D-Raffinose	Salicin	Sedoheptulosan	L-Sorbose	Stachyose	D-Tagatose	Turanose	Xylitol	N-Acetyl-D-Glucosaminitol	γ-Amino Butyric Acid	δ-Amino Valeric Acid	Butyric Acid
E	Capric Acid	Caproic Acid	Citraconic Acid	Citramalic Acid	D-Glucosamine	2-Hydroxy Benzoic Acid	4-Hydroxy Benzoic Acid	β-Hydroxy Butyric Acid	γ-Hydroxy Butyric Acid	a-Keto-Valeric Acid	Itaconic Acid	5-Keto-D-Gluconic Acid
F	D-Lactic Acid	Methyl Ester	Malonic Acid	Melibionic Cid	Oxalic Acid	Oxalomalic Acid	Quinic Acid	D-Ribono-1,4-Lactone	Sebacic Acid	Sorbic Acid	D-Tartaric Acid	L-Tartaric Acid
G	Acetamide	L-Alaninamide	N-Acetyl-L-Glutamic Acid	L-Arginine	Glycine	L-Histidine	L-Homoserine	Hydroxy-L-Proline	L-Isoleucine	L-Leucine	L-Lysine	L-Methionine
H	L-Ornithine	L-Phenylalanine	L-Pyroglutamic Acid	L-Valine	D,L-Carnitine	Sec-Butylamine	D,L-Octopamine	Putrescine	Dihydroxy Acetone	2,3-Butanediol	2,3-Butanedione	3-Hydroxy 2-Butanone

Figure A2. Biolog Omnilog® PM plate 2A layout and contents.

Plate 3B	1	2	3	4	5	6	7	8	9	10	11	12
A	Negative Control	Ammonia	Nitrite	Nitrate	Urea	Bluret	L-Alanine	L-Arginine	L-Asparagine	L-Aspartic Acid	L-Cysteine	L-Glutamic Acid
B	L-Glutamine	Glycine	L-Histidine	L-Isoleucine	L-Leucine	L-Lysine	L-Methionine	L-Phenylalanine	L-Proline	L-Serine	L-Threonine	L-Tryptophan
C	L-Tyrosine	L-Valine	D-Alanine	D-Asparagine	D-Aspartic Acid	D-Glutamic Acid	D-Lysine	D-Serine	D-Valine	L-Citruline	L-Homoserine	L-Ornithine
D	N-Acetyl-L-Glutamic Acid	N-Phthaloyl-L-Glutamic Acid	L-Pyroglutamic Acid	Hydroxylamine	Methylamine	N-Amylamine	N-Butlamine	Ethylamine	Ethanolamine	Ehtylenediamine	Putrescine	Agmatine
E	Histamine	β-Phenylethyl-amine	Tyramine	Acetamide	Formamide	Glucuronamide	D,L-Lactamide	D-Glucosamine	D-Galactosamine	D-Mannosamine	N-Acetyl-D-Glucosamine	N-Acetyl-D-Galactosamine
F	N-Acetyl-D-Mannosamine	Adenine	Adenosine	Cytidine	Cytosine	Guanine	Guanosine	Thymine	Thymidine	Uracil	Uridine	Inosine
G	Xanthine	Xanthosine	Uric Acid	Alloxan	Allantoin	Parabanic Acid	D,L-α-Amino-N-Butyric Acid	γ-Amino-N-Caproic Acid	ε-Amino-N-CaproicAcid	D,L-α-Amino-Caprylic Acid	δ-Amino-N-ValericAcid	α-Amino-N-Valeric Acid
H	Ala-Asp	Ala-Gln	Ala-Glu	Ala-Gly	Ala-His	Ala-Leu	Ala-Thr	Gly-Asn	Gly-Gln	Gly-Glu	Gly-Met	Met-Ala

Figure A3. Biolog Omnilog® PM plate 3B layout and contents.

Plate 4A	1	2	3	4	5	6	7	8	9	10	11	12
A	Negative Control	Phosphate	Pyrophosphate	Trimeta-phosphate	Tripoly-phosphate	Triethyl Phosphate	Hypophosphite	Adenosine-2'-monophosphate	Adenosine-3'-monophosphate	Adenosine-5'-monophosphate	Adenosine-2'-3'-cyclic monophosphate	Adenosine-3'-5'-cyclic monophosphate
B	Thiophosphate	Dithiophosphate	D,L-α-Glycerol Phosphate	β-Glyverol Phosphate	Carbamyl Phosphate	D-2-Phospho-Glyceric Acid	D-3-Phospho-Glyceric Acid	Guanosine-2'-monophosphate	Guanosine-3'-monophosphate	Guanosine-5'-monophosphate	Guanosine-2',3'-cyclic monophosphate	Guanosine-3',5'-cyclic monophosphate
C	Phosphoenol Pyruvate	Phospho-Glycolic Acid	D-Glucose-1-Phosphate	D-Glucose-6-Phosphate	2-Deoxy-D-Glucose 6-Phosphate	D-Glucosamine-6-Phosphate	6-Phospho-Gluconic Acid	Cytidine-2'-monophosphate	Cytidine-3'-monophosphate	Cytidine-5'-monophosphate	Cytidine-2',3'-cyclic monophosphate	Cytidine-3',5'-cyclic monophosphate
D	D-Mannose-1-Phosphate	D-Mannose-6-Phosphate	Cysteamine-S-Phosphate	Phospho-L-Arginine	O-Phospho-D-Serine	O-Phospho-L-Serine	O-Phospho-L-Threonine	Uridine-2'-monophosphate	Uridine-3'-monophosphate	Uridine-5'-monophosphate	Uridine-2',3'-cyclic monophosphate	Uridine-3',5'-cyclic monophosphate
E	O-Phospho-D-Tyrosine	O-Phospho-L-Tyrosine	Phosphocreatine	Phosphoryl Choline	O-Phosphoryl-Ethanolamine	Phosphono Acetic Acid	2-Aminoethyl Phosphonic Acid	Methylene Diphosphonic Acid	Thymidine-3'-monophosphate	Thymidine-5'-monophosphate	Inositol Hexaphosphate	Thymidine 3',5'-cyclic monophosphate
F	Negative Control	Sulfate	Thiosulfate	Tetrathionate	Thiophosphate	Dithiophosphate	L-Cysteine	D-Cysteine	L-Cysteinyl-Glycine	L-Cysteic Acid	Cysteamine	L-Cysteine Sulfinic Acid
G	N-Acetyl-L-Cysteine	S-Methyl-L-Cysteine	Cystathionine	Lanthionine	Glutathione	D,L-Ethionine	L-Methionine	D-Methionine	Glycyl-L-Methionine	N-Acetyl-D,L-Methionine	L-Methionine Sulfoxide	L-Methionine Sulfone
H	L-Djenkolic Acid	thiourea	1-Thio-β-D-Glucose	D,L-Lipoamide	Taurocholic Acid	Taurine	Hypotaurine	p-Amino Benzene Sulfonic Acid	Butane Sulfonic Acid	2-Hydroxyethane Sulfonic Acid	Methane Sulfonic Acid	Tetramethylene Sulfone

Figure A4. Biolog Omnilog® PM plate 4A layout and contents.

Plate 5	1	2	3	4	5	6	7	8	9	10	11	12
A	Negative Control	Positive Control	L-Alanine	L-Arginine	Lasparagine	L-aspartic Acid	L-Cysteine	L-Glutamic Acid	Adenosine-3',5'-cyclic monophosphate	Adenine	Adenosine-3',5'-cyclic monophosphate	2'-Deoxy Adenosine
B	L-Glutamine	Glycine	L-Histidine	L-Isoleucine	L-Leucine	L-Lysine	L-Methionine	L-Phenylalanine	Guanosine-3',5'-cyclic monophosphate	Guanine	Guanosine-3',5'-cyclic monophosphate	2'-Deoxy Guanosine
C	L-Proline	L-Serine	L-Threonine	L-Tryptophan	L-Tyrosine	L-Valine	L-Isoleucine + L-Valine	trans-4-Hydroxy L-Proline	(5) 4-Amino-imidazole-4(5)-Carboxamide	Hyoznathine	Inosine	2'-Deoxy inosine
D	L-Ornithine	L-Citruline	Chorismic Acid	(-)Shikimic Acid	L-Homoserine Lactone	D-Alanine	D-Aspartic Acid	D-Glutamic Acid	D,L-α,ε-Diamino-pimelic Acid	Cutosine	Cytidine	2'-Deoxy Cytidine
E	Putrescine	Spermidine	Spermine	Pyridoxine	Pyridoxal	Pyridoxamine	β-Alanine	D-Pantothenic Acid	Orotic Acid	Uracil	Uridine	2'-Deoxy Uridine
F	Quinolinic Acid	Nicotinic Acid	Nicotinamide	β-Nicotinamide Adenine Dinucleotide	δ-Amino-Levulinic Acid	Hematin	Deferoxamine Mesylate	D-(+)-Glucose	N-Acetyl D-Glucosamine	Thymine	Glutathione (reduced form)	Thymidine
G	Oxaloacetic Acid	D-Biotin	Cyano-Cobalamine	p-Amino-Benzoic Acid	Folic Acid	Inosine + Thiamine	Thiamine	Thiamine Pyrophosphate	Riboflavin	Pyrrolo-Quinoline Quinone	Menadione	m-Inositol
H	Butyric Acid	D,L-α-Hydroxy-Butyric Acid	α-Keto-Butyric Acid	Caprylic Acid	D,L-α-Lipoic Acid (oxidized form)	D,L-Mevalonic Acid	D,L-Carnitine	Choline	Tween 20	Tween 40	Tween 60	Tween 80

Figure A5. Biolog Omnilog® PM plate 5 layout and contents.

Plate 6	1	2	3	4	5	6	7	8	9	10	11	12
A	Negative Control	Positive Control: L-Glutamine	Ala-Ala	Ala-Arg	Ala-Asn	Ala-Glu	Ala-Gly	Ala-his	Ala-Leu	Ala-Lys	Ala-Phe	Ala-Pro
B	Ala-Ser	Ala-Thr	Ala-Trp	Ala-Tyr	Arg-Ala	Arg-Arg	Arg-Asp	Arg-Gln	Arg-Glu	Arg-Ile	Arg-Leu	Arg-Lys
C	Arg-Met	Arg-Phe	Arg-Ser	Arg-Trp	Arg-Tyr	Arg-Val	Asn-Glu	Asn-Val	Asp-Asp	Asp-Glu	Asp-Leu	Asp-Lys
D	Asp-Phe	Asp-Trp	Asp-Val	Cys-Gly	Gln-Gln	Gln-Gly	Glu-Asp	Glu-Glu	Glu-Gly	Glu-Ser	Glu-Trp	Glu-Tyr
E	Glu-Val	Gly-Ala	Gly-Arg	Gly-Cys	Gly-Gly	Gly-His	Gly-Leu	Gly-Lys	Gly-Met	Gly-Phe	Gly-Pro	Gly-Ser
F	Gly-Thr	Gly-Trp	Gly-Tyr	Gly-Val	His-Asp	His-Gly	His-Leu	His-Lys	His-Met	His-Pro	His-Ser	His-Trp
G	His-Tyr	His-Val	Ile-Ala	Ile-Arg	Ile-Gln	Ile-Gly	Ile-His	Ile-Ile	Ile-Met	Ile-Phe	Ile-Pro	Ile-Ser
H	Ile-Trp	Ile-Tyr	Ile-Val	Leu-Ala	Leu-Arg	Leu-Asp	Leu-Glu	Leu-Gly	Leu-Ile	Leu-Leu	Leu-Met	Leu-Phe

Figure A6. Biolog Omnilog® PM plate 6 layout and contents.

Plate 7	1	2	3	4	5	6	7	8	9	10	11	12
A	Negative Control	Positive Control: L-Glutamine	Leu-Ser	Leu-Trp	Leu-Val	Lys-Ala	Lys-Arg	Lys-Glu	Lys-Ile	Lys-Leu	Lys-Lys	Lys-Phe
B	Lys-Pro	Lys-Ser	Lys-Thr	Lys-Trp	Lys-Tyr	Lys-Val	Met-Arg	Met-Asp	Met-Gln	Met-Glu	Met-Gly	Met-His
C	Met-Ile	Met-Leu	Met-Lys	Met-met	Met-Phe	Met-Pro	Met-Trp	Met-Val	Phe-Ala	Phe-Gly	Phe-Ile	Phe-Phe
D	Phe-Pro	Phe-Ser	Phe-Trp	Pro-Ala	Pro-Asp	Pro-Gln	Pro-Gly	Pro-Hyp	Pro-Leu	Pro-Phe	Pro-Pro-	Pro-Tyr
E	Ser-Ala	Ser-Gly	Ser-His	Ser-Leu	Ser-Met	Ser-Phe	Ser-Pro	Ser-Ser	Ser-Tyr	Ser-Val	Thr-Ala	Thr-Arg
F	Thr-Glu	THr-Gly	Thr-Leu	Thr-Met	Thr-Pro	Trp-Ala	Trp-Arg	Trp-Asp	Trp-Glu	Trp-Gly	Trp-Leu	Trp-Lys
G	Trp-Phe	Trp-Ser	Trp-Trp	Trp-Tyr	Tyr-Ala	Tyr-Gln	Tyr-Glu	Tyr-Gly	Tyr-His	Tyr-Leu	Tyr-Lys	Tyr-Phe
H	Tyr-Trp	Tyr-Tyr	Val-Arg	Val-Asn	Val-Asp	Val-Gly	Val-His	Val-Ile	Val-Leu	Val-Tyr	Val-Val	γ-Glu-Gly

Figure A7. Biolog Omnilog® PM plate 7 layout and contents.

Plate 8	1	2	3	4	5	6	7	8	9	10	11	12
A	Negative Control	Positive Control: L-Glutamine	Ala-Asp	Ala-Gln	Ala-Ile	Ala-Met	Ala-Val	Asp-Ala	Asp-Gln	Asp-Gly	Glu-Ala	Gly-Asn
B	Gly-Asp	Gly-Ile	His-Ala	His-Glu	His-His	Ile-Asn	Ile-Leu	Leu-Asn	Leu-His	Leu-Pro	Leu-Tyr	Lys-Asp
C	Lys-Gly	Lys-met	Met-Thr	Met-Tyr	Phe-Asp	Phe-Glu	Gln-Glu	Phe-Met	Phe-Tyr	Phe-Val	Pro-Arg	Pro-Asn
D	Pro-Glu	Pro-Ile	Pro-Lys	Pro-Ser	Pro-Trp	Pro-Val	Ser-Asn	Ser-Asp	Ser-Gln	Ser-Glu	Thr-Asp	Thr-Gln
E	Thr-Phe	Thr-Ser	Trp-Val	Tyr-Ile	Tyr-Val	Val-Ala	Val-Gln	Val-Glu	Val-Lys	Val-Met	Val-Phe	Val-Pro
F	Val-Ser	β-Ala-Ala	β-Ala-Gly	β-Ala-His	Met-β-Ala	β-Ala-Phe	D-Ala-D-Ala	D-Ala-Gly	D-Ala-Leu	D-Leu-D-Leu	D-Leu-Gly	D-Leu-Tyr
G	γ-Glu-Gly	γ-D-Glu-Gly	Gly-D-Ala	Gly-D-Asp	Gly-D-Ser	Gly-D-Thr	Gly-D-Val	Leu-β-Ala	Leu-D-Leu	Phe-β-Ala	Ala-Ala-Ala	D-Ala-Gly-Gly
H	Gly-Gly-Ala	Gly-Gly-D-Leu	Gly-Gly-Gly	Gly-Gly-Ile	Gly-Gly-Ile	Gly-Gly-Leu	Val-Tyr-Val	Gly-Phe-Phe	Leu-Gly-Gly	Leu-Leu-Leu	Phe-Gly-Gly	Tyr-Gly-Gly

Figure A8. Biolog Omnilog® PM plate 8 layout and contents.

Plate 9	1	2	3	4	5	6	7	8	9	10	11	12
A	NaCl 1%	NaCl 2%	NaCl 3%	NaCl 4%	NaCl 5%	NaCl 5.5%	NaCl 6%	NaCl 6.5%	NaCl 7%	NaCl 8%	NaCl 9%	NaCl 10%
B	NaCl 6%	Nacl 6% + Betaine	NaCl 6% + N-N Dimethyl Glycine	NaCl 6% + Sarcosine	NaCl 6% + Dimethyl sulphonyl propionate	NaCl 6% + MOPS	NaCl 6% + Ectoine	NaCl 6% + Choline	NaCl 6% + Phosphoryl Choline	NaCl 6% + Creatine	NaCl 6% + Creatinine	NaCl 6% + L-Carnitine
C	NaCl 6% + KCl	NaCl 6% + L-Proline	NaCl 6% + N-Acetyl L-Glutamine	NaCl 6% + β-Glutamic Acid	NaCl 6% + γ-Amino-N-Butyric Acid	NaCl 6% + Glutathione	NaCl 6% + Glycerol	NaCl 6% + Trehalose	NaCl 6% + Trimethylamine-N-oxide	NaCl 6% + Trimethylamine	NaCl 6% + Octopine	NaCl 6% + Trigonelline
D	Potassium Chloride 3%	Potassium Chloride 4%	Potassium Chloride 5%	Potassium Chloride 6%	Sodium sulfate 2%	Sodium sulfate 3%	Sodium sulfate 4%	Sodium sulfate 5%	Ethylene glycol 5%	Ethylene glycol 10%	Ethylene glycol 15%	Ethylene glycol 20%
E	Sodium formate 1%	Sodium formate 2%	Sodium formate 3%	Sodium formate 4%	Sodium formate 5%	Sodium formate 6%	Urea 2%	Urea 3%	Urea 4%	Urea 5%	Urea 6%	Urea 7%
F	Sodium Lactate 1%	Sodium Lactate 2%	Sodium Lactate 3%	Sodium Lactate 4%	Sodium Lactate 5%	Sodium Lactate 6%	Sodium Lactate 7%	Sodium Lactate 8%	Sodium Lactate 9%	Sodium Lactate 10%	Sodium Lactate 11%	Sodium Lactate 12%
G	Sodium Phosphate pH 7 20mM	Sodium Phosphate pH 7 50mM	Sodium Phosphate pH 7 100mM	Sodium Phosphate pH 7 200mM	Sodium Benzoate pH 5.2 20mM	Sodium Benzoate pH 5.2 50mM	Sodium Benzoate pH 5.2 100mM	Sodium Benzoate pH 5.2 200mM	Ammonium sulfate pH 8 10mM	Ammonium sulfate pH 8 20mM	Ammonium sulfate pH 8 50mM	Ammonium sulfate pH 8 100mM
H	Sodium Nitrate 10mM	Sodium Nitrate 20mM	Sodium Nitrate 40mM	Sodium Nitrate 60mM	Sodium Nitrate 80mM	Sodium Nitrate 100mM	Sodium Nitrite 10mM	Sodium Nitrite 20mM	Sodium Nitrite 40mM	Sodium Nitrite 60mM	Sodium Nitrite 80mM	Sodium Nitrite 100mM

Figure A9. Biolog Omnilog® PM plate 9 layout and contents.

Plate 10	1	2	3	4	5	6	7	8	9	10	11	12
A	pH 3.5	pH 4	pH 4.5	pH 5	pH 5.5	pH 6	pH 7	pH 8	pH 8.5	pH 9	pH 9.5	pH 10
B	pH 4.5	pH 4.5 + L-Alanine	pH 4.5 + L-Arginine	pH 4.5 L-Asparagine	pH 4.5 + L-Aspartic Acid	pH 4.5 + L-Glutamic Acid	pH 4.5 + L-Glutamine	pH 4.5 + Glycine	pH 4.5 + L-Histidine	pH 4.5 + L-Isoleucine	pH 4.5 + L-Leucine	pH 4.5 + L-Lysine
C	pH 4.5 + L-Methionine	pH 4.5 + L-Phenylalanine	pH 4.5 + L-Proline	pH 4.5 + L-Serine	pH 4.5 + L-Threonine	pH 4.5 + L-Tryptophan	pH 4.5 + L-Citrulline	pH 4.5 + L-Valine	pH 4.5 + Hydroxy-L-Proline	pH 4.5 + L-Ornithine	pH 4.5 + L-Homoarginine	pH 4.5 + L-Homoserine
D	pH 4.5 + Anthranilic Acid	pH 4.5 + L-Norleucine	pH 4.5 + L-Norvaline	pH 4.5 + α-Amino-N-Butyric Acid	pH 4.5 + p-Amino-Benzoic Acid	pH 4.5 + L-Cysteic Acid	pH 4.5 + D-Lysine	pH 4.5 + 5-Hydroxy Lysine	pH 4.5 + 5-Hydroxy Tryptophan	pH 4.5 + D,L-Diamino pimelic Acid	pH 4.5 + Trimethylamine-N-oxide	pH 4.5 + Urea
E	pH 9.5	pH 9.5 + L-Alanine	pH 9.5 + L-Arginine	pH 9.5 + L-Asparagine	pH 9.5 + L-Aspartic Acid	pH 9.5 + L-Glutamic Acid	pH 9.5 + L-Glutamine	pH 9.5 + Glycine	pH 9.5 + L-Histidine	pH 9.5 + L-isoleucine	pH 9.5 + L-Leucine	pH 9.5 + L-Lysine
F	pH 9.5 + L-Methionine	pH 9.5 + L-Phenylalanine	pH 9.5 + L-Proline	pH 9.5 + L-Serine	pH 9.5 + L-Threonine	pH 9.5 + L-Tryptophan	pH 9.5 + L-Tyrosine	pH 9.5 + L-Valine	pH 9.5 + Hydroxy-L-Proline	pH 9.5 + L-Ornithine	pH 9.5 + L-Homoarginine	pH 9.5 + L-Homoserine
G	pH 9.5 + Anthranilic acid	pH 9.5 + L-Norleucine	pH 9.5 + L-Norvaline	pH 9.5 + Agmatine	pH 9.5 + Cadaverine	pH 9.5 + Putrescine	pH 9.5 + Histamine	pH 9.5 + Phenylethylamine	pH 9.5 + Tyramine	pH 9.5 + Creatine	pH 9.5 + Trimethylamine-N-oxide	pH 9.5 + Urea
H	X-Caprylate	X-α-D-Glucoside	X-β-D-Glucoside	X-α-D-Galactoside	X-β-D-Galactoside	X-α-D-Glucuronide	X-β-D-Glucuronide	X-β-D-Glucosaminide	X-β-D-Galactosaminide	X-α-D-Mannoside	X-PO4	X-SO4

Figure A10. Biolog Omnilog® PM plate 10 layout and contents.

Plate 11C	1	2	3	4	5	6	7	8	9	10	11	12
A	Amikacin				Chlortetracycline				Lincomycin			
B	Amoxicillin				Cloxacillin				Lomefloxacin			
C	Bleomycin				Colisitin				Minocycline			
D	Capreomycin				Demeclocycline				Nafcillin			
E	Cefazolin				Enoxacin				Nalidixic acid			
F	Chloramphenicol				Erythromycin				Neomycin			
G	Ceftriaxone				Gentamicin				Potassium tellurite			
H	Cephalothin				Kanamycin				Ofloxacin			

Figure A11. Biolog Omnilog® PM plate 11C layout and contents.

Plate 12B	1	2	3	4	5	6	7	8	9	10	11	12
A	Penicillin G				Tetracycline				Carbenicillin			
B	Oxacillin				Penimepicycline				Polymyxin B			
C	Paromomycin				Vancomycin				D,L-Serine hydroxamate			
D	Sisomicin				Sulfamethazine				Novobiocin			
E	2,4-Diamino-6,7-diisopropyl-pteridine				Sulfadiazine				Benzethonium chloride			
F	Tobramycin				Sulfathiazole				5-Fluoroorotic acid			
G	Spectinomycin				Sulfamethoxazole				L-Aspartic-β-hydroxamate			
H	Spiramycin				Rifampicin				Dodecyltrimethyl ammomium bromide			

Figure A12. Biolog Omnilog® PM plate 12B layout and contents.

Plate 13B	1	2	3	4	5	6	7	8	9	10	11	12
A	Ampicillin				Adequalinium chloride				Nickel chloride			
B	Aziocillin				2,2'-Dipyridul				Ocoolinic acid			
C	6-Mercapto-purine				Doxycycline				Potassium chromate			
D	Cefuroxime				5-Fluorouracil				Rolltetracycline			
E	Cytosine-1-beta-D-arabino-furanoside				Geneticin (G418)				Ruthenium red			
F	Cesium Chloride				Clycine				Thalium (I) acetate			
G	Cobalt chloride				Manganese chloride				Trifluoperazine			
H	Cupric chloride				Moxalactam				Tylosin			

Figure A13. Biolog Omnilog® PM plate 13B layout and contents.

Plate 14A	**1**	**2**	**3**	**4**	**5**	**6**	**7**	**8**	**9**	**10**	**11**	**12**
A	Acriflavine				Furaltadone				Sanguinarine			
B	9-Amicoacridine				Fusaric acid				Sodium arsenate			
C	Boric Acid				1-Hydroxypyridine-2-thione				Sodium cycanate			
D	Cadmium chloride				Iodoacetate				Sodium dichromate			
E	Cefoxitin				Nitrofurantoin				Sodium metaborate			
F	Chloramphenicol				Piperacillin				Sodium metavanadate			
G	Chlerythrine				Carbenicillin				Sodium nitrite			
H	EGTA				Promethazine				Sodium orthovanadate			

Figure A14. Biolog Omnilog® PM plate 14A layout and contents.

Plate 15B	1	2	3	4	5	6	7	8	9	10	11	12
A	Procaine				Guanidine hydrochloride				Cefmatazole			
B	D-Cycloserine				EDTA				5,7-Dichloro-8-hydroxy-quinaidine			
C	5,7-Dichloro-8-hydroxy-quinoline				Fusidic acid				1,10-Phenanthroline			
D	Phleomycin				Domiphen bromide				Nordihydroguaia retic acid			
E	Alexidine				5-Nitro-2-furaldehyde semicarbazone				Methyl viologen			
F	3,4-Dimethoxy-benzyl alcohol				Oleandomycin				Puromycin			
G	CCCP				Sodium azide				Menadione			
H	2-Nitroimidazole				Hydroxyurea				Zinc chloride			

Figure A15. Biolog Omnilog® PM plate 15B layout and contents.

Plate 16A	1	2	3	4	5	6	7	8	9	10	11	12
A	Cefotaxime				Phosphomycin				5-Chloro-7-iodo-8-hydroxy-quinoline			
B	Norfloxacin				Sulfanilamide				Trimethoprim			
C	Dichiofluanid				Protamine sulfate				Cetylpryidinium chloride			
D	1-Chloro-2,4-dinitrobenzene				Diamide				Cinoxacin			
E	Streptomycin				5-Azacytidine				Rifamycin SV			
F	Potassium tellurite				Sodium selenite				Aluminum sulfate			
G	Chromium chloride				Ferric chloride				L-Glutamic-g-hydroxamate			
H	Glycine hydroxamate				Chloroxylenol				Sorbic acid			

Figure A16. Biolog Omnilog® PM plate 16A layout and contents.

Plate 17A	**1**	**2**	**3**	**4**	**5**	**6**	**7**	**8**	**9**	**10**	**11**	**12**
A	D-Serine				β-Chloro-L-alanine hydrochloride				Thiosalicylic acid			
B	Sodium salicylate				Hygromycin B				Ehtionamide			
C	4-Aminopyridine				Sulfachloro-pyridazine				Sulfamono-methoxine			
D	Oxycarboxin				3-Amino-1,2,4-triazole				Chlorpromazine			
E	Nioproof				Compound 48/80				Sodium tungstate			
F	Lithium chloride				DL-Methionine hydroxamate				Tannic acid			
G	Chlorambucil				Cefamandole nafate				Cefoperazone			
H	Cefsulodin				Caffeine				Phenylarsine oxide			

Figure A17. Biolog Omnilog® PM plate 17A layout and contents.

Plate 18C	1	2	3	4	5	6	7	8	9	10	11	12
A	Ketoprofen				Sodium pyrophosphate decahydrate				Thiamphenicol			
B	Trifuorothymidin				Pipemidic Acid				Azathioprine			
C	Poly-L-lysine				Sulfisoxazole				Pentachloro-phenol			
D	Sodium m-arsenite				Sodium bromate				Lidocaine			
E	Sodium metasilicate				Sodium m-periodate				Antimony (III) chloride			
F	Semicarbazide				Tinidazole				Aztreonam			
G	Triclosan				3,5-Diamino-1,2,4-triazole (Guanazole)				Myricetin			
H	5-fluoro-5'-deoxyuridine				2-Phenylphenol				Plumbagin			

Figure A18. Biolog Omnilog® PM plate 18C layout and contents.

Plate 19	**1**	**2**	**3**	**4**	**5**	**6**	**7**	**8**	**9**	**10**	**11**	**12**
A	Josamycin				Gallic acid				Coumarin			
B	Methyltrioctyl-ammomium chloride				Harmane				2,4-Dinitrophenol			
C	Chlorhexidine				Umbelliferone				Cinnamic acid			
D	Disulphiram				Iodonitro Tetrazolium Violet				Phenyl-methyl-sulfonyl-fluoride (PMSF)			
E	FCCP				D,L-Thioctic acid				Lawsone			
F	Phenethicillin				Blasticidin S				Sodium caprylate			
G	Laurul sulfobetaine				Dihydro-streptomycin				Hydroxylamine			
H	Hexammine cobalt (III) chloride				Thioglycerol				Polymixin B			

Figure A19. Biolog Omnilog® PM plate 19 layout and contents.

Plate 20B	**1**	**2**	**3**	**4**	**5**	**6**	**7**	**8**	**9**	**10**	**11**	**12**
A	Amitriptyline				Apramycin				Beserazide			
B	Ophenadrine				D,L-Propanolol				Tetrazolium violet			
C	Thioridazine				Atropine				Ornidazole			
D	Proflavine				Ciprofloxacin				18-Crown-6-ether			
E	Crystal violet				Dodine				Hexa-chlorophene			
F	4-Hydroxy-coumarin				Oxytetracycline				Pridinol			
G	Captan				3,5-Dinitro-benzene				8-Hydroxy-quinoline			
H	Patulin				Tolylfluanid				Troleandomycin			

Figure A20. Biolog Omnilog® PM plate 20B layout and contents.

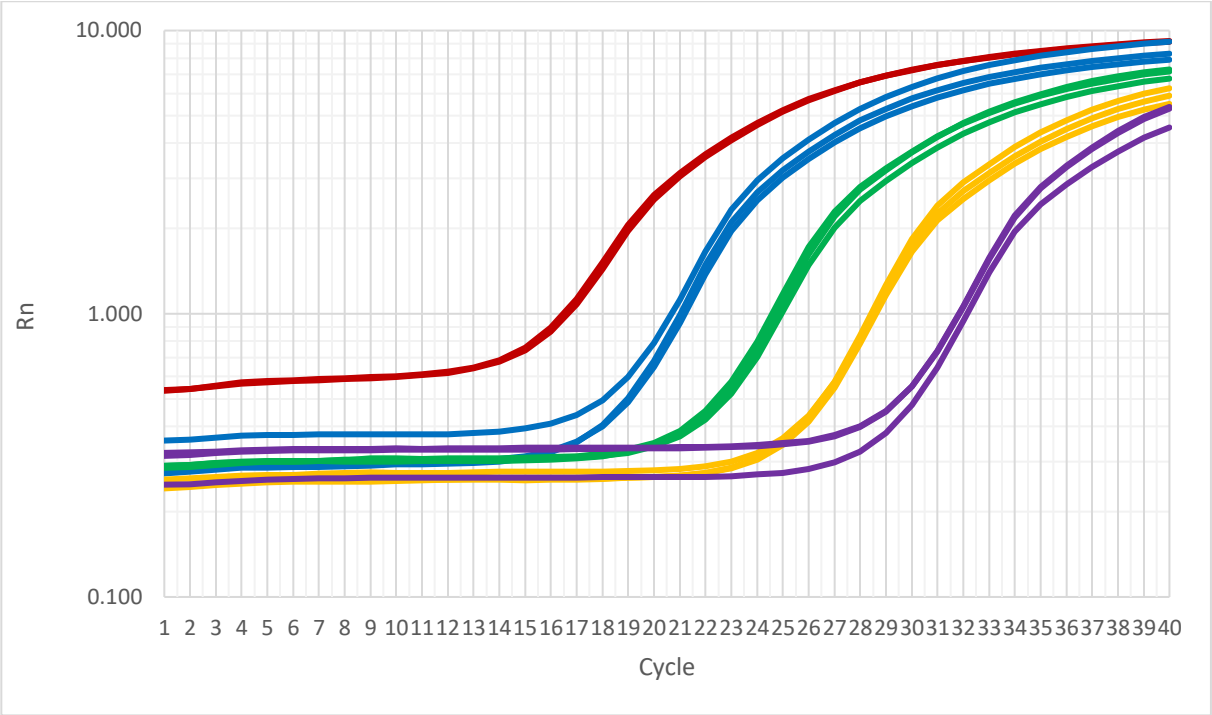


Figure A21. qPCR amplification curve for *invA* gene amplification from N13-01291. qPCR was performed in triplicate to amplify a fragment of *invA* from 10 ng (red), 1 ng (blue), 100 pg (green), 10pg (yellow), and 1 pg (purple) of *S.* Heidelberg gDNA. The real-time PCR was performed on an Applied Biosystems ViiA™ 7 Real-Time PCR System (Applied Biosystems, Foster City, CA, USA).

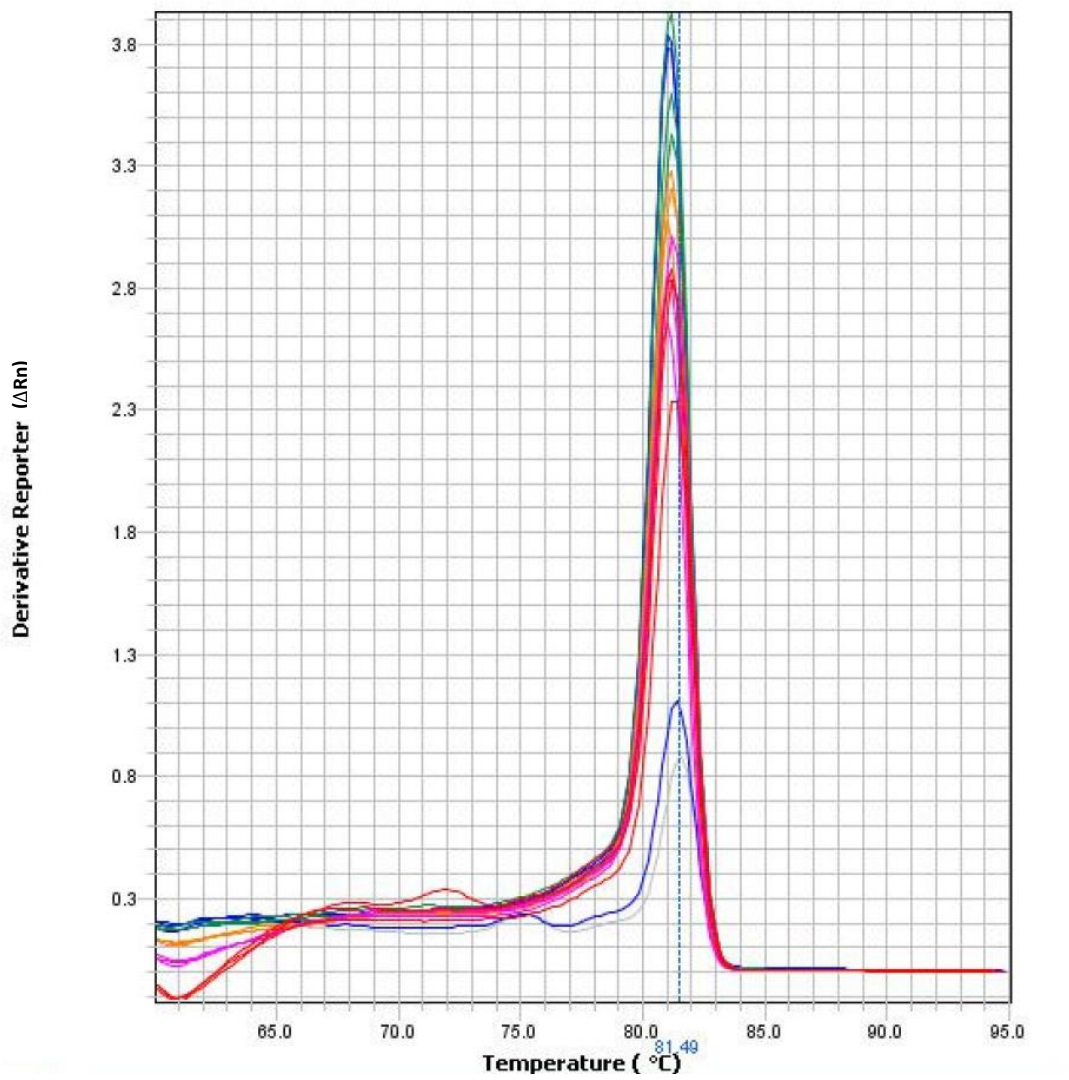


Figure A22. Melt curve of the *invA* real-time PCR product generated in Figure 12, from 1 ng of *S. enterica* serotype Heidelberg gDNA input. Rn indicates the normalized reporter; calculated as the intensity of fluorescence emission by the reporter dye divided by the intensity of fluorescence emission by the passive reference dye. Blue; 10 ng sample, Green; 1 ng sample, Orange; 100 pg sample, Pink; 10 pg sample, Red; 1 pg sample, and Grey; NTC.

Table 4. Chromosomally-derived proteins identified with a 2-fold or greater change in the presence of either plasmid[151].

Identified Proteins (2778)	Functional Annotation	GenBank Accession Number	Log_2-Fold Change in the Presence of pCMYN13-02944A	Log_2-Fold Change in the Presence of pCMY12-2460C
copper oxidase	Unclassified: metabolism	ALN26780.1	1.58	1.03
glucose dehydrogenase	Carbohydrate metabolism	ALN26781.1	2	-2.1
peptide chain release factor-like protein	Protein families: genetic information processing	ALN26924.1	-1.73	-1.05
hNH endonuclease	No annotation	ALN26938.1	-1.02	1.14
hypothetical protein APS45_02195	No annotation	ALN27026.1	1.58	-1.12
hypothetical protein APS45_02285	No annotation	ALN27044.1	2.47	-2.78
dimethyl sulfoxide reductase	Energy metabolism	ALN27553.1	-1.5	-2.45
dimethyl sulfoxide reductase	Energy metabolism	ALN27554.1	-1.42	-2.39
hypothetical protein APS45_06020	No annotation	ALN27742.1	1.7	1.87
peptidase T	Protein families: metabolism	ALN27811.1	-1.12	-1.55
lipoprotein EnvE	No annotation	ALN27826.1	-1.09	-1.72

lysozyme inhibitor	No annotation	ALN27831.1	1.45	-1.46
nickel ABC transporter substrate-binding protein	Cellular processes	ALN27840.1	-1.06	-1.65
ferredoxin	No annotation	ALN27846.1	2.8	-1.49
acetylornithine aminotransferase	Amino acid metabolism	ALN27886.1	1.22	-1.23
arginine N-succinyltransferase	Amino acid metabolism	ALN27887.1	1.18	-1.35
N-succinylglutamate 5-semialdehyde dehydrogenase	Amino acid metabolism	ALN27888.1	1.38	-1.52
succinylarginine dihydrolase	Amino acid metabolism	ALN27889.1	1.04	-1.05
hypothetical protein APS45_06820	Protein families: genetic information processing	ALN27891.1	2.32	3.22
dethiobiotin synthetase	Metabolism of cofactors and vitamins	ALN28060.1	-1.27	-1.25
hypothetical protein APS45_07775	No annotation	ALN28071.1	1.46	1.34
hypothetical protein APS45_07850	No annotation	ALN28086.1	2.33	-1.21
nitrate reductase	Energy metabolism	ALN28151.1	1.74	-1.24
TonB-dependent receptor	Protein families: signalling and cellular processes	ALN28161.1	1.74	-1.44

colanic acid/biofilm transcriptional regulator	Protein families: genetic information processing	ALN28162.1	1.59	-1.53
hypothetical protein APS45_08425	Amino acid metabolism	ALN28194.1	1.34	-1.24
hypothetical protein APS45_08965	No annotation	ALN28299.1	2.6	-1.93
hypothetical protein APS45_08970	No annotation	ALN28300.1	2.24	-1.78
Mn-containing catalase	Unclassified: signalling and cellular processes	ALN28301.1	3.09	-1.64
nitrate reductase	Energy metabolism	ALN28328.1	-1.13	-1.64
nitrate/nitrite transporter NarK	Energy metabolism	ALN28330.1	-1.7	-1.23
carbon-nitrogen hydrolase	No annotation	ALN28432.1	1.2	2.62
glucose-6-phosphate dehydrogenase	No annotation	ALN28491.1	-1.6	-1.29
cobalt-precorrin-6X reductase	Metabolism of cofactors and vitamins	ALN28570.1	-1.15	-1.1
cobalt-precorrin-3B C(17)-methyltransferase	Metabolism of cofactors and vitamins	ALN28571.1	-1.04	-1.34
ethanolamine utilization protein EutM	No annotation	ALN28589.1	1.49	-1.88

disulfide bond formation protein DsbE	Protein families: genetic information processing	ALN28786.1	-1.19	-1.07
cytochrome C biogenesis protein CcmE	Unclassified: signalling and cellular processes	ALN28788.1	-1.09	-1.12
cytochrome C	Unclassified: metabolism	ALN28793.1	-1.26	-2.82
nitrate reductase	Energy metabolism	ALN28796.1	-1.49	-2.42
glycerol-3-phosphate dehydrogenase, anaerobic, A subunit	Lipid metabolism	ALN28819.1	-1.66	-1.32
glycerol-3-phosphate dehydrogenase, anaerobic, B subunit	Lipid metabolism	ALN28820.1	-1.5	-1.42
glycerol-3-phosphate dehydrogenase, anaerobic, C subunit	Lipid metabolism	ALN28821.1	-2.32	-1.24
carbon starvation induced protein	Amino acid metabolism	ALN29252.1	2.09	-4
hydroxyglutarate oxidase	Amino acid metabolism	ALN29253.1	1.03	-1.08
NAD-dependent succinate-semialdehyde dehydrogenase	Carbohydrate metabolism	ALN29254.1	1.17	-1.92
peptidoglycan-binding protein	No annotation	ALN29258.1	2.97	-1.44

sorbitol-6-phosphate 2-dehydrogenase	Carbohydrate metabolism	ALN29294.1	1.79	1.04
hydrogenase assembly chaperone	Unclassified: genetic information processing	ALN29315.1	-1.4	-1.22
transcriptional regulator SirC	No annotation	ALN29326.1	-2.66	-1.76
type III secretion system protein PrgI	Environmental Information Processing	ALN29332.1	-1.24	-1.65
type III secretion system protein PrgH	Protein families: signalling and cellular processes	ALN29333.1	-1.5	-1.21
transcriptional regulator HilD	No annotation	ALN29334.1	-1.58	-1.2
ribose 5-phosphate isomerase	Carbohydrate metabolism	ALN29506.1	-2.53	1.49
PTS galactitol transporter subunit IIB	Carbohydrate metabolism	ALN29508.1	-1.65	1.31
xylanase deacetylase	No annotation	ALN29601.1	1.2	-1.51
hydrogenase 2-specific chaperone	No annotation	ALN29614.1	-1.32	-1.06
hydrogenase 2 maturation endopeptidase	Protein families: metabolism	ALN29615.1	-1.29	-1.4
hydrogenase 2 large subunit	Xenobiotics biodegradation and metabolism	ALN29616.1	-1.03	-1.59

hydrogenase 2 protein HybA	No annotation	ALN29618.1	-1.22	-2.77
putrescine aminotransferase	Amino acid metabolism	ALN29686.1	1.2	-1.33
hypothetical protein APS45_16485	No annotation	ALN29705.1	-1.26	-2.02
pyruvate formate-lyase	Carbohydrate metabolism	ALN29707.1	-1.23	-1.8
propionate kinase	Carbohydrate metabolism	ALN29708.1	-1.17	-2.29
threonine dehydratase	Amino acid metabolism	ALN29710.1	-1.24	-3.47
hypothetical protein APS45_17075	Unclassified: genetic information processing	ALN29810.1	2.09	-1.16
large-conductance mechanosensitive channel	Protein families: signalling and cellular processes	ALN29851.1	1.2	-1.58
nitrite reductase	Energy metabolism	ALN29913.1	-1.32	-2.32
nitrite reductase	Energy metabolism	ALN29914.1	-1.75	-2.59
peptide ABC transporter substrate-binding protein	Environmental information processing	ALN30062.1	1.71	-1.39
cold-shock protein	Unclassified: genetic information processing	ALN30080.1	-1.47	-1.2
aldehyde dehydrogenase	Carbohydrate metabolism	ALN30110.1	1.09	-1.59
sugar kinase	Unclassified: metabolism	ALN30111.1	1.73	1.47
acyltransferase	No annotation	ALN30388.1	-1.09	-1.95

autoinducer	Environmental information processing	ALN30464.1	1.06	-1.67
conjugal transfer protein TraF	No annotation	ALN30606.1	3.12	-1.49
cation/acetate symporter ActP	Protein families: signalling and cellular processes	ALN30636.1	1.17	-1.72
cytochrome C nitrite reductase	Energy metabolism	ALN30640.1	-1.49	-1.61
fumarate hydratase	Carbohydrate metabolism	ALN30666.1	-1.52	-2.6
C4-dicarboxylate transporter	Environmental Information Processing	ALN30667.1	-1.5	-3.11
C4-dicarboxylate transporter	Protein families: signalling and cellular processes	ALN30689.1	-1.08	-1.66
DNA alkylation response protein	Unclassified: metabolism, lipid	ALN30736.1	1.58	-1.13
ornithine carbamoyltransferase	Amino acid metabolism	ALN30802.1	-1.07	-2.63
carbamate kinase	Energy metabolism	ALN30803.1	-1.68	-2.26
arginine deiminase	Amino acid metabolism	ALN30804.1	-1.41	-2.21
1-pyrroline dehydrogenase	Amino acid metabolism	ALN30991.1	1.18	-1.11
PTS galactitol transporter subunit IIA	Carbohydrate metabolism	ALN31044.1	-1.49	1.1